MODELLING OF THE SOIL MECHANICAL PROPERTIES TO SOIL MOISTURE CONDITIONS AND THEIR APPLICATIONS TO STUDY THE TRACTION DEVELOPED BY LUGGED TIRES

by

OMAR SOLIMAN ALI HASSAN

A thesis submitted to the Faculty of Graduate Studies and Research in partial fulfilment of the requirements for the degree of Doctor of Philosophy

Department of Agricultural Engineering
Macdonald Campus of McGill University
Sainte-Anne-de-Bellevue
Quebec, Canada

July 1980

ABSTRACT

Ph.D. OMAR SOLIMAN ALI HASSAN Agricultural Engineering

MODELLING OF THE SOIL MECHANICAL PROPERTIES TO SOIL MOISTURE CONDITIONS AND THEIR APPLICATIONS TO STUDY THE TRACTION DEVELOPED BY LUGGED TIRES

The variations of soil mechanical properties, cohesion, c, internal friction angle, ϕ, soil-rubber adhesion, c'_r, soil-steel adhesion, c'_s, soil-steel friction angle, δ_s, soil-rubber friction angle, δ_r, the sinkage moduli, kc, $k\phi$, and n, have been studied under field conditions for different soil depths of sandy loam and clay soils. Models to predict these parameters were developed in this study. These models were functions of soil moisture content, soil plastic limit or liquid limit and two constants which depend on the soil type and depth. Also, a model to estimate the soil moisture content by a simple and accurate method was developed using the data of daily precipitation and evaporation pan reading (class A) in southern Quebec. The soil mechanical properties models were used to study the traction characteristics of lugged tires. The investigation shows that lug design could have a significant role in improving the traction force for agricultural tires. The optimal lug angle was found for different soil types during the farming season in an average climatic year of southern Quebec.

RESUME

Ph.D. OMAR SOLIMAN ALI HASSAN Génie Rurale

MODELES DE PROPRIETES MECANIQUES DES SOLS EN FONCTION DE LEUR TENEUR EN HUMIDITE ET LEURS INFLUENCES SUR LA GEOMETRIE IDEALE DES ERGOTS DE PNEUS POUR FAVORISER LA TRACTION

Les variations qui existent en matière de mécanique des sols dans les paramètres cohésion, c, angle de friction interne, ϕ, adhesion sol-caoutchouc, c'_r, adhesion sol-acier, c'_s, angle de friction sol-acier, δ_s, angle de friction sol-caoutchouc, δ_r, les modules de penetration kc, $k\phi$ et n, ont été étudiées "in situ" pour différents types de sol et à différentes profondeurs. Des modèles ont été développés afin de pouvoir prédire ces paramètres et sont fonction du degré d'humidité du sol, de sa limite plastique, de la limite liquide et de deux constantes reliées au type de sol et à sa profondeur.

De plus, un modèle a été développé afin d'estimer la teneur en humidité par des méthodes simples et précises en mettant en jeu la pluriométrie journalière et l'evaporation par bac evapométrique de Classe "A" aux environs du sud du Quebec.

Les modèles des propriétés mécaniques furent utilisées pour vérifier les caractéristiques de traction des ergots de roues de tracteurs. Les essais ont démontré que le design des ergots peut influencer la force de traction des tracteurs agricoles. L'angle idéal des ergots a été défini pour certains types de sol durant la période de culture lors d'une période moyenne de climat au sud du Québec.

ACKNOWLEDGEMENTS

The author is sincerely grateful to his supervisor, Professor Edward McKyes, Chairman of the Agricultural Engineering Department, Macdonald College of McGill University, for the valuable guidance, assistance and encouragement throughout this research and in the preparation of the thesis.

Gratitude is also expressed to Professors R. S. Broughton, G. S. V. Raghavan and G. Mehuys for their valuable help and enthusiasm; and to Professor P. J. Jutras for translating the Abstract into French.

Thanks are extended to the technical staff of the Agricultural Engineering Department, W. R. Nattress and R. G. Cassidy, for assistance in the construction of equipment for use in this project.

Many thanks are expressed to my friends, Dr. S. Chieng, Dr. S. A. Ba-Angood, Dr. A. Inteaz and Dr. U. G. N. Anazado for their help and encouragement during this study. Thanks are also extended to Mrs. M. Couture for typing the manuscript.

The author is grateful to Agriculture Canada and the Agricultural Engineering Department for financial support, without which this study would not have been possible.

TABLE OF CONTENTS

Page

LIST OF TABLES

LIST OF FIGURES

Figure Page

LIST OF SYMBOLS

The symbols used are listed below, except those used in Table 1 which have been defined in the same table.

a	area of slipping surface
b	width of loaded surface or wheel length in contact with the soil
c	soil cohesion
c_1 and c_2	constants which depend on the soil type and depth
c'_s	soil-steel adhesion
c'_r	soil-rubber adhesion
C.V.	coefficient of variation
D	wheel outside diameter
d	lug depth
DM	daily soil moisture changes
E	end of lug clearance
ET	evapotranspiration
Eva	pan evaporation
Fs	side force developed by lug on the horizontal plane
g	number of lugs across the soil-wheel contact area
GWo	subsurface runoff
ΔGW	change in groundwater storage
H	soil shearing resistance or soil thrust
h	grouser height

h_1	Planck's constant
IRR	irrigation
kc	cohesion modulus
$k\phi$	friction modulus
L	length of loaded area or lug length
LL	soil liquid limit
m	number of lugs along the contact area
MC	soil moisture content percentage by weight
M_u	moisture holding capacity of a layer
N	normal load on the slipping surface
n	sinkage factor
N_v	Avogadro's number
PL	soil plastic limit
PI	soil plasticity index
Pn_2	soil thrust due to the adhesion force
PE	potential evapotranspiration
PRE	precipitation
q	vertical contact pressure
r	wheel radius
r_i	inside radius of the shear ring
r_o	outside radius of the shear ring
S	lug space
S_c	critical lug spacing
SD	standard deviation
ΔSM	change in the soil moisture content
SR	surface runoff

SMC	soil moisture content percentage by volume
T	torque on a lug in contact with the soil
t	absolute temperature
T_o	intercept of the torque vs normal pressure line with the y axis
W	lug width
Wd	wheel width
Z	sinkage
γ	soil bulk density
δ_r	soil-rubber friction angle
δ_s	soil-steel friction angle
θ	lug angle
θ_k	angle between the wheel tangential and horizontal thrust force of a lug
ε	angle of the soil movement on the lug face with the vertical
ε°	strain rate
ϕ	soil internal friction angle
τ	shear strength
σ'_f	effective stress on the shear plane
λ	slope of the line, torque vs normal pressure
λ_1	distance between successive equilibrium positions of soil particle

CHAPTER I

INTRODUCTION

Soil moisture conditions change very widely during the farming season. Accordingly, the soil mechanical properties will vary. On the other hand, the performance of many farm vehicles or equipment depends mainly upon the soil mechanical properties to a considerable extent. The farmer today is faced with the problem of selecting proper traction devices and tractor parameters for efficient field work when the moisture content and mechanical properties of field soils are continually changing throughout the year. If these properties can be estimated in advance, a suitable machine could be designed or selected to perform a given farming operation at the desirable time.

Since the measurement of soil moisture is less costly and easier to estimate than the soil mechanical properties, the modelling of the soil mechanical properties to the soil moisture content would offer a good means of identifying those properties. In addition, the prediction of soil moisture conditions by using such models leads to the prediction of the soil mechanical properties. Hence, a simple and reliable method for the prediction of soil moisture content is required.

Several topics can be studied by using models of soil mechanical properties. For example, these properties are required for the

calculation of values of traction capacity, flotation, slipperiness, and stickiness of the vehicle running gear or soil resistance against any tillage tool, as well as to estimate the amount of soil failure in front of these tools (McKyes and Ali 1977; Hettiaratchi and Reece 1967, 1974; Osman 1964; Yong and Chen 1970). In the field, however, the soil mechanical properties are known to vary mainly with soil moisture content, soil type, soil depth, and location. The variation of these properties has not been studied widely (Lumb 1970; Bekker 1969). In the present study, modelling of these properties to the soil moisture content of different soil types at different depths in southern Quebec will be investigated. Also, a method to predict the soil moisture content will be proposed.

The effects of lugs on the wheel traction force have been the subject of relatively few reported investigations. However, some of the developed models of soil mechanical properties will be used to study the characteristics of soil thrust developed by the lugs. There is no theory available in the literature to calculate the soil thrust due to lugs for a rubber lugged tire; nevertheless, with some modifications of the existing theory on soil failure, the thrust could be calculated. In this study the theory developed by Hettiaratchi and Reece (1974) will be modified in order to predict the traction force due to the lugs.

The modified theory for predicting the soil thrust as well as the soil mechanical properties models can be verified experimentally by measuring the soil thrust due to the lugs. The meaning of the growing or the farming season in this study was the period of the year when the ground is not frozen and the field work is possible.

Objectives

The present work will deal with modelling the following soil mechanical properties to the soil moisture content:

a) soil cohesion (c)

b) soil-steel adhesion (c_s')

c) soil-rubber adhesion (c_r')

d) soil-soil friction angle (ϕ)

e) soil-steel friction angle (δ_s)

f) soil-rubber friction angle (δ_r)

g) cohesion modulus of stiffness or deformation (kc)

h) friction modulus of stiffness or deformation ($k\phi$)

i) sinkage factor (n)

The detailed objectives of this study can be stated, however, as follows:

1) To measure and determine the relationships between (a) soil moisture content and (b) the depth and the following soil mechanical properties in two soil types, namely a sandy loam and a clay:
   (i) soil adhesion (c)
   (ii) soil adhesion (to steel and rubber, c_s', c_r')
   (iii) soil-soil friction angle (ϕ)
   (iv) soil-steel or rubber friction angle (δ_s, δ_r)
2) To measure and determine the relationships between the soil moisture content and the following parameters:
   (i) cohesion modulus (kc)

(ii) friction modulus ($k\phi$)

(iii) sinkage factor (n)

3) To determine the variations in the above-mentioned parameters during the growing season.

4) To establish a simple and reliable method which will predict the soil moisture content during the growing season, taking into account potential evapotranspiration, rainfall, evaporation from a free water surface and actual evapotranspiration.

5) To demonstrate the use of the above-mentioned relationships by using variable soil strength properties to find the best lug angle for agricultural tires under a wide range of soil conditions, i.e., a year-round best tire lug design, if possible.

6) To find a method to calculate the soil thrust developed by lugs of tires.

Scope

The scope of this study with respect to models of soil mechanical properties is restricted to a soil with moisture content under the liquid limit. The method which calculates the soil moisture content is also expected to be applicable to flat land with soil moisture conditions under the field capacity in southern Quebec during the growing season. In addition, in this thesis a modified theory of soil failure in front of a flat plate will be proposed to calculate the soil thrust for lugs of tires.

The studies were carried out on sandy loam and clay soils.

CHAPTER II
REVIEW OF LITERATURE

A. Modelling of soil mechanical properties to soil moisture content

The few models of soil mechanical properties reported in the literature were found to be empirical relationships (Wroth and Wood 1978; Bekker 1969). The available models deal only with the parameters c, ϕ, Kc, Kϕ and n in certain regions (Nichols 1932; Wells and Treesuwan 1977). Nevertheless, there are no models available for the soils in southern Quebec. Bekker (1969) and Raghavan and McKyes (1979) stated that it is desirable to identify these parameters in terms of well known physical properties such as soil water content.

The soil mechanical properties (c, ϕ, c'_s, c'_r, δ_s, δ_r, Kc, Kϕ and n) depend on the soil plasticity index (Neal 1966). Four decades ago Casagrande (1939, from Terzaghi and Peck 1948) related soil strength to the soil liquid and plastic limits. Nichols (1932) presented the following empirical relationship between soil shear strength and soil moisture content:

$$\tau = \frac{(LL - MC)(0.66\ PI + q + 1.8)}{PL} \qquad \ldots (1)$$

where τ = shear strength

LL = soil liquid limit

PL = soil plastic limit

MC = soil moisture content

q = average vertical contact pressure

PI = plasticity index = LL - PL

The general trend of the relationship between the soil mechanical properties and its moisture content shows that an increase in the soil moisture content resulted in increased values for the soil properties (c, ϕ, c'_s, c'_r, δ_s, δ_r) up to the plastic limit. This is followed by decreased values for these properties with further increase in the soil moisture content up to a point around the liquid limit (Bekker 1960; Payne 1956). Wells and Treesuwan (1977) found that the soil internal friction angle (ϕ) increased with increasing soil moisture content according to the regression relationship.

$$\phi = 1129.20 + 0.39\ MC - 1127.5\ \gamma^2 \quad \ldots (2)$$

where MC = soil moisture content (% by weight)

γ = soil bulk density (kg/m^3)

Lumb (1966, 1970) and Lee (1974) studied the variations of the soil mechanical properties c and ϕ for undisturbed soil. The conclusion was that the coefficient of variations in the ϕ values was higher than in the c values. They found soil cohesion varied in a linear fashion with the soil depth.

A comprehensive test was conducted by Youssef et al. (1965), who used different types of clay to show that soil shear strength is a function of soil plasticity index.

Neal (1966) carried out investigations on the effect of the soil moisture content on the soil-rubber adhesion and frictional angle. The values of the two parameters increased with increasing soil moisture content up to the plastic limit and then decreased until the liquid limit was reached. Increasing the soil moisture content beyond the liquid limit did not change the soil-rubber friction or adhesion significantly. Some characteristics of the friction between soil and metal were determined by Nichols (1932), Fountaine (1954), Neal (1966) and Payne (1956).

The reported studies on the relationships between the n, kc, $k\phi$ values were very few. Wells and Treesuwan (1977) stated that n values change between 0.5 and 0.7 with varying the soil moisture content. Smith (1964) and Stong and Buchele (1962) also reported that the n values changed by small amounts with changing soil moisture content. Similar findings were reported by Bailey and Webber (1965).

There is, however, no general relationship between soil mechanical properties and soil moisture content that has been established. The only relationships reported are regression relationships for a particular soil (McKyes and Stemshorn 1977). In addition, the few studies which have been carried out on the relationships between the parameters δ_r, δ_s, c_r' and c_s' and the soil moisture content are not comprehensive enough to establish firm relationships.

The soil mechanical properties (c, ϕ, c_r', c_s', δ_r, δ_s) are used mainly to determine the soil shear strength (shown in equation 3) or

the shearing resistance at soil and rubber or steel surface (equation 4).

$$H = ac + N \tan \phi \quad \ldots (3)$$

$$H = ac' + N \tan \delta \quad \ldots (4)$$

where

H = shearing resistance

N = the normal load on the slipping surface

a = the area of the slipping surface

c = soil cohesion

c' = the adhesion between the rubber or the steel and the soil

δ = the friction angle between the soil and rubber or steel

ϕ = soil internal frictional angle.

Most of the known theory which explains soil-machine interactions uses these parameters. Other theories have been developed to predict soil strength such as the critical state theory (Schofield and Worth 1968) and the rate process theory (Mitchell 1976). However, these two theories have not been used in the study of soil-machine interactions. Therefore, modelling the soil parameters presented in equations (3) and (4) is needed because of their wide use in the field of agricultural engineering.

The detailed development of the rate process theory is based on statistical mechanics and physical chemistry (Mitchell 1976). According to this theory the soil shear strength can be evaluated by equation (5).

$$\tau = A_1 + A_2 \sigma_f \quad \ldots (5)$$

where

τ = soil shear strength

$A_1 = \frac{2a_1 \Delta F}{\lambda_1 N_v} + \frac{2b\ kt}{\lambda_1} \ln \frac{\varepsilon^\circ}{B}$

$A_2 = \frac{2b\ \Delta F}{\lambda_1 N_v} + \frac{2b\ kt}{\lambda_1} \ell\ \frac{\varepsilon^\circ}{B}$

N_v = Avogadro's number (6.02×10^{23})

ΔF = value of activation energy which depends on the soil type (kcal/mole)

t = absolute temperature

λ_1 = distance between successive equilibrium positions

ε° = strain rate

$B = Xkt/h_1$

a_1 and b = constants

k = Boltzmann's constant (1.38×10^{-16} erg $^\circ k^{-1}$)

δ_f = effective stress on the shear plane

h_1 = Planck's constant (6.624×10^{-27} erg sec^{-1})

X = parameter which depends on time and soil structure.

The critical state theory as presented by Schofield and Worth (1968) describes the critical state of soil under load after which the soil could flow as a frictional fluid. This state can be defined by two equations:

$$q = MP \quad \ldots (6)$$

$$\Gamma = \gamma + \lambda \ln P \quad \ldots (7)$$

where

M, Γ, and λ depend on the soil properties

γ = specific volume

q = axial deviator stress

P = effective spherical pressure

In this theory, the possibilities of degradation or orientation of the particles were not considered in calculating the power dissipation.

The most widely used equation to calculate the sinkage (Z) of a machine under normal load (N) is Bekker's equation:

$$N = \left(\frac{kc}{b} + k\phi \right) Z^n \quad \text{(Bekker 1952)} \qquad \ldots (8)$$

where

kc, kϕ, and n are empirically measured soil constraints which are mentioned in the objectives, and b is the width of the loaded surface.

It should be mentioned that there are many other theories available to calculate the sinkage of a machine under certain normal load, as shown in Table 1 (Wong and Bekker 1977). These theories, however, have not received the wide acceptance which has led to practical applications that Bekker's equation has (Wong 1979).

TABLE 1. The relationships between the load and sinkage, soil shear strength and slip as reported by Wong and Bekker (1977)

Date of origin (approx.)	Name of the originator (or user)	Soil-value (parameter) definition	Soil value (parameters)	Country
1913	R.Bernstein	$p = k'(1-3-nz)$	k', n	Germany
1936	M.N.Letoshnev	$p = k_B z^{1/2} = (a'U + a''A)z^{1/2}$	a',a'', or k_B; 1/2	
1940	I.S.Vernikov	$p = k_L z^n = (a' + a''b)z^n$	a',a'', or k_L; n	U.S.S.R.
1947	M.N.Troitskaya	$p = k_v z = \gamma\gamma'/[2(\gamma'-\gamma)]$	γ, γ', or k_v; n = 1	U.S.S.R.
		$p = p_c(e^{k_T\lambda}-1)$	p_c, k_T, λ	U.S.S.R.
1948	S.S.Korchunov	$\tau = \tau_o(1 - e^{-k_T\lambda})$	τ_o, k_T, λ	
1959	S.S.Suakyan	$p = p_{KO}(1 - e^{-z/k_{ko}})$	p_{KO}, k_{ko}	U.S.S.R.
1963	V.V.Katsygin	$p = k_s\lambda^n = k_s(z/D)^n$	k_s, n	U.S.S.R.
		$p = p_{kA} \tan h\,[k_{KA}/p_{KA}]z$	k_{KA}, p_{KA}	U.S.S.R.
		$\tau = p\mu_m[1 + \frac{\mu_{KA}}{\cos h\,\frac{x}{k_\tau}}]\tan h[\frac{s}{k_\tau}]$	μ_m, μ_{KA}	U.S.S.R.
1959	Ya S.Ageikin (user)	$p = kz^n$	k, n	U.S.S.R.
		$\tau = c + p\mu_A$	c, μ_A	
1963	V.A.Skotnikov (user)	$p = k_{SK}z$	k_{SK}, n=1	U.S.S.R.

(table continued)

TABLE 1 (continued)

Date of origin (approx.)	Name of the originator (or user)	Soil-value (parameter) definition	Soil value (parameters)	Country
1964-66	V.V.Guskov et al. (user)	$p = p_{KA} \tan h\, [k_{KA}/p_{KA}]z$	p_{KA}, k_{KA}	U.S.S.R.
		$\tau = c + p \tan\phi$	c, ϕ	
		$\tau = p\mu_m[1 + \frac{\mu_{KA}}{\cos h(\frac{s}{k_\tau})}] \tan h\, [\frac{s}{k_\tau}]$	μ_m, μ_{KA}	
1967	S.G.Volskii (user)	$p = kz^n$	k, n	U.S.S.R.
		$\tau = c + \tan\phi$	c, ϕ	
1968-69	M.Z.Nafikov & I.S.Poliakov	$p = [k_{NP}/K_{NP}][e^{K_{NP}z} - 1]$	k_{NP}, K_{NP}	U.S.S.R.
		$\tau = c + p \tan\phi$	c, ϕ	
1970	Ya S.Ageikin	$p = 1/[(1/p_s) + (\pi m_z D/2k_z z)]$	p_s, m_z, k_z	U.S.S.R.
1970	Lunar Rover "Lunokhod"	Unknown. Penetrometer, the "ninth wheel," cone-cum vanes torque-slip measurement	Unknown	U.S.S.R.
1955	M.G.Bekker	$p = [(k_c/b) + k_\phi]z^n$	k_c, k_ϕ, n	U.S.A.
		$\tau = c + p \tan\phi$	c, ϕ	
1965	A.R.Reece	$p = (ck'_c + b\gamma k'_\phi)(z/b)^n$	ck'_c, $\gamma k'_\phi$, n	England
		$\tau = c + p \tan\phi$	c, ϕ	
1965	A.Soltynski (user)	$p = [k_c/b) + k_\phi]z^n$	k_c, k_ϕ, n	Poland
		$\tau = c + p \tan\phi$	c, ϕ	
1967	G.Sitkei (user)	$p = [k_c/b) + k_\phi]z^n$	k_c, k_ϕ, n	Hungary
		$\tau = c + p \tan\phi$	c, ϕ	
1969	A.Wislicki (user)	$p = [k_c/b + k_\phi]z^n$	k_c, k_ϕ, n	Poland
		$\tau = c + p \tan\phi$	c, ϕ	

B. Measurement of the soil mechanical properties

The value of soil mechanical properties can be obtained by using any of the following devices.

1. Devices used in the laboratory

a. Direct shear box (Freitag et al. 1970).—The direct shear device is shown in Figure 1. The soil sample in this device is confined under a vertical load and sheared by fixing one-half of the frame and translating the other to cause simple shear. The results of the direct shear test are shear stress, normal stress (on the failure plane), and shear displacement. The values of normal stress and maximum shear stress can be plotted directly from the test data, and the cohesion c and the angle of internal friction ϕ can be derived.

b. Triaxial test.--The test usually is conducted on a cylindrical soil specimen loaded axially while under hydrostatic confinement (Figure 2a). The measurements obtained in this device can be used to determine the soil properties c and ϕ.

c. Shear plate.--This apparatus provides a tangential stress deformation relation at the ground surface level under certain normal loads which can be used for estimating the c and ϕ values (Figure 2b).

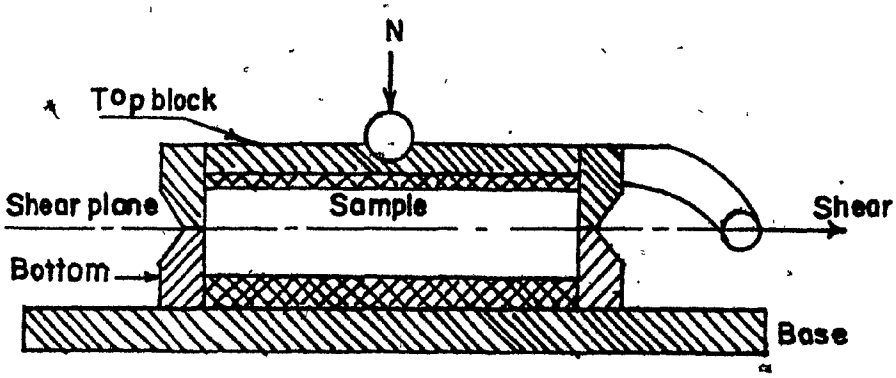

(a) Direct Shear Box

Figure 1. Direct shear box.

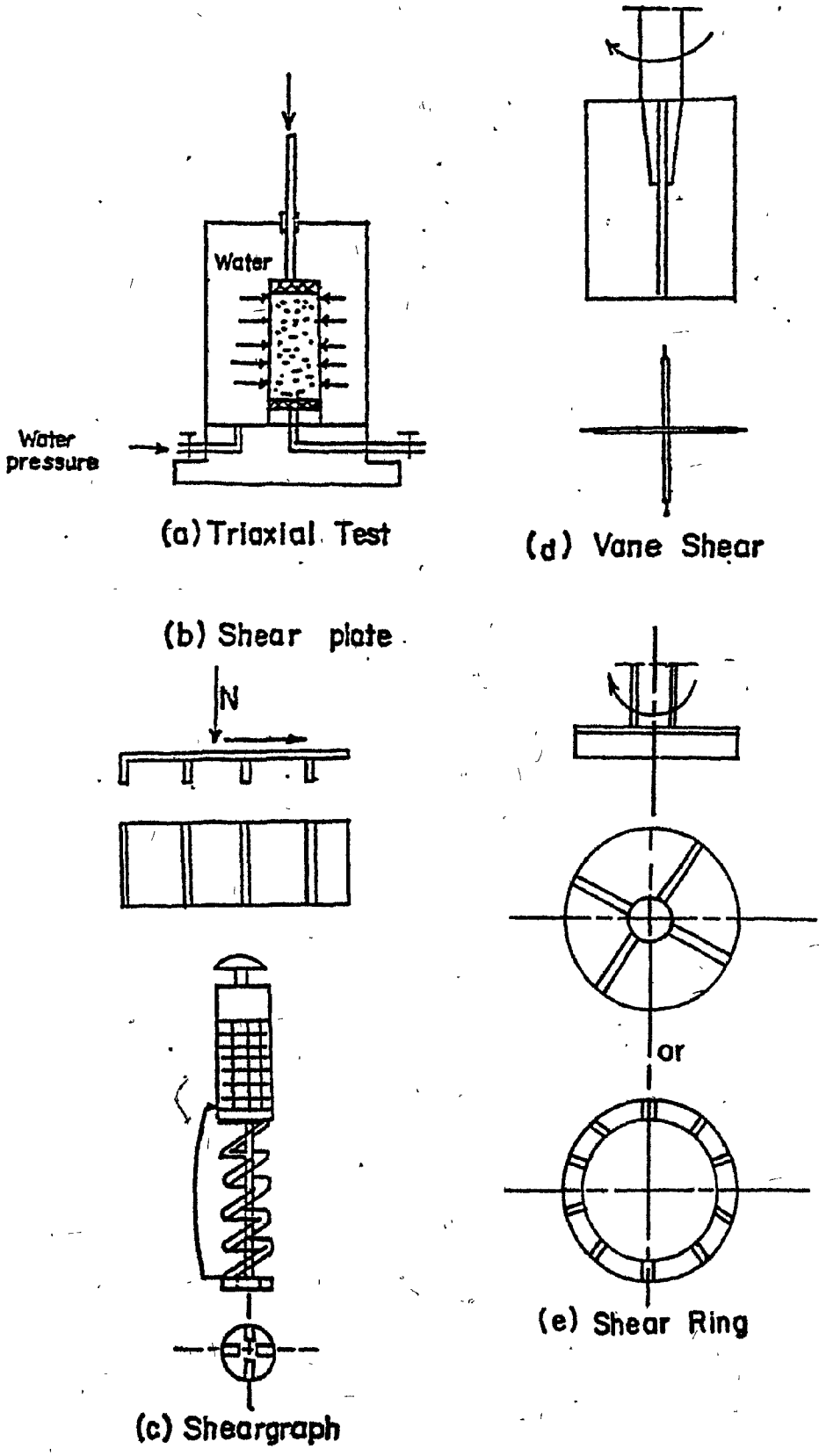

Figure 2. Devices for measuring soil mechanical properties (c and ϕ).

2. Devices used in the field

a. Sheargraph.--This device utilizes a small circular cup with radial vanes as shown in Figure 2c. The soil is sheared by the rotation of the cup under imposed normal stress. The device is intended to measure the ultimate shear strength at different normal loads. The parameters c and ϕ can be estimated.

b. Shear vane.--The device consists of four vanes mounted perpendicularly to each other and the torque value required to rotate the blades gives an indication of soil shear strength (Figure 2d).

c. Shear ring.--This device consists of a grousered ring imbedded in the soil, which is rotated at a certain normal load N (Bekker 1969). The torque (T) is plotted as a function of the normal load. The torque-normal load relationship can be fitted by a line, the intercept of this line with the torque axis gives T_o and the slope of the line is given by the angle λ. The soil parameters c and ϕ can be calculated by using equations (9) and (10) developed by Reece (1964) (Figure 2e).

$$\tan \phi = (\tan \lambda)(2\pi/3)(r_o^3 - r_i^3) \quad \ldots (9)$$

$$c = T_o/(2\pi/3)(r_o^3 - r_i^3) + 2\,h\,\pi(r_o^2 + r_i^2)\,\eta \quad \ldots (10)$$

where

r_o = outside radius of the shear ring

r_i = inside radius of the shear ring

h = grouser height

η = 1 (as long as the shear ring does not sink appreciably)

η = $2 \sin^2 (45 + \phi/2)$ (if the shear ring sinks more than r_o).

d. Plate sinkage test.--This device exists in many shapes and sizes, but the main components are two or more plates pressed into the ground and the mean contact pressure is recorded as a function of sinkage. The pressure sinkage curves for each plate size are plotted on log-log paper and fitted by straight lines of the same slope. This slope gives n value, and from the n values at Z = 1, kc and kϕ are obtained from equation (8) (Bekker 1960).

The values of the soil mechanical properties may depend upon the method used to carry out the measurements (Osman 1964). However, some investigations were conducted to select the best apparatus to measure these properties.

Ghani (1966) determined the soil shear stress at several soil moisture contents by using a torsion shear apparatus with five heads. The shear strength value did not vary significantly by using different shear heads. Payne and Fountaine (1952) introduced a torsional shear box for measuring the soil shear strength in the field. Comparisons between the values of cohesion and soil internal frictional angle using this apparatus and a direct shear box in the laboratory resulted in differences of about 5% between the two methods.

Neal (1966) reported that the basic theory of adhesion between soil and metal is applicable for soil and rubber as well and he also recommended that a hand-powered torquemeter for twisting the shear box be used to measure the soil shear strength and soil rubber friction properties. Payne (1956) described a field method to measure the

soil-to-implement friction coefficient. The technique gave adequate results because there was little disturbance of the soil in the field. O'Callaghan et al. (1964), Fountaine and Brown (1959) and Fountaine (1954) reported that the torsion shear test could be used as long as the normal pressure on the shear surface was less than 137.9 kPa. If the normal pressure exceeds this value, the triaxial test is more reliable as a laboratory test in producing the actual failure plane and thus determining the appropriate c and ϕ values. Bekker (1969) and Reece (1964) recommended the shear ring for measuring c and ϕ values in the field. This type of shear device would give the most accurate values of these two parameters. On the other hand, the sheargraph can be used to measure c_r', c_s', δ_s and δ_r values in the field (Payne 1956).

C. Prediction of soil moisture content

From the literature available, it would appear that considerable efforts have been expended on prediction of soil moisture content during the past decade. Most of the models which have been developed to achieve this goal use precipitation as the main variable along with many other meteorological data. The use of any of these models, however, requires a considerable amount of data and/or computer time. This makes the prediction of soil moisture content at any time of the growing season an expensive and complicated procedure.

The water content of a soil at a particular time depends on the balance between water inflow and outflow. In flat land, most of the inflow is from precipitation by rain, irrigation or snow. Outflow, on the other hand, is produced by one or more of the following methods: evaporation, subsurface drainage, surface drainage, or evapotranspiration.

In order to get good trafficability conditions in a short time after a rainstorm, water in excess of the field capacity must be removed as soon as possible by use of any possible drainage methods. When the soil moisture content reaches the field capacity the decreasing soil moisture will depend strongly on the climate and soil surface conditions until a dry layer of about 3-5 mm thick is formed on the soil surface (Penman 1941, 1948, 1949b). After this limit the moisture loss decreases rapidly and depends upon the soil properties more than on external conditions.

The most important soil, crop, and climatic factors affecting soil moisture losses (Bond and Willis 1969, 1970; Lemon 1956) are: (a) relative humidity, (b) dry bulb temperature, (c) wind speed, (d) the latitude of the area, (e) the length of the sunshine period (daylight), (f) the crop cover, (g) transpiration as influenced by leaf area, (h) the characteristics of the leaves as crop cover develops, and (i) soil water movement characteristics.

The models which could be used to predict the soil moisture content can be divided into five main groups (Lake 1968):

(a) models based on saturation deficit

(b) models based on temperature and sunshine

(c) models based on energy budget

(d) models based on mass transfer

(e) coefficients applied to evaporation data from pans.

The first four groups required a lot of meteorological data and some of the procedures require computer analysis. On the other hand, the last group of models (e) is easy to handle and gives a reasonable answer (Shimshi et al. 1975).

Water balance models have been studied by a number of researchers including Lewis and Burgy (1964), Ayers (1968), Lake (1968), Chieng (1975), Bahattacharya (1977) and Foroud and Broughton (1974). They applied their models for different purposes but the basic equation which was used in all the models was:

$$IRR + PRE = SR_o + \Delta SM + \Delta GW + GW_o + ET \quad \ldots (11)$$

where

IRR = irrigation

PRE = precipitation

SR_o = surface runoff

Δ SM = change in soil moisture content

Δ GW = change in ground water storage

GW_o = subsurface runoff

ET = evapotranspiration

Holmen and Robertson (1963, 1964) reported that in order to estimate the daily soil moisture content, records of rainfall and estimates of the potential evapotranspiration (PE) must be available. The procedure is based on the assumption that all moisture from the uppermost zone is evapotranspirated at the potential rate and the available moisture is withdrawn from any upper zone before extraction occurs from the adjacent lower zone. A general equation has been presented for estimating daily evapotranspiration (ET):

$$ET_i = \sum_{i=r}^{n} k_j \frac{SM_j(i-1)}{SM_j} Z_j \, PE_i \, e^{-w(PE_i - \overline{PE})} \quad \ldots (12)$$

where

ET_i = actual evapotranspiration for day i ending at morning of observation of day i + 1

j = zone number

k_j = coefficient accounting for soil and plant characteristics in the j zone

$SM_j(i-1)$ = available soil moisture in the j^{th} zone at the end of day i-1, that is, at the morning of observation of day i

SM_j = capacity for available soil moisture in the j^{th} zone

Z_j = adjustment factors for different types of soil drying curves

PE_i = potentional evapotranspiration

w = adjustment factor

$\overline{PE}$ = average of PE for month or season.

Young and Ligon (1972) reported that the evapotranspiration can be taken as a ratio from potentional evapotranspiration. This ratio is dependent on the precipitation occurring as follows:

$$ET = PE/2, \quad (PRE > 0.01) \qquad \ldots (13)$$

$$ET = PE, \quad (PRE < 0.01, \ 0 < Mu < 1.00) \qquad \ldots (14)$$

$$ET = (PE)(Mu/Mu_{max}); \quad (PRE < 0.01, \ Mu = 0) \qquad \ldots (15)$$

where the daily moisture changes (DM) were taken as:

$$DM = PRE - ET - SR \qquad \ldots (16)$$

where

PRE = precipitation for the day (mm)

SR = surface runoff (mm)

Mu = the quantity of moisture brought forward from the previous day in the lower soil layer (mm)

Mu_{max} = the maximum moisture holding capacity of this layer (mm)

Saxton et al. (1974) produced a mathematical model which was developed to compute daily actual ET and soil moisture profiles from inputs of daily potential ET, crop and soil moisture characteristics. Evaporation and plant transpiration were computed separately by several relationships; these values were then combined to provide daily actual ET estimates.

Potential evapotranspiration and evaporation are both affected by several important factors (Saxton et al. 1974): (1) net radiation, (2) vapour pressure, (3) height above the soil, (4) slope of the psychrometric saturation line over psychrometric constant,

(5) horizontal wind movement, (6) wind profile displacement height, (7) wind profile roughness. He also found that there is a correlation of daily potential ET with daily pan evaporation (in mm). This is represented by the equation:

$$PE = 0.01 + 0.83\ (Eva) \quad \ldots (17)$$

where

Eva = pan evaporation

Generally, the evaporation from the free water surface is considered as a reliable index of energy. Consequently, the relationship between evapotranspiration and pan evaporation has been investigated by Shimshi et al. (1975). They found an empirical relationship between the evapotranspiration and the daily evaporation from class A pan. This relationship is represented by the equation

$$ET = a + cSM + dEva \quad \ldots (18)$$

where

SM = soil water content

a, c, d = coefficients estimated by multiple regression from two years data for wheat land. These coefficients varied with soil depth.

Monteith (1965) reported that the potentional evapotranspiration of a dense short green crop was 60-80% of the pan evaporation. Cackett and Metelerkamp (1963) studied the effect of the ground percentage of cover by beans on the ratio of the evapotranspiration to open pan evaporation. This ratio increased with increasing percentage

of crop cover. Penman (1948) found that the evapotranspiration from grass in England was approximately 0.75 Eva. Baier and Robertson (1966) found that, for sugar beets, the value of the ET/EP ratio decreased only a small amount before harvest as the cold autumn weather began.

Chieng (1975) calculated the evapotranspiration value by means of the product of the ET/PE ratio and the daily potential evapotranspiration value. The daily potential evapotranspiration value has been calculated by Baier and Robertson (1966) and stored on magnetic tape at the McGill University Computing Centre (Chieng 1975). The ET/PE ratio was developed from data given by Van Hylckama (1956).

D. The role of the lugged tire in traction

There appears to be a lack of knowledge about the principal limiting factor which determines the design or the choice of the best lug shape on the wheel surface of lugged tires. This is required in order to obtain the maximum soil thrust from the same tire size. Figure 3 presents the shape of the lug on the tire surface.

Lugs are necessary for the production of traffic forces on off-road vehicle running gears on most soils (Reece 1964; Gill and VandenBerg 1967; Vasey and Naylor 1958). The factors of lug design affecting traction are shown in Figure 3, but the most important variables are the lug angle, lug length, and lug depth.

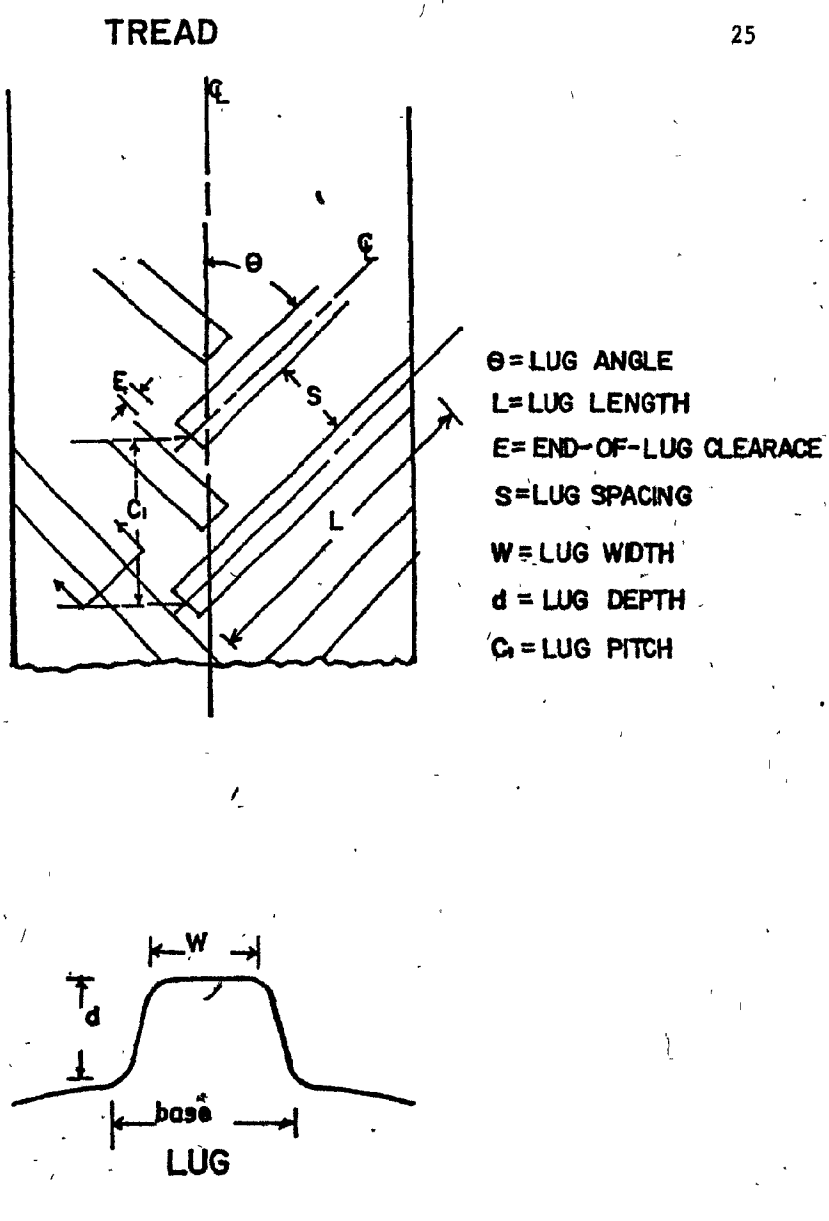

Figure 3. Tire lug and tread diagram (Yearbook of ASAE 1979).

Artemov and Serebryakov (1967) tested different pneumatic wheels in the Moscow area. On each wheel, nine auxiliary lugs were mounted on a special ring with the help of a locking arrangement. The lugged tires were better than the smooth tire in all the soil conditions tested (after rain, loose soil, normal moisture, and wet meadow). The average increase of the pull due to the lugs was 27%.

The beneficial effect of lugs of pneumatic tires on traction can be explained in two ways:

(i) The space between the lugs is filled by soil and soil failure may occur across the tips of the lugs. In this case the lugs help to ensure that failure occurs between soil-soil and not between rubber-soil (Reece 1964).

(ii) The soil fails in front of each individual lug (Bekker 1952).

It should be noted that in the first case, the effect of the lug is mainly due to increasing the wheel diameter by an amount equivalent to the lug height (Reece 1964; Bekker 1956). In the second case, the effect of the lug is attributed to each individual lug in a fashion similar to a moving blade in the soil.

Taylor (1973, 1974, 1976) has studied the effect of varying (a) the number of lugs on the wheel surface, (b) lug angle and (c) lug shape on the dynamic traction ratio. The results are presented in Figure 4 (a,b,c). Figure 4c shows that one tire might be slightly superior in sandy loam, clay loam, silty clay, and clay soil. In a related study, Yong et al. (1977) studied the effect of the track

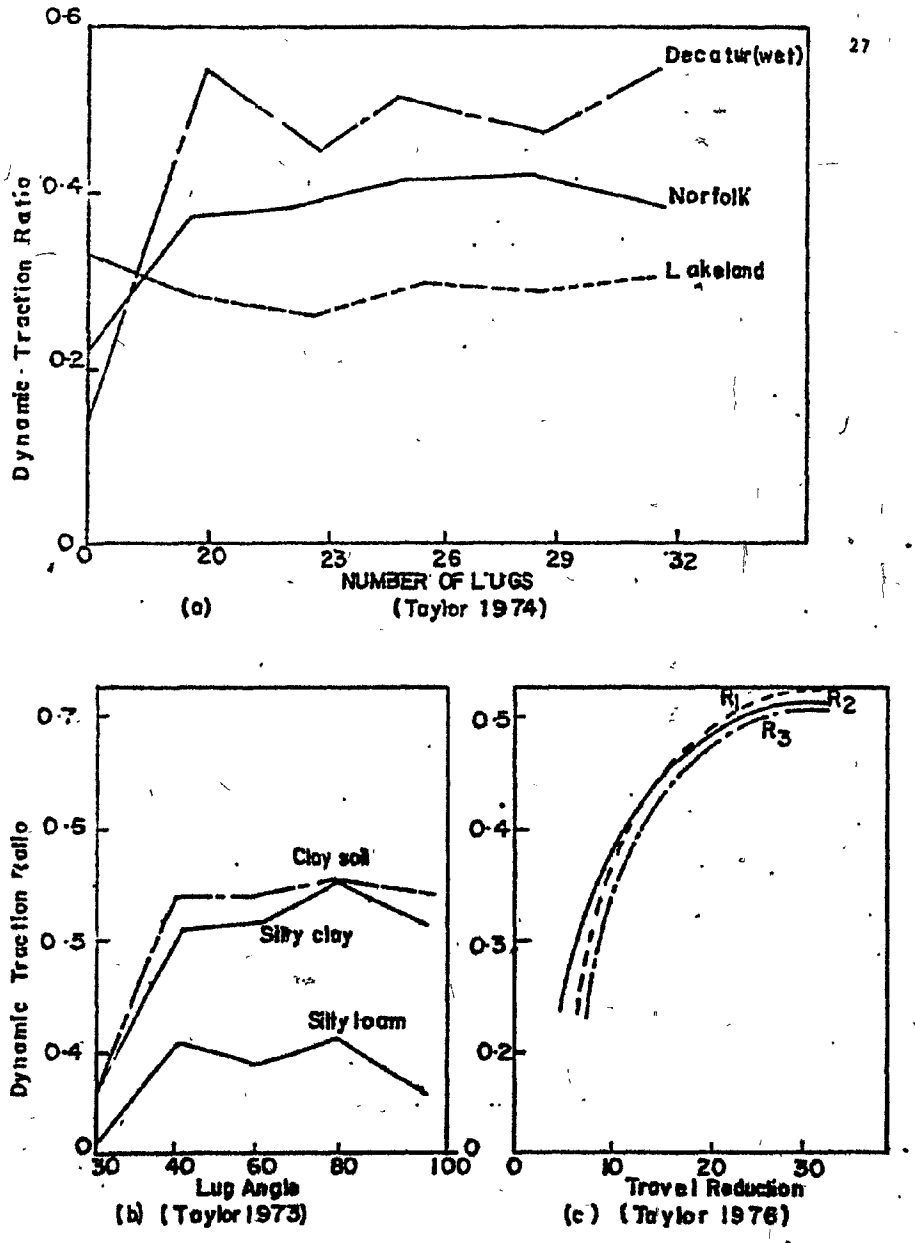

Figure 4. Effect of lug number and lug angle and different lug design on the dynamic traction ratio.

grouser shape on the traction force. The traction force varied significantly with the lug shape and soil conditions.

Bailey et al. (1976) tested the effect of the shape of the lug on a rigid wheel surface. Vertical and triangular grousers made of steel and rubber were used in this investigation. There was no difference in the traction coefficient between the triangular and vertical lugs for either material, steel or rubber.

Burt and Bailey (1974, from Bailey et al. 1976) developed an equation which was used in the above study to calculate the soil thrust (Bailey et al. 1976):

$$H = \sum_{i=1}^{n-1} \frac{T_{i+1} - T_i}{r} \cos \theta_k \qquad \ldots (19)$$

where

H = soil thrust

T_i = torque on i^{th} lug (the number of lugs in contact with the soil is i)

θ_k = angle between the wheel tangential and horizontal thrust force for the i^{th} lug

r = wheel radius

1. Lug angle

Very few investigations have been made on the effect of lug angle on the traction force. Taylor (1973) tested commercial tires of the same size (18.4-15/34, 6 ply) on silt loam, loamy sand, sandy

loam, silty clay, and clay loam soils with lug angles of 40°, 50°, 70°, and 80°. The experiment indicated that lug angles of 40°, 70° and 80° resulted in a higher traction force than lugs at a 50° angle. He concluded that the effect of lug angle on traction performance was very small and the lug angle effect may interact with other lug design variables. The conclusions from these investigations were only partially in agreement with those reported by Reed and Shields (1950). However, a generalized trend cannot be established since there was no separation of the variables.

Taylor (1976) made comparative tests on three different agricultural tires which had different lug shapes and geometry. The experiment showed that one tire might be slightly superior in some conditions, but the contribution of each lug in geometrical dimension had a small effect.

Pandey and Ojha (1973) also studied the effect of lug angle on traction force using three steel wheels and varying the lug angle between 15° and 30°. The test results showed that the wheels with a 20° lug angle produced a better trative performance on sandy clay loam soil.

2. Effect of soil type and consistency

Flotation is so closely related to traction that no conclusions regarding mobility can be made without considering fully both factors and their inter-relationship with the full range of soil types and conditions. Most of the research work done on the effect of lug

design on traction characteristics of commercial tires was on different soil types and moisture contents. There has been no established trend about the effect of soil types and consistency on the wheel traction force until now..

Randolph (1926, 1927) used sandy soil at different moisture contents to measure the effect of lug variables on traction. The difference in the moisture content did not change the relationships between the lug design factors (angle, depth, and width) and the traction force, but the magnitude was changed. Gross and Elliott (1946) found that the drawbar pull increased with increasing moisture content up to the plastic limit of the soil, and after that the drawbar pull decreased with increasing moisture content of loam soil. Dwyer et al. (1974) studied the traction performance of driving wheel tires of farm tractors and they concluded that soil shear strength and soil rubber friction were likely to provide the best indication of the coefficient of traction.

Artemov and Serbryakov (1967) found that auxiliary tire lugs (steel grousers mounted on the surface of a rubber tire) increased the traction by 50% on a muddy soil surface compared with a normal tire. This increase was 25% in normal moisture content conditions and 20% on wet meadow grass. VandenBerg and Reed (1962) used four different soil types (clay loam, silty loam, sandy loam, and sand) with six lugged tires in a field experiment in which the lugs increased the maximum coefficient of traction within the range of 0 to 70% travel reduction regardless of the soil type.

It is generally recognized that tire lugs increase the wheel traction force for a given wheel size and vertical load (Gee-Clough et al. 1977). This increase depends mainly upon the lug dimension (depth, angle, and length) for a given soil. It is expected that an investigation of these three parameters to define the optimal lug dimensions could define the tire design which can develop the maximum traction force due to the lugs.

E. Prediction of the soil thrust developed by lugs of tires

The theoretical development of the failure of soil in front of a lug has not been studied. On the other hand, several investigations have been carried out to explain the interaction between a vertical plate and soil (Reece 1964; Ikeda and Persson 1968; Yong and Sylvestre-Williams 1969). The analysis of soil failure in two dimensions can be explained by a number of theoretical methods. Theories of mechanics have been applied to the analysis of forces on the loaded interface using spiral failure surfaces (Terzaghi and Peck 1948; Hettiaratchi and Reece 1974) or by characteristic solutions (Yong and Chen 1970).

Halkinov (1931, from Bekker 1952) was the first to present a description of soil failure by lugs. The lug was considered as a soil cutter in the vertical position, which produced a straight-line shear sloped to the horizontal at an angle of $45° - \phi/2$. Figure 5b shows this case with lugs spaced such that a fully developed soil failure is

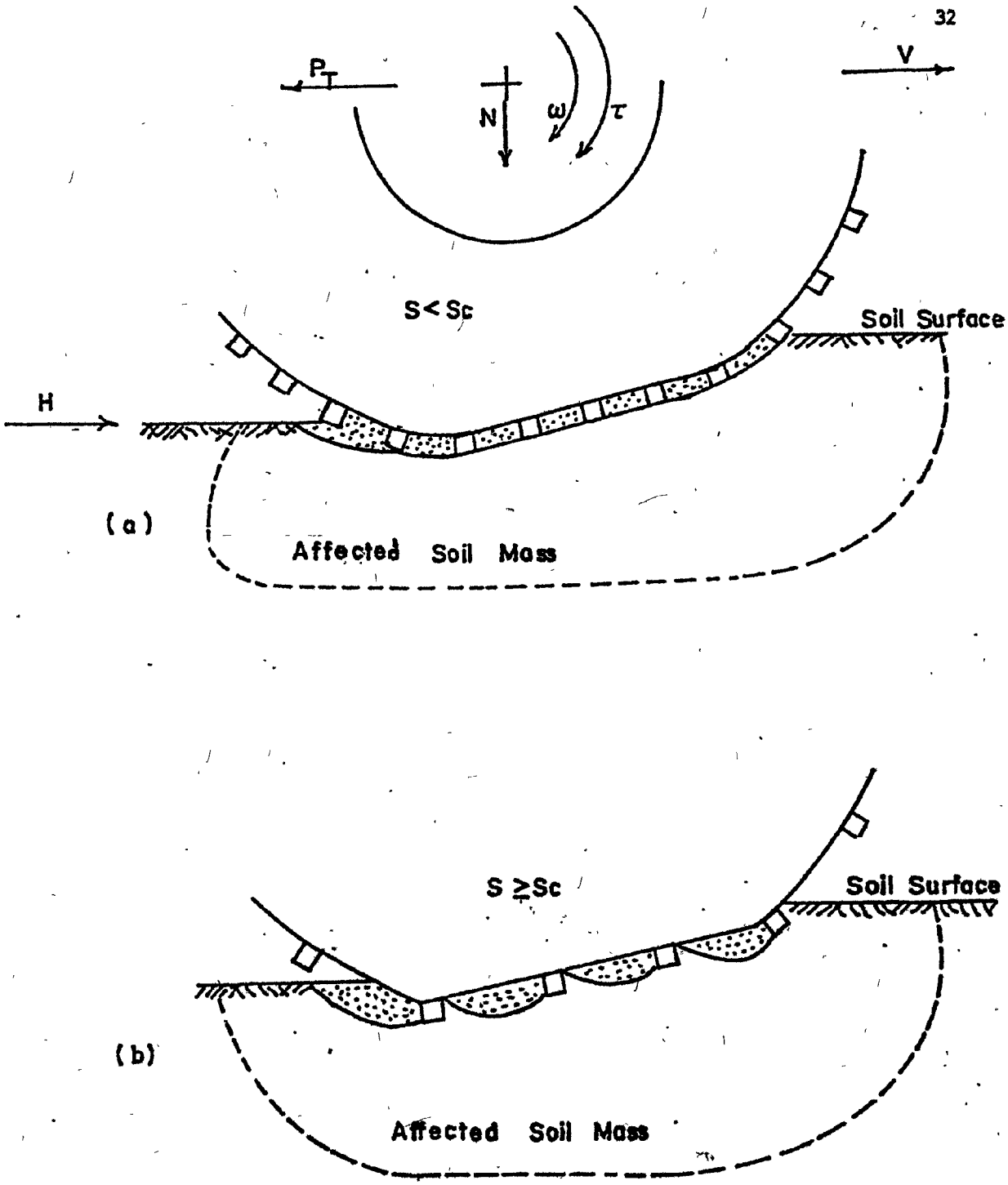

Figure 5. Model of soil failures due to the lug.
(a) Lug space "S" less than the critical lug space "Sc".
(b) Lug space greater than the critical lug space.

permitted between the lugs. Bekker (1956) used the assumptions of the soil failure as shown in Figure 5b to predict the maximum soil thrust H under normal load N of vertical lugs on a rigid wheel, and presented the following equation.

$$H = WdLc\left(1 + \frac{2d}{Wd}\right) + N \tan\phi\left[1 + 0.64\left(\frac{d}{Wd}\right) \cot^{-1}\left(\frac{d}{Wd}\right)\right] \quad \ldots (20)$$

where

Wd = width of the wheel

c = soil cohesion

d = lug depth

ϕ = soil-soil friction angle

N = normal load

L = length of the contact area

It should be noted that the lug angle, soil-rubber adhesion and friction angle were not taken into consideration in this equation. The traction force produced by the lugged tire could be represented as the soil resistance against plate movement having the shape of the soil-wheel contact area. Hettiaratchi and Reece (1974) described a failure in front of a wide plate (see Figure 6).

The Hettiaratchi and Reece (1967) equations used to calculate the traction P are:

$$P = [\gamma d^2 N_\gamma + cdN_c + qdN_q] L \quad \ldots (21)$$

where

γ = soil density (kN/m^3)

d = lug depth (m)

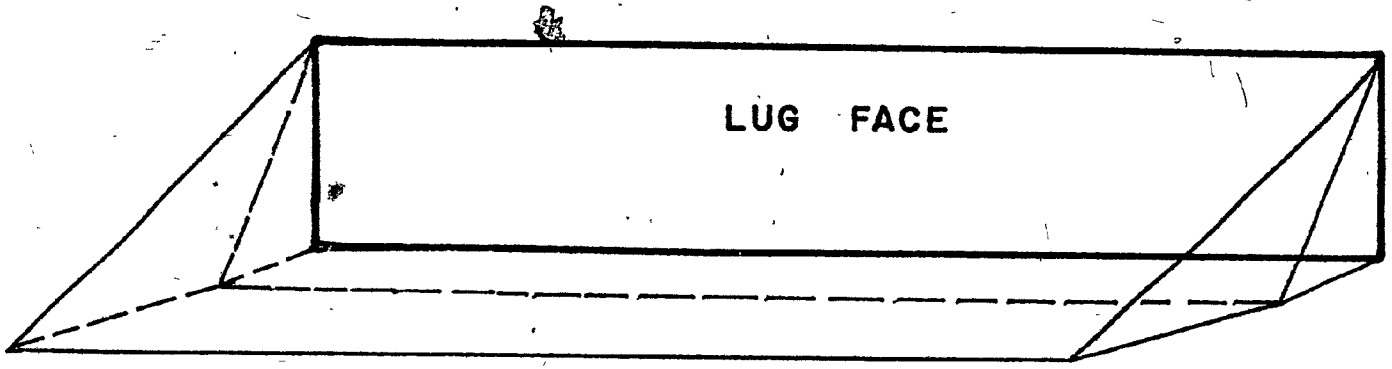

Figure 6. Soil failure ahead of flat wide lug, in 3 dimensions (Hettiaratchi and Reece 1974).

The $N\gamma$, Nc, Nq factors can be estimated from figures presented by Hettiaratchi and Reece (1967) at $\delta_r = o$ and $\delta_r = \phi$. Equation (22) could be used to calculate the N factors at the exact value of δ_r.

$$N \text{ (factors at } \delta) = \left(\frac{N \text{ at } \delta = o}{N \text{ at } \delta = \phi} \right)^{\lambda w} \quad \ldots (22)$$

where

$$\lambda = \delta/\phi$$

$$w = e^{xf}$$

$$x = 0.4(1-\lambda)\ \phi \cot \phi \ (\phi \text{ in radians})$$

and f can be estimated from Table 2.

TABLE 2. Equations to calculate f factors

N factors	f factors
N_γ	$1 - 0.5 \text{ sech } [2\ (\phi - 0.26)]e^{\tan \phi}$
N_c	coth (1.745)
N_q	tanh (90 - 1/2 ϕ)

Equation (22) could be used to calculate the soil thrust of a lug with 90° angle but for lugs with an angle less than 90° this equation is not sufficient. For lugs with an angle less than 90° the soil movement on the lug face will take another direction rather than the vertical direction which has been considered by Hettiaratchi and Reece (1967).

However, the necessary modification of this theory with respect to the direction of soil movement on the lug face with any lug angle would make the predicted soil thrust more accurate. Also, adequate equations to predict the soil thrust due to the lugs for a lugged tire are required to provide more understanding of the interaction between soil and lugged tire with any tread design.

CHAPTER III

EMPIRICAL AND THEORETICAL DEVELOPMENT

A. Modelling of soil mechanical properties to soil moisture content

On the basis of the information from the literature and the sufficient number of data available in this study from the field tests for the parameters c, ϕ, c_s', c_r', δ_s, δ_r, kc, kϕ and n at different soil moisture contents, the models stated in the objectives were developed for a sandy loam and clay soil. Among the many equations which have been used for curve fitting of the measured data, the sine function gives the best presentation for the relationships between the soil moisture content and the soil mechanical properties. These relationships can be presented by the following equation:

$$Y = C_2\left(\sin\left(\frac{\pi}{2}\frac{MC}{PL}\right)\right) + C_1 \qquad \ldots (23)$$

where

Y can take the values of the properties c, ϕ, c_s', c_r', δ_s and δ_r

MC = soil moisture content (% by weight)

PL = soil plastic limit (% by weight)

C_2 = constant depending upon the soil depth

C_1 = constant depending upon the soil type

Also, the properties kc, $k\phi$, and n might be expected to have similar relationships with the soil moisture contents. The models which resulted in good agreement with the measured data are discussed in Chapter V. It should be noticed that these models are applicable only to cohesive soils.

B. Prediction of soil moisture content

In flat land with a subsurface and surface drainage system, the soil moisture content does not increase more than the field capacity. Any excess water due to rainfall or irrigation is considered as a surplus and could be moved from the soil by subsurface drainage in a period of approximately 48 hours. This fact can be considered as valid within the rooting depth of the growing plant. The water balance model which was assumed to be applicable to the field situation is as follows:

$$SMC_i = SMC_{i-1} + PRE - ET \quad \ldots (24)$$

where

SMC_i = soil moisture content at i^{th} day

SMC_{i-1} = soil moisture content at day before i^{th} day

PRE = precipitation

ET = actual evapotranspiration at i^{th} day

Note that the SMC_i and SMC_{i-1} are volumetric soil water contents in mm. However, from equation (24) the soil moisture content for any particular day can be calculated if the soil moisture content, evapotranspiration and rainfall of the previous day are known. The

components of equation (24) are all easy to obtain with the exception of evapotranspiration, which is difficult to measure or to calculate. Chieng et al. (1978) successfully used the Van Hylckama curvilinear relationship of the ratio ET/PE with the available water remaining in the soil in the range between the soil field capacity and permanent wilting point in southern Quebec.

For the clay and sandy loam soils used in this study the available water in the root zone (corn crop) is 61 mm and 45 mm, respectively (Taylor et al. 1978). Figure 7 presents the relationship between the ratio ET/PE and available water remaining in the soil for the soils used in this investigation. In order to estimate the evapotranspiration from this graph the PE must be known. The value of PE is not easy to estimate since its computation requires a lot of data (day length, latitude, geographic and climatic region, temperature, maximum and minimum temperature, wind speed, cloud cover, relative humidity, and net radiation); these parameters are not easily obtained by the machine designer and the farm manager. Consequently, a simple method estimating the PE value would be very helpful.

From the available literature (Young and Ligon 1972; Saxton et al. 1974; Shimshi et al. 1975) it could be stated that there is a high correlation between values of the potential evapotranspiration (PE) and the values of evaporation from an open water surface (Eva). In addition, the factors which affect PE are similar to those which affect Eva values. Saxton et al. (1974) reported that the $\frac{PE}{Eva}$ ratios can be

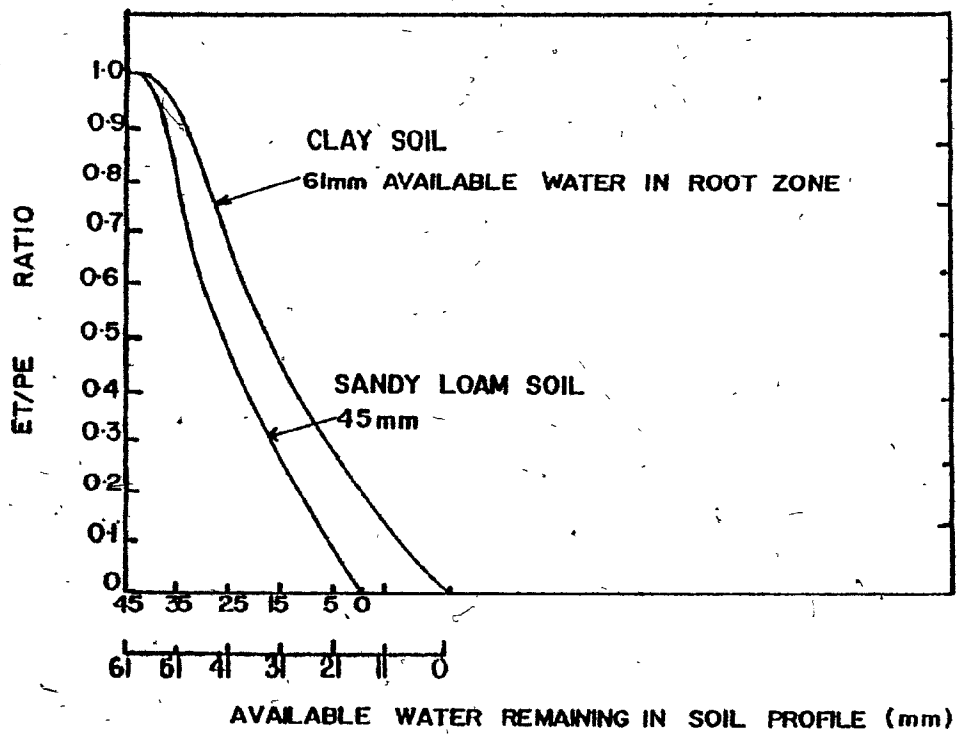

Figure 7. The relations of ET/PE ratio vs the remaining available water in the soil profile for sandy loam and clay soils.

presented by a constant value for a specific crop and region. Therefore, if the ratio of $\frac{PE}{Eva}$ values is known for a particular area, by measuring the Eva from evaporation pan class A, the PE can be estimated accurately enough without any complex calculation or use of computer time. In this study the data reported by Lake (1968) will be used to estimate the PE in the region under investigation.

Lake (1968) calculated the PE during the growing season for irrigated, non-irrigated, corn, wheat, oats and barley. The class A evaporation pan reading was reported simultaneously in the findings during the calculation of PE. These data were estimated and measured for the same region that was used in the present study. Consequently, the changes in the $\frac{PE}{Eva}$ ratios at different times of the growing season for a different soil surface condition can be obtained from the graphs shown in Figure 8. Thus, the soil moisture content can be estimated by using Figures 7 and 8 and equation (24) with the pan evaporation and rain gage reading at a specific time of the farming season. The testing of this model will be presented in Chapter V.

C. Calculation of the soil thrust developed by a lug of lugged tires

The theory put forward by Hettiaratchi and Reece (1974) to calculate the soil resistance to the movement of a wide plate ($\theta \approx 90°$) will be used in this study along with some modifications in order to make the theory applicable to a lug with an angle $\theta \leq 90°$. In addition, equations to calculate the total soil thrust produced by a lugged tire

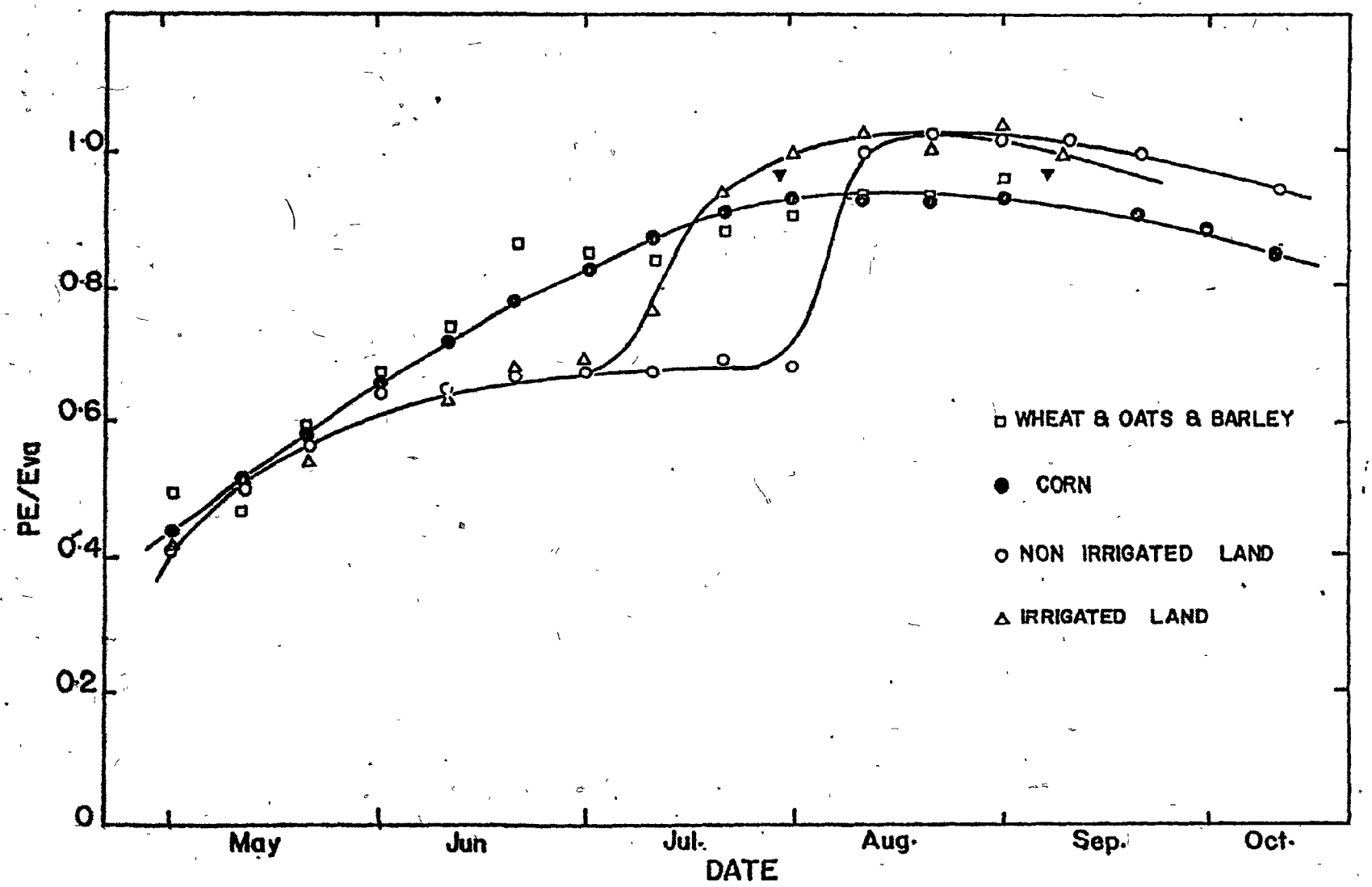

Figure 8. The changes in the PE/Eva ratio during the farming season in southern Quebec.

will be developed. The soil failure due to the lugs on the wheel is very similar to the failure which occurs in front of a wide moving plate. Figure 9 shows the shape of a cross-section area of soil failure as presented by Hettiaratchi and Reece (1974).

Forces produced by the lug on a tire (H) must be classified according to the lug spacing. Two cases can be defined as follows:

(a) The lug space S is less than the critical lug space Sc. In this case the soil failure between two lugs is not fully developed (Figure 5a). The critical lug space can be calculated using the equation developed from Figure 9 as follows:

$$Sc = \left[\frac{\tan \phi + \cot B}{1 + \tan \theta_1 \tan \phi} \right] d \qquad \ldots (25)$$

where

$$B = 45 - \phi/2$$

$$\theta_1 = 45 - [\phi + \delta_1 + \sin^{-1} [\frac{\sin \delta_r}{\sin \phi}]]/2 \text{ (Hettiaratchi and Reece 1967)} \ldots (26)$$

d = lug depth (cm) from the soil surface.

In this case the traction force (H_p) produced by a lugged tire due to the lugs in contact with the soil can be calculated by summation of all the forces acting on the lugs. This results in the following equation:

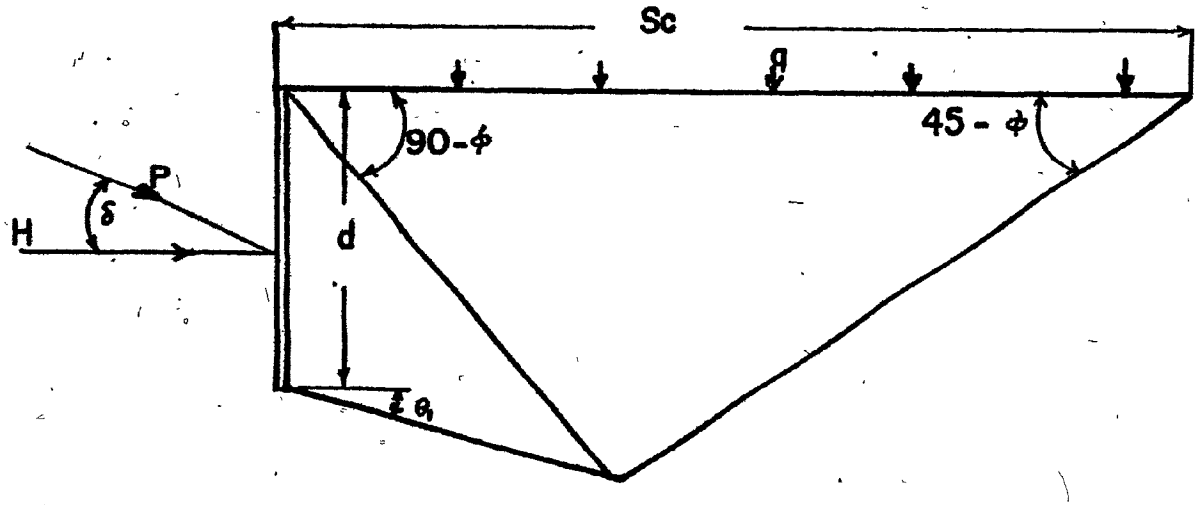

Figure 9 . The shape of the soil failure in front of wide lug in the vertical plane (Hettiaratchi and Reece 1967).

$$H_p = \left[\sum_{i=1}^{i=q} \sum_{j=1}^{j=m} (WL_{ij}\ c_i' + Q \tan \delta) \right] + 2dS$$

$$\left[c + (q + \gamma d) \frac{1 - \sin \phi}{1 + \sin \phi} \tan \phi \right] + \left[\sum_{i=1}^{i=q-1} \sum_{j=1}^{j=m-1} \right.$$

$$\left. S\, L_{ij} (c + Q \tan \phi) \right] \qquad \ldots (27)$$

where

γ = soil bulk density

W = lug width

Q = $q + \gamma d$

S = lug space

L_{ij} = lug length in row number i and line number j (see Figure 10).

q = normal pressure on the soil

It should be noted that equation (27) contains three terms. The first term is the force due to the friction between the lug face (AB in Figure 10) and the soil, the second term is the force due to the shear of the soil on both sides of the wheel, and the third term is the force due to shearing the soil trapped between two lugs.

(b) The lug space S is greater than the critical space. In this case the soil failure between two lugs is fully developed, as shown in Figure 5b.

For this case, the theory developed by Hettiaratchi and Reece (1967) could be used in order to calculate the soil thrust due to one

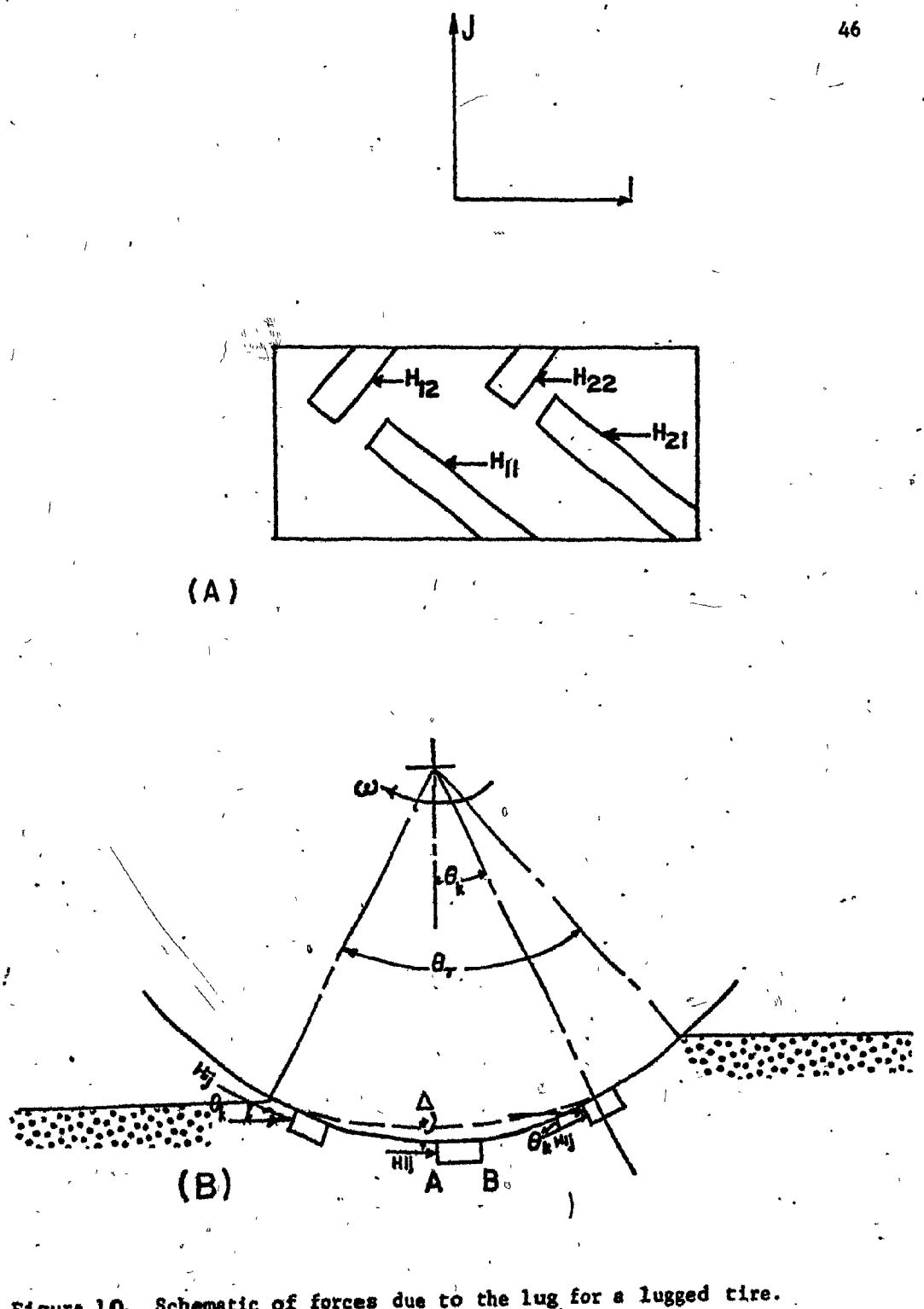

Figure 10. Schematic of forces due to the lug for a lugged tire.
A- Plan view
B- Vertical view.

lug P as shown in Figure 11. This figure shows that the total soil resistance P predicted by Hettiaratchi and Reece (1967) (see equations 21 and 22) lying on a cone has an angle δ_r and base critical with radius equal to $P_p \tan \delta_r$ where P_p can be calculated according to equation (28):

$$P_p = P \cos \delta_r \quad \ldots (28)$$

From Figure 11, the force P_p is perpendicular to the lug face and the component $P_p \tan \delta_r$ is in the direction of the soil movement on the lug face which has an angle ε with the horizontal. In order to define the angle ε, experiments were conducted in the laboratory to measure this angle using dry sand and clay at different moisture contents. These experiments were carried out by pushing a plate in the soil manually for a short distance (5-10 cm) with different angles θ (Figure 12a). The angle ε was obtained at each θ value by calculating the horizontal and the vertical displacements of a point on the chain located in front and in contact with the moving plate (Figure 12b). Figure 13 shows the relationships between the two angles θ and ε for the two soil types, sand and clay under different levels of moisture content. These experiments show that the angle ε was approximately equal to the lug angle θ in all the tests.

However, the component of the force $P_p \tan \delta$ acting on the direction of travel in the horizontal plane, the soil thrust, can be calculated from the geometry of Figure 11 according to the equation:

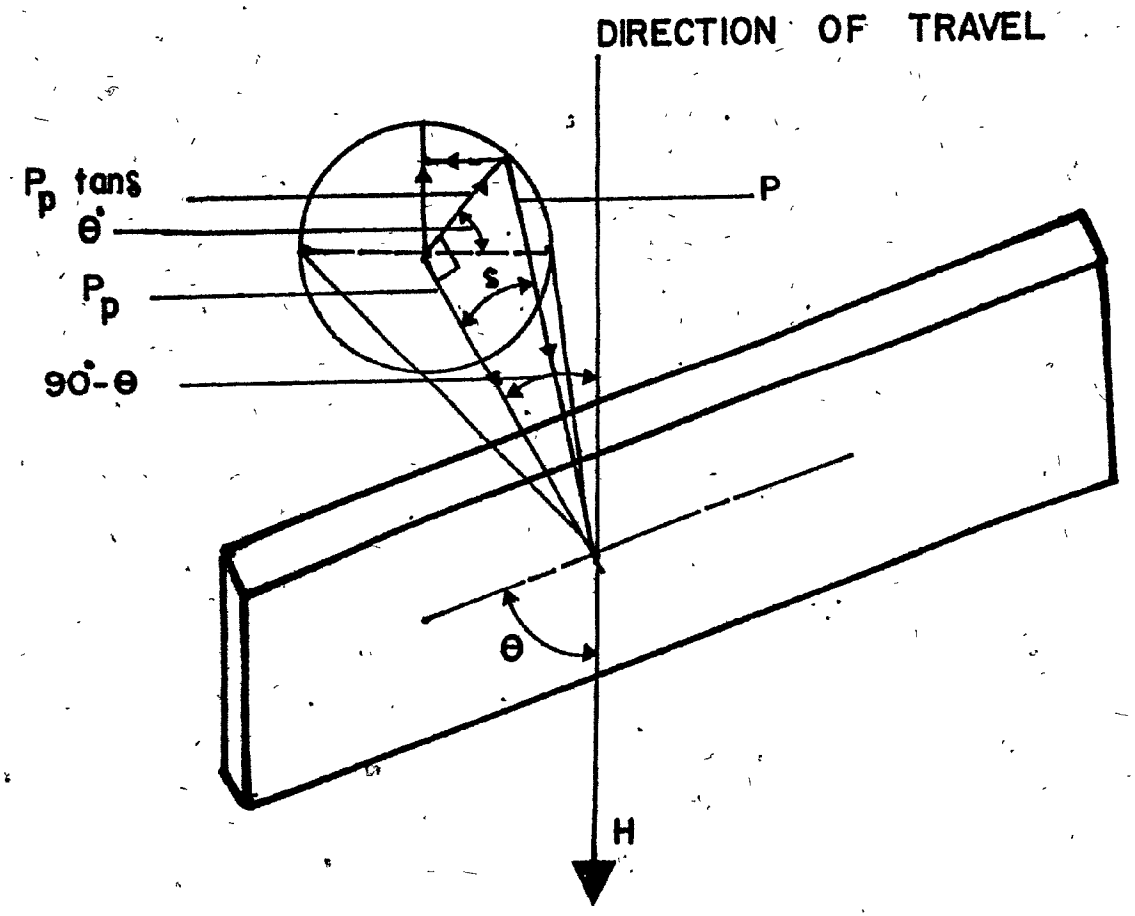

Figure 11 Diagram of forces acting on a lug.

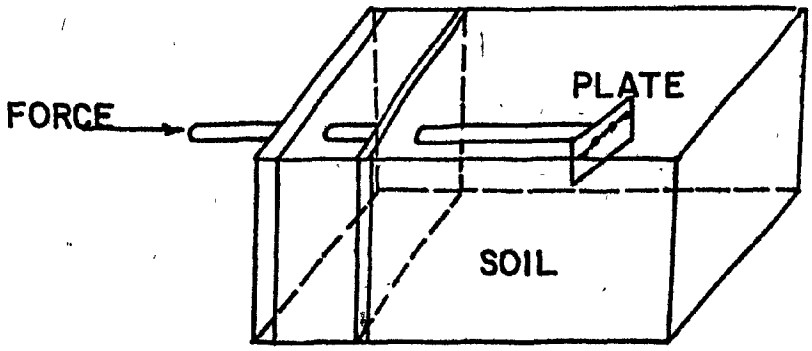

Figure 12-a. The soil bin which was used to push the plate with an angle θ to measure the soil movement angle ε.

y = vertical displacement
x = horizontal displacement

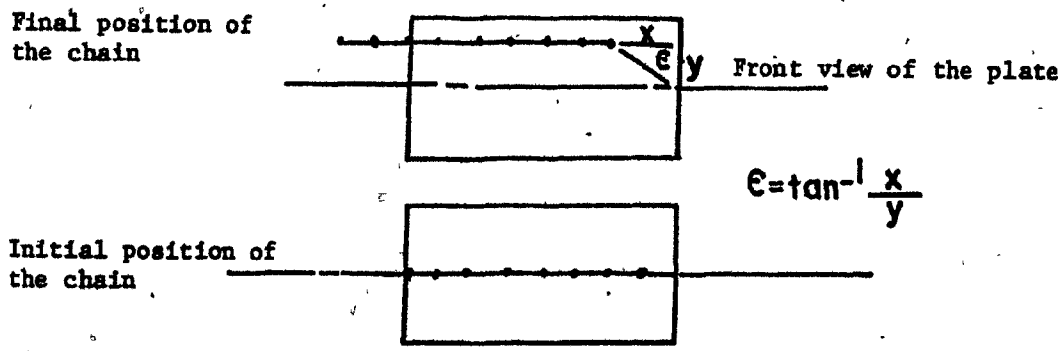

Figure 12-b. The measurement of the soil movement angle on the plate face

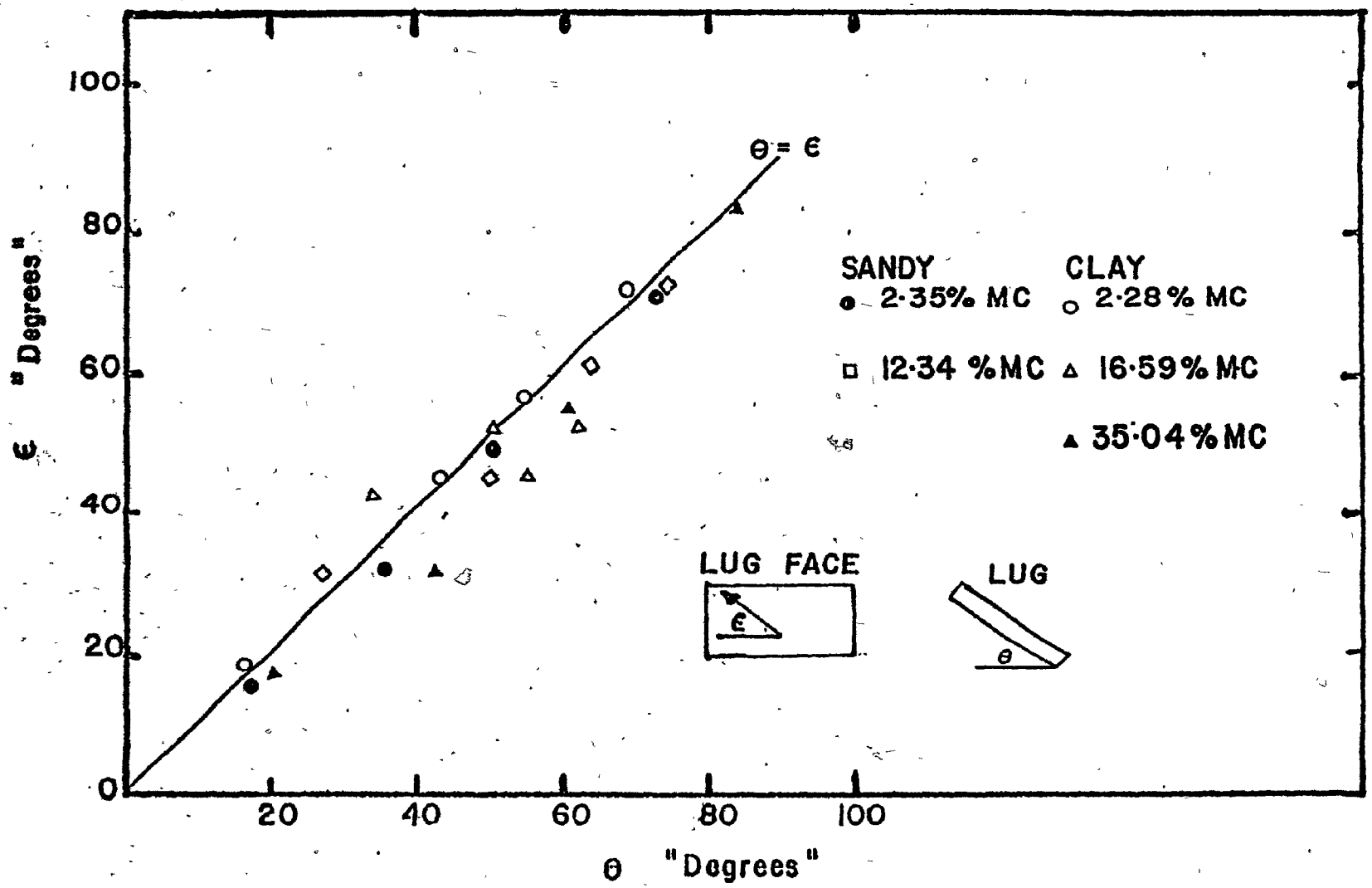

Figure 13. The relationship between the lug angle "θ" and the soil movement direction

$$P_{n1} = P_p \tan \delta \cos^2 \theta \quad \ldots (29)$$

Also, there is a force component which adds to the soil thrust due to the soil adhesion to the lug face as presented in equation (30).

$$P_{n2} = c'_r L d \cos^2 \theta \quad \ldots (30)$$

where

L = lug length

d = lug depth

θ = lug angle

However, the total soil thrust in the direction of travel due to a single lug can be obtained from:

$$H = P_p \sin \theta + P_p \tan \delta \cos^2 \theta + c'_r L d \cos^2 \theta \quad \ldots (31)$$

The total wheel traction force due to the lugs (H_p) can be obtained by summing the forces produced by each individual lug along and across the wheel contact areas as presented in Figure 10 from:

$$H_p = \sum_{i=1}^{i=g} \sum_{j=1}^{j=m} Hij \cos \theta_k \quad \ldots (32)$$

where

g = the number of lugs across the contact area

m = the number of lugs along the contact area

θ_k = the angle between the central line axis of a lug and the vertical line passing through the wheel centre

Hij = traction force due to one lug perpendicular on the lug vertical face.

From the lug geometry on the wheel surface shown in Figure 3, the lug length on the wheel surface can be calculated as a function of number of lugs g, end-of-lug clearance E, wheel width Wd, and lug angle according to:

$$L = \frac{Wd + E\,(g-1)\,\sin\theta}{g\,\sin\theta} \qquad \ldots (33)$$

This value of lug length L can be used in equation (31). Consequently the traction force due to an individual lug also becomes a function of the end-of-lug clearance E in addition to the other factors stated previously.

I: Soil-wheel contact area and lug rake angle

Bekker (1960) stated that the pneumatic tire on agricultural soil can behave as a rigid tire if the inflation pressure is higher than a critical value. In this case the lug rake angle (the angle between the horizontal and the perpendicular to the vertical lug face, θk) depends upon the lug position on the wheel surface. This is true except when there is a bending deflection in the lug itself caused by the soil thrust and the applied normal load. Moreover, the lug deflection is related to the characteristics of the rubber. This lug deflection decreases the lug rake angle. However, if the inflation pressure is less than the critical pressure, the tire will behave as an elastic body, and in this case, calculation of the contact area will depend upon the soil properties as well as the tire construction

(tire size, inflation pressure, tire material, tread shape, normal load, geometry of the terrain surface, and the vehicle vibration). All these factors, in addition to the soil thrust, affect the lug rake angle. Therefore, calculating the area and lug rake angle is not possible by rigorous methods, especially since some of these factors have an unpredictable behavior (Bekker 1956). Thus, systematic investigations which would elucidate this problem have been very limited. Only experimental studies in a limited number of test conditions have been made so far.

In order to estimate tire contact area, the tire manufacturers have developed an approximate method for calculating the contact area at the recommended normal load and inflation pressure on medium-soft agricultural soil, not including the very hard or severely muddy conditions, as follows (Tire Guides Inc. 1976):

$$a = (D/2)wd \qquad \ldots (34)$$

where

D = wheel outside diameter

wd = wheel width

This equation can help to estimate the number of lugs in contact with the soil (g and m).

Bekker (1960) reported that most of the ground contact area could be considered as a flat horizontal surface. The soil-wheel contact area of an unloaded farm tractor is shown in Figure 14. This photograph, taken during a field test, shows that most of the lugs in

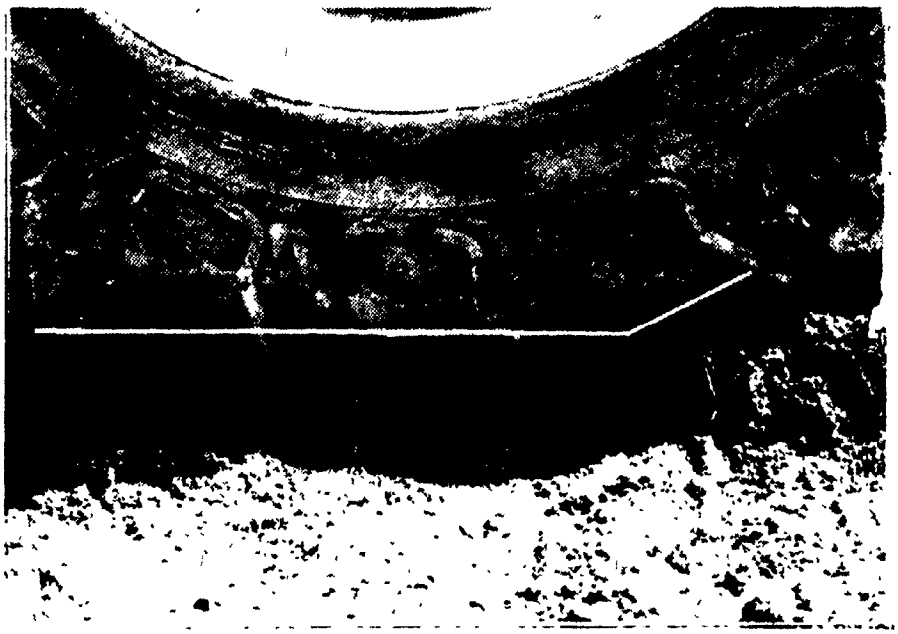

Figure14 . Shape of soil-wheel contact area of an unloaded farm tractor.

contact with the soil are nearly vertical, and they become even more vertical with increasing pull or normal load on the wheel. In the case of lugs with a rake angle, the soil thrust produced by the lugs should be different from vertical lugs.

2. Flow chart for prediction of the best lug angle and soil thrust of lugged tire during the farming season

Bekker (1960) reported that the soil thrust of a tire is due to the shearing strength between the tire carcass and the lug action. For a lugged tire with a lug space equal to or higher than the critical space (S > Sc), the soil thrust could be estimated as a summation of two forces. These forces are:

(i) Soil thrust due to the lug (equation 31).

(ii) Soil thrust (Hc) due to the shear strength between the tire carcass and the soil contact area:

$$Hc = Wd \left(Sc - \sum_{i=1}^{i=g} S\right) (c' + q \tan \delta) \quad \ldots (35)$$

Processes for predicting soil thrust forces of lugged tires are presented in the flow chart shown in Figure 15.

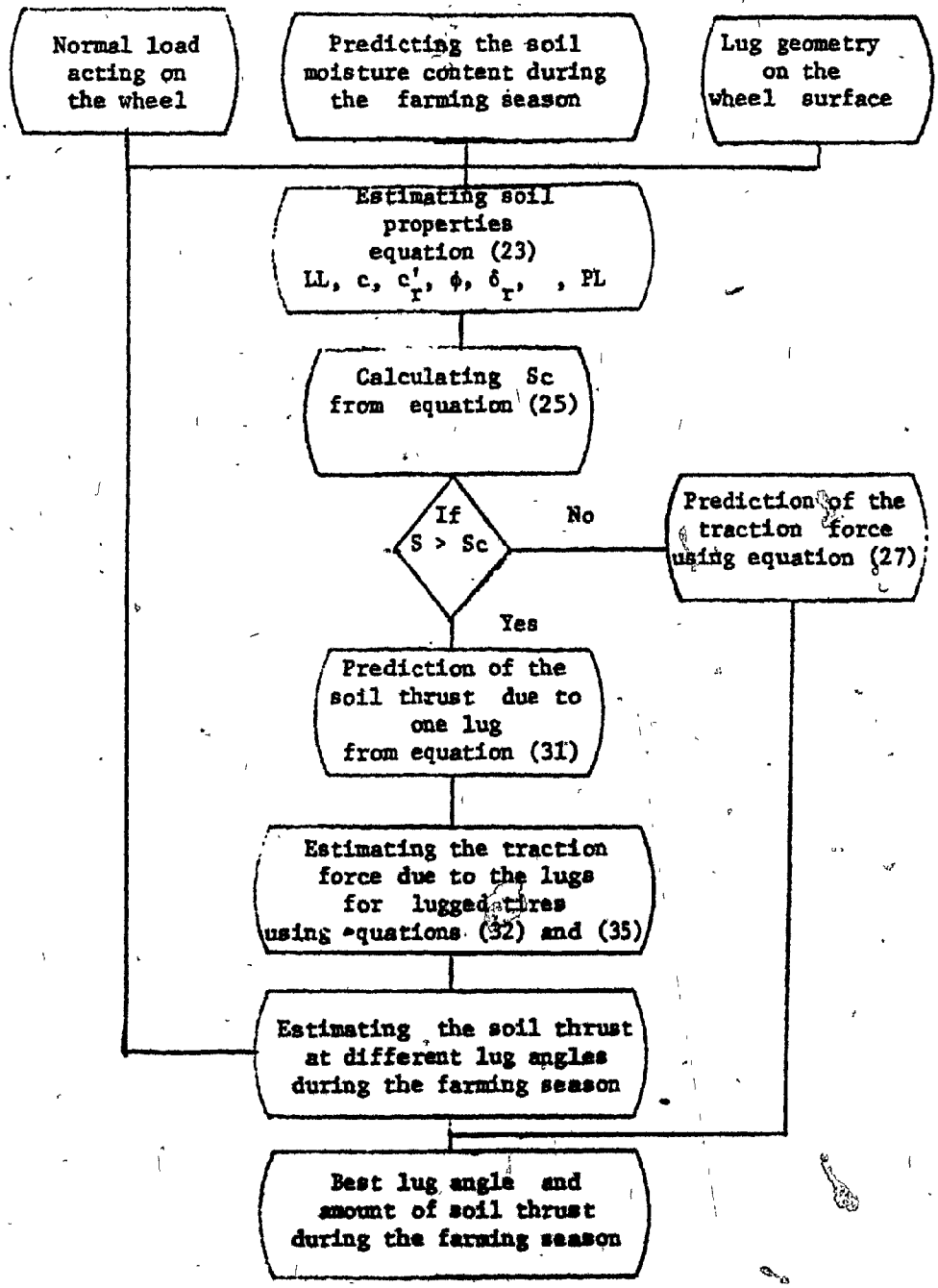

Figure 15. Flow chart for estimating the best lug angles and the amount of soil thrust during the farming season.

CHAPTER IV
MATERIALS AND EXPERIMENTAL METHODS

A. Soil properties

1. Grain size distribution

Mechanical analysis was carried out (in duplicate) on samples of each soil type by the hydrometer method as outlined by Lambe and Whitman (1969). Table 3 shows the mean value of the analyses, and Figures A1 and A2 show the grain size distribution curves of samples from these soils (Appendix A). In these tests, the mean values for each of the soil components had a coefficient of variability in the range of 7 to 11%. According to these grain size distributions the soils can be classified as sandy loam and clay. The U.S.D.A. texture triangle system was used for the soils classifications (Terzaghi and Peck 1948).

TABLE 3. Mechanical analysis of the soils

Soil type	Sand % > 0.05 mm	Silt % 0.05-0.002 mm	Clay % < 0.002 mm
Sandy loam	70.0	22.0	8.0
Clay	16.8	17.2	66.0

2. Soil consistency

The Atterberg limits were obtained using the method described by Lambe and Whitman (1969). The results are shown in Table 4.

TABLE 4. The Atterberg limits of the two soil types

Soil type	% of moisture content (dry weight basis)		
	Liquid limit	Plastic limit	Plasticity index
Sandy loam	32.5	23.6	8.8
Clay	42.0	32.1	9.9

B. Rubber properties

Rubber blocks were used to make the individual lug models for the various tests. The rubber material (black neoprene 60-70 share) is similar to the material used in the manufacture of tires.

The maximum compression and tensile stresses of rubber samples were measured using an Instron testing machine (American Society for Testing Materials, 1968). The results are summarized below:

Modulus of elasticity:

Compression (see Figure A-3, Appendix A) . . . . 10,000 kPa

Tension (see Figure A-4, Appendix A) . . . . . 9,500 kPa

Maximum strength

Compression . . . . . 4,900 kPa

Tension . . . . . 4,600 kPa

The specific unit weight of this material was 1440 kg/m^3.

C. Measurements of soil mechanical properties in the field

1. Measuring soil cohesion (c) and friction angle (ϕ)

A manual shear ring apparatus was designed and built for this purpose; a photograph and a diagram of the apparatus are shown in Figures 16 and 17. The apparatus was made from aluminium to make it lighter and the stand was made from steel. The shear ring apparatus was made from hard acrylic plastic to which small steel plates were fixed at 12-mm spacings. The shear ring carried a 6-mm grouser and had dimensions of 150 mm and 112 mm outside and inside diameter, respectively (Figure 18). The shear ring dimensions used were recommended by Reece (1964) on the basis of field experience.

From Figure 16 it will be noted that the shear ring is fixed with a vertical rod at point D. In addition, the disc (e) which carries the normal load can be freely rotated on the top of the disc (e_1). A single ball bearing was used between the disc e and e_1. In order to measure the torque required to rotate the shear ring, a proving ring was connected between points A and B. By rotating the torque arm from position C and taking a reading of the dial gauge connected to the proving ring, the torque applied can be obtained by using the calibration curve of the proving ring (Figure A5, Appendix A). The torque measurements were taken under different normal loads. The linear relationship between the torque and normal pressure is plotted and then the values of λ and T_o can be obtained graphically (Figure 19).

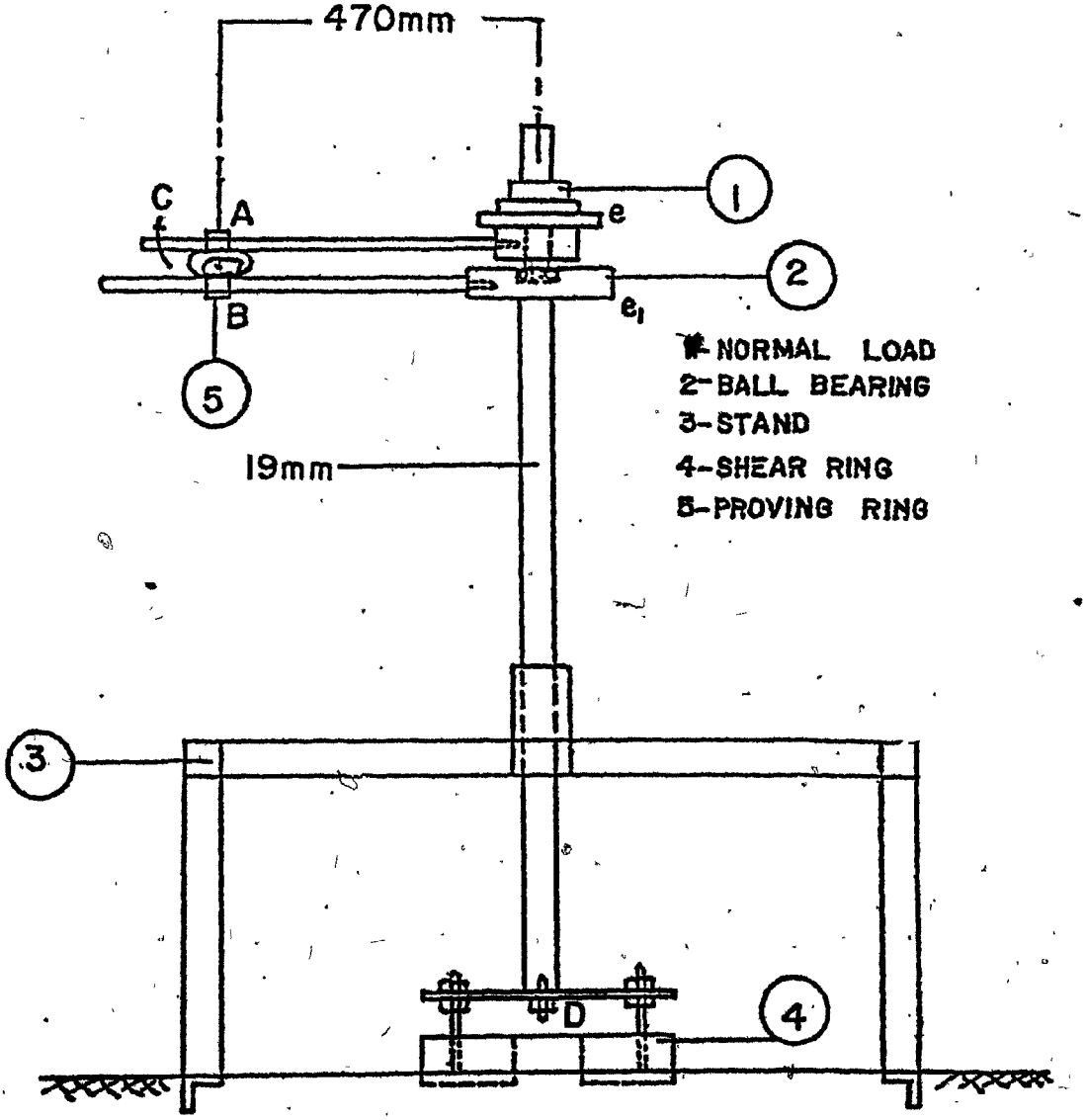

Figure 16. Diagram of shear ring apparatus.

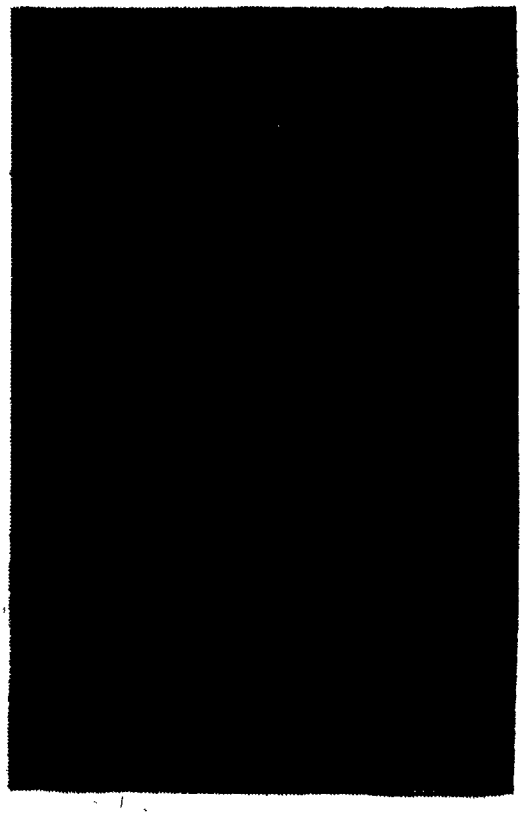

Figure 17. Shear ring apparatus.

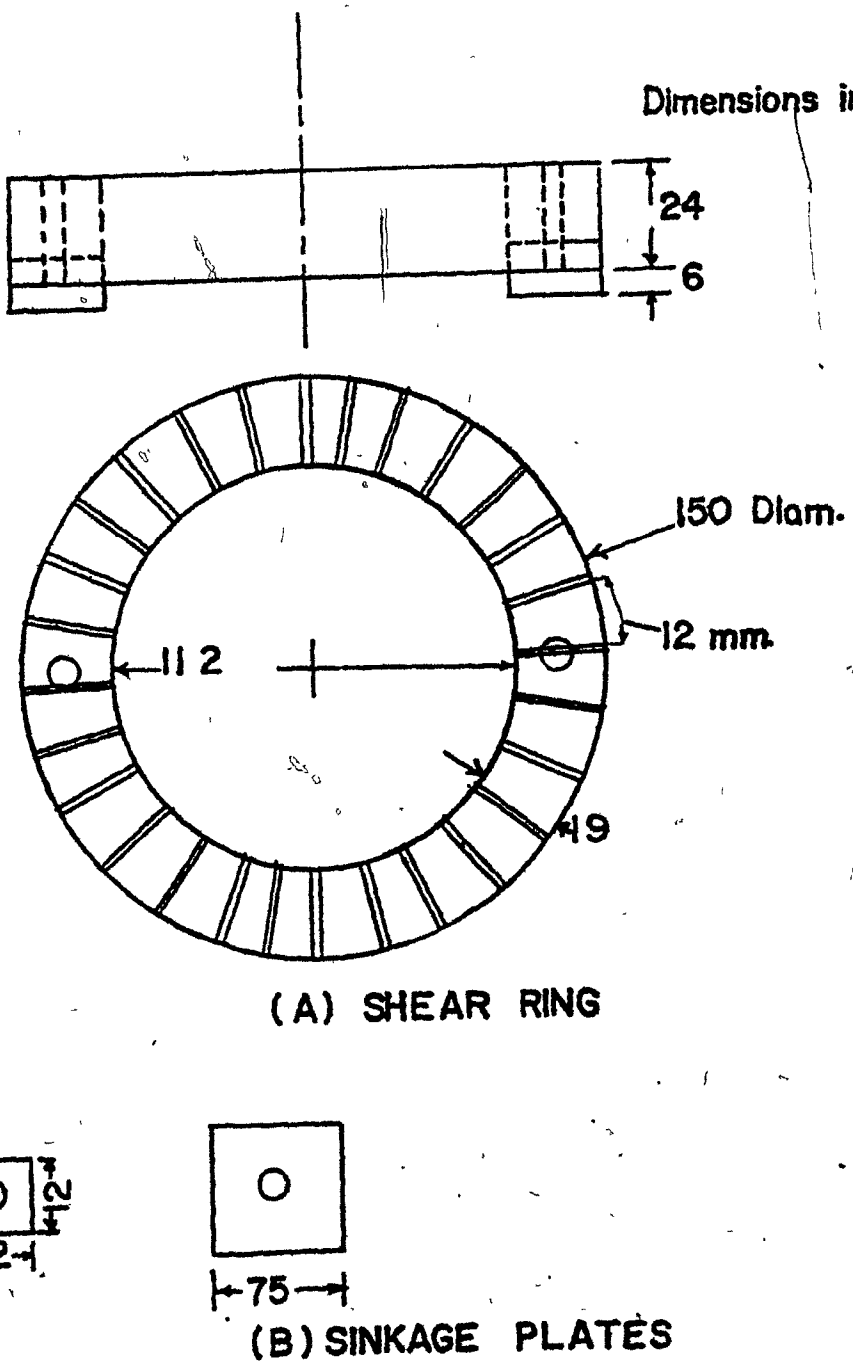

Figure 18. Diagram of the shear ring and the sinkage plates.

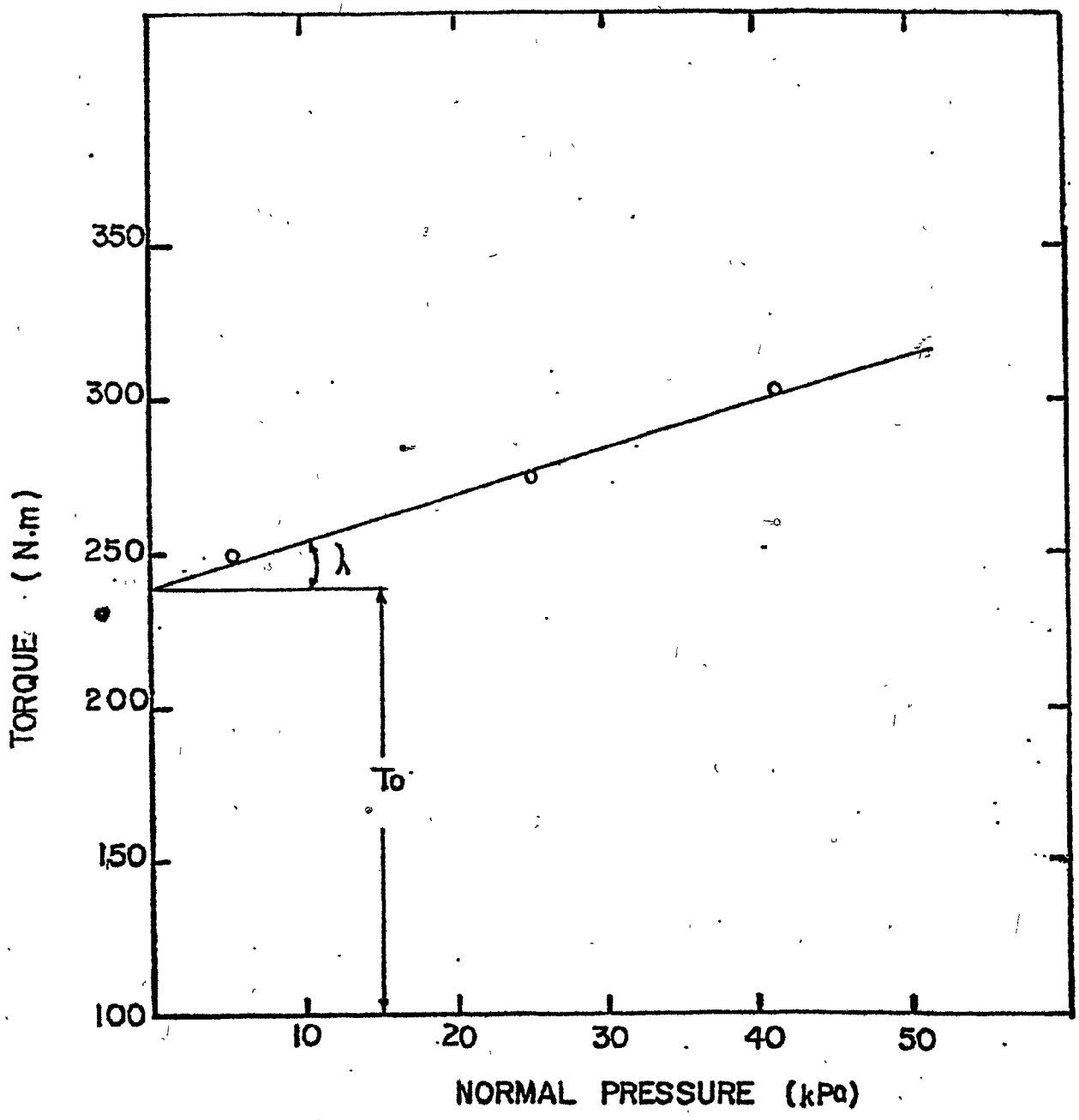

Figure 19. Relationship between normal pressure and the torque required to rotate the shear ring in the soil.

Using these two values in equations (5) and (6), the cohesion and soil internal friction angles were obtained.

This apparatus was used to measure the c and ϕ values at different soil depths (0 cm, 5 cm, 10 cm) and at four different locations in two fields of sandy loam and clay soils. Areas of 25 x 25 cm were excavated in the field by using a spatula in order not to disturb the soil at all the tested depths. These measurements were taken during the farming season of 1979 at different soil moisture conditions. These two fields were used for growing corn. The soil moisture content in the tested fields ranged from 5% to the soil's plastic limit.

2. Measurement of the c_r', δ_r, c_s', δ_s parameters

Measurement of soil-machine mechanical properties, adhesion to the rubber (c_r'), adhesion to the steel (c_s'), friction angle between the soil and rubber (δ_r) and steel (δ_s) was carried out by the shear-graph apparatus shown in Figure 20 (Payne 1956; Osman 1964). Rubber discs were used to measure c_r', δ_r and then replaced by a steel disc to measure c_s', δ_s. These measurements were carried out at three soil depths (5 cm, 10 cm, and 15 cm) and at four locations in two soils. These measurements were also taken during the farming season at different soil moisture conditions.

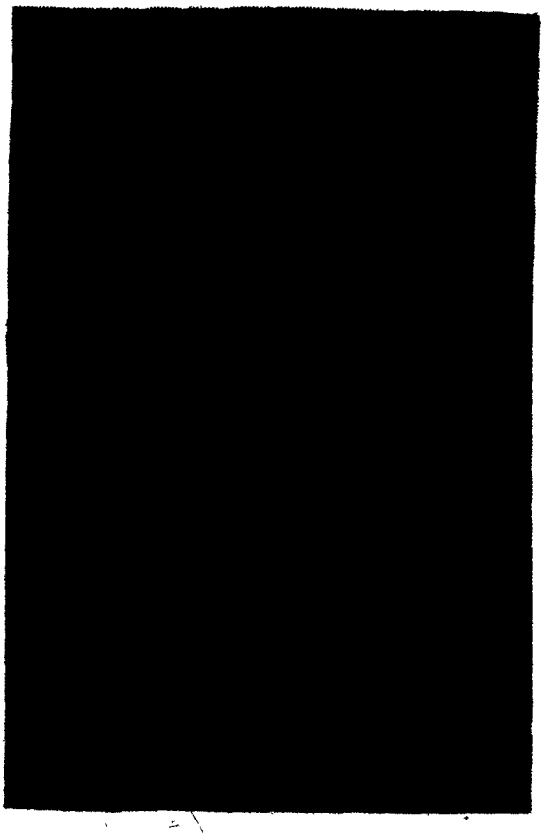

Figure 20. Shear graph apparatus.

3. Measuring soil sinkage parameters (kc, kϕ, and n)

The same apparatus used with the shear-ring was used to obtain the load-sinkage relationships. Figure 21 shows the same apparatus shown in Figure 16 with the exception that the shear ring was replaced by a plate. As mentioned in Chapter II, in order to measure the kc, kϕ, and n factors, the load-sinkage relationship must be obtained for two plates (Figure 22). Two square plates having dimensions of 12 mm and 75 mm were used (Figure 18).

The tests were carried out by connecting a given plate to the apparatus and applying different normal loads. After each normal load, the plate sinkage in the soil was measured from a constant point at which the apparatus was located. By applying the procedure described in Chapter II, the factors, kc, kϕ, and n were obtained.

4. Measurements of the soil moisture content and bulk density

For each test carried out in this study, the soil moisture content and bulk density were also measured. The soil bulk density was measured by using a core to take a specific volume of soil ($88.8\ cm^3$) and measuring its dry weight. The ring was pushed into the soil and then the samples were cut flush with the ring. At the same time, the gravimetric soil moisture content was calculated after oven-drying at 105°C.

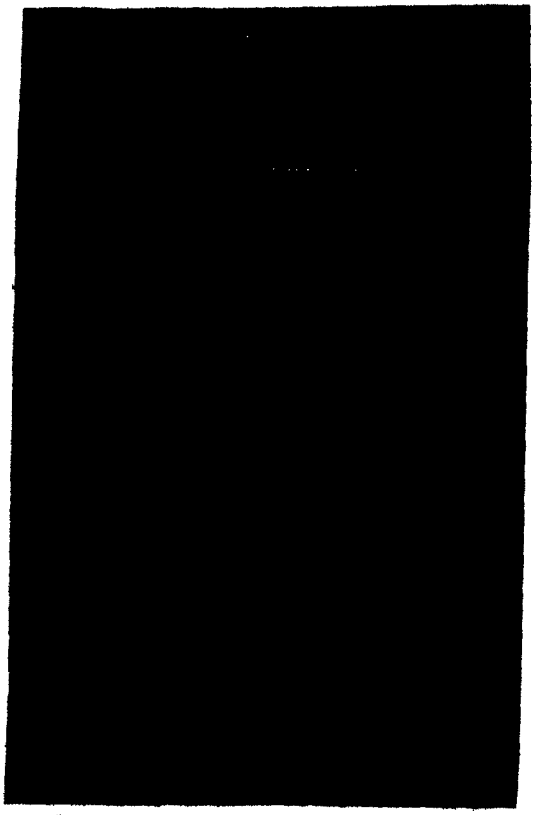

Figure 21. Apparatus to measure the load-sinkage relationship.

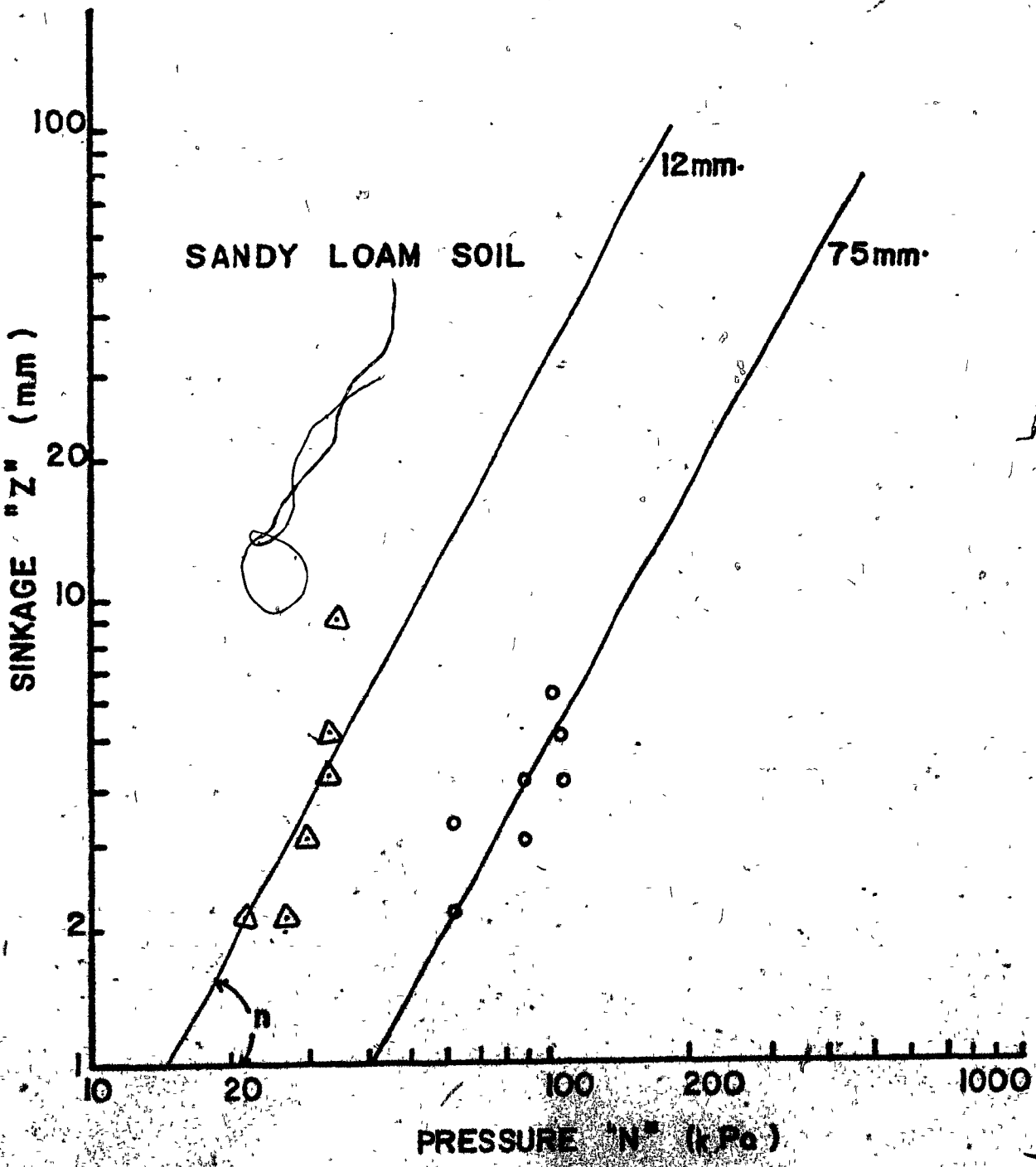

Figure 22. Sinkage pressure relationship for two plates in sandy loam soil.

Variations in soil bulk density in the sandy loam or the clay were small at the depths and locations where the measurements were taken. In the sandy loam soil, the mean value of the soil bulk density was 1590 kg/m^3 with a standard deviation of 140 kg/m^3 and a coefficient of variation of 8.8%. For the clay soil, the mean value was 1325 kg/m^3 with a standard deviation of 120 kg/m^3 and coefficient of variation of 9.1%.

The variations of some of the measured values of soil moisture contents in the clay and sandy loam soils are presented in Table A1 in Appendix A. The variation in soil moisture content with depth or location has a coefficient of variation of about 10%.

D. Field experimentation

1. Single wheel apparatus

A field test to find the effect of the lug variables of lugged tires was performed through the use of a single wheel apparatus developed by the author specifically for this study. The main components of the apparatus (Figure 23) consist of a pneumatic tire on which lugs were changeable, driven by a hydraulic motor. The soil thrust was calculated according to the equation shown in Figure 23A. The R_1 and R_{10} are the reactions on the transducer 3. R_1 is the difference between the reaction during the development of the soil thrust and the zero level. The R_{10} value is the difference between the reaction while the apparatus is on the ground, the wheel not rotating, and the zero level (see Figure A6). The whole assembly was mounted on a farm tractor (Figures 24 and 25), which also provided the hydraulic power. A portable electric generator provided the electrical power needed for the recording and measuring devices.

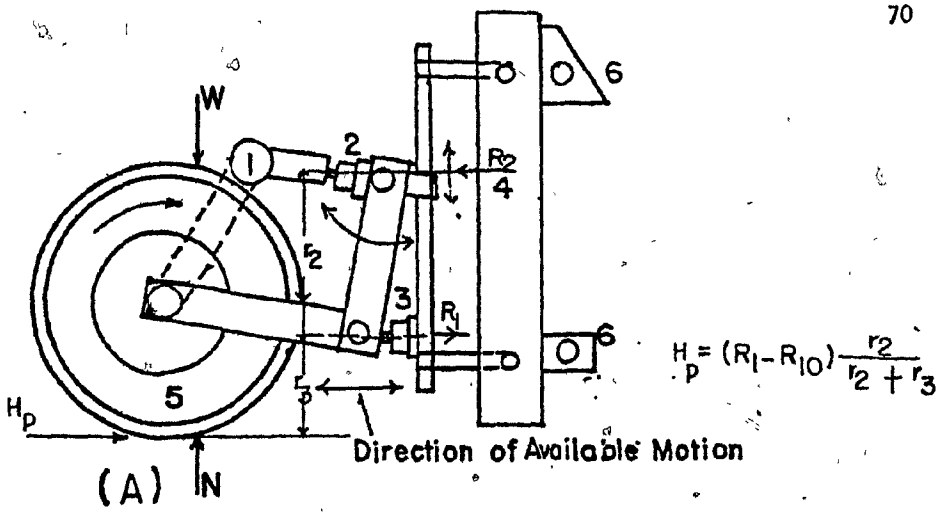

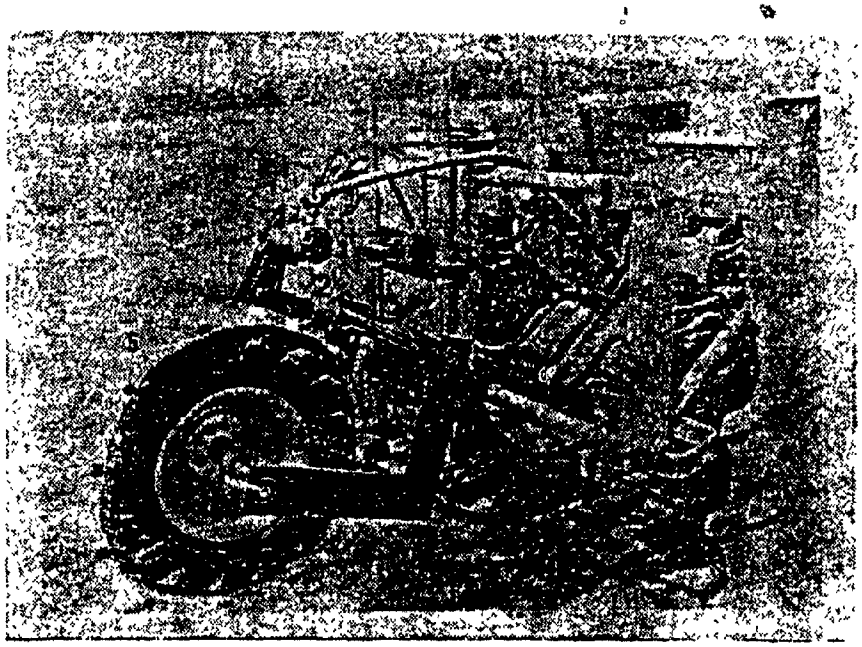

(B)

Figure 23. Construction of the single wheel apparatus (SWA).

1. hydraulic motor; 2 and 3. transducers;
4. frame; 5. tested single wheel;
6. hitching points.

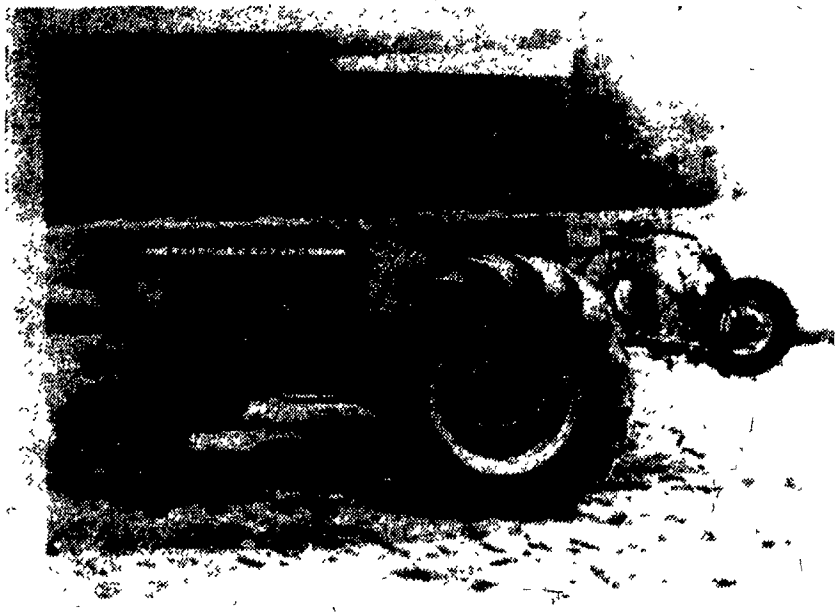

Figure 24. Single wheel test apparatus mounted on the tractor.

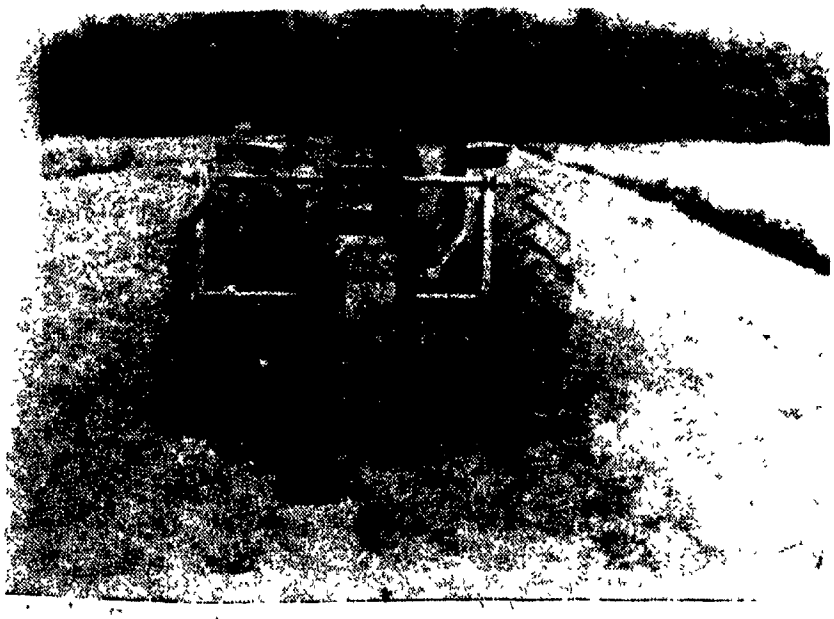

Figure 25. Rear view of the single wheel tester.

The wheel was a pneumatic rubber tire (Good Year 6 x 12) with inflation pressure of 100 kPa. This wheel was used to compare different lug designs. The wheel was fixed on a 2.5 cm diameter axle with a ball-bearing assembly on each end of that axle. The axle had a sprocket gear fixed on one side of the wheel and a chain provided the connection between the wheel and the hydraulic motor.

In order to use different lug designs, lugs of the desired dimensions and orientation were mounted on a flexible metal sheet with a rubber layer on the outside. The lugs were fixed on the wheel surface with a spacing which ensured the full development of soil failure between two lugs. A lug space of 16 cm was used to serve this purpose in all the tested models. The metal and rubber sheets with the lugs were mounted and fixed tightly on the pneumatic rubber tire to form a continuous surface on the circumference. This assembly approximated the flexibility of a pneumatic tire and a facility for changing the lug designs.

The wheel was driven by a hydraulic motor which was connected to the hydraulic system of the tractor. The torque and speed of the hydraulic motor was dependent upon the oil pressure and delivery rate of the tractor's hydraulic system, and therefore, the engine speed provided the control of the final speed of the wheel.

The wheel assembly was connected to the mounting frame in such a way that allowed free motion of the wheel in the vertical plane (Figure 23), and rotation about the same point to avoid rolling resistance.

The horizontal forces acting on the wheel activated the transducer, which sent a signal to the force recording devices.

The single wheel apparatus was attached to a farm tractor (Massey Ferguson 165D), through a mounting frame using the 3-point hitch of the tractor. The whole system could be lifted or lowered by using the tractor's hydraulic lift system. This arrangement proved to be versatile in providing an efficient method for transporting the equipment to the field site, and for dismounting the assembly in the machine shop for maintenance or modifications.

2. Measurement and recording

The traction force produced by the wheel was measured by an LVDT force transducer, which was mounted on the wheel assembly and connected by a cable to the signal conditioner (TSC-5AC) and finally to a four-channel recorder (Gulton, Model TR-444). The electric power was supplied to the recorder from a portable generator (Honda 350 watts). The transducer was calibrated using a dead load before and after each measurement. Figure A6 in Appendix A shows a typical recording of traction force as obtained in a field test. The frequency of the portable generator was held quite constant and the variation in voltage produced was ± 8 V. This variation in the amount of the voltage could be tolerated by the recorder without any effect on its performance.

3. Test procedure

The test was run by lowering the single wheel apparatus using the linear quadrat control lever in the tractor until the total load of the apparatus was transferred to the contact surface between the wheel and the soil. The system was fixed in this position and the tractor's engine speed was increased up to the calibrated limit to give a wheel speed of 3 r.p.m. At the same time the traction force was recorded directly.

The following experimental procedures were followed to standardize the determination of soil wheel thrust:

(i) The length of the contact area between the tire and soil was measured in all tests using the test wheel under a normal load of 622.7 N. This length was found to be nearly equal to a constant value of 31.5 cm for all lug parameters tested.

(ii) At least one lug was ensured to be in contact with the soil over its full length.

E. Tested lugged rubber tires

The lugged rubber tires tested are shown schematically in Figure 26. These wheels were tested in two different fields, sandy loam and clay soil, on the Macdonald College Farm, using the single wheel apparatus. In each range, four levels of moisture were used for each soil type. Each lug design was tested under one normal load of 622.7 N and a linear speed of 8.5 cm/sec.

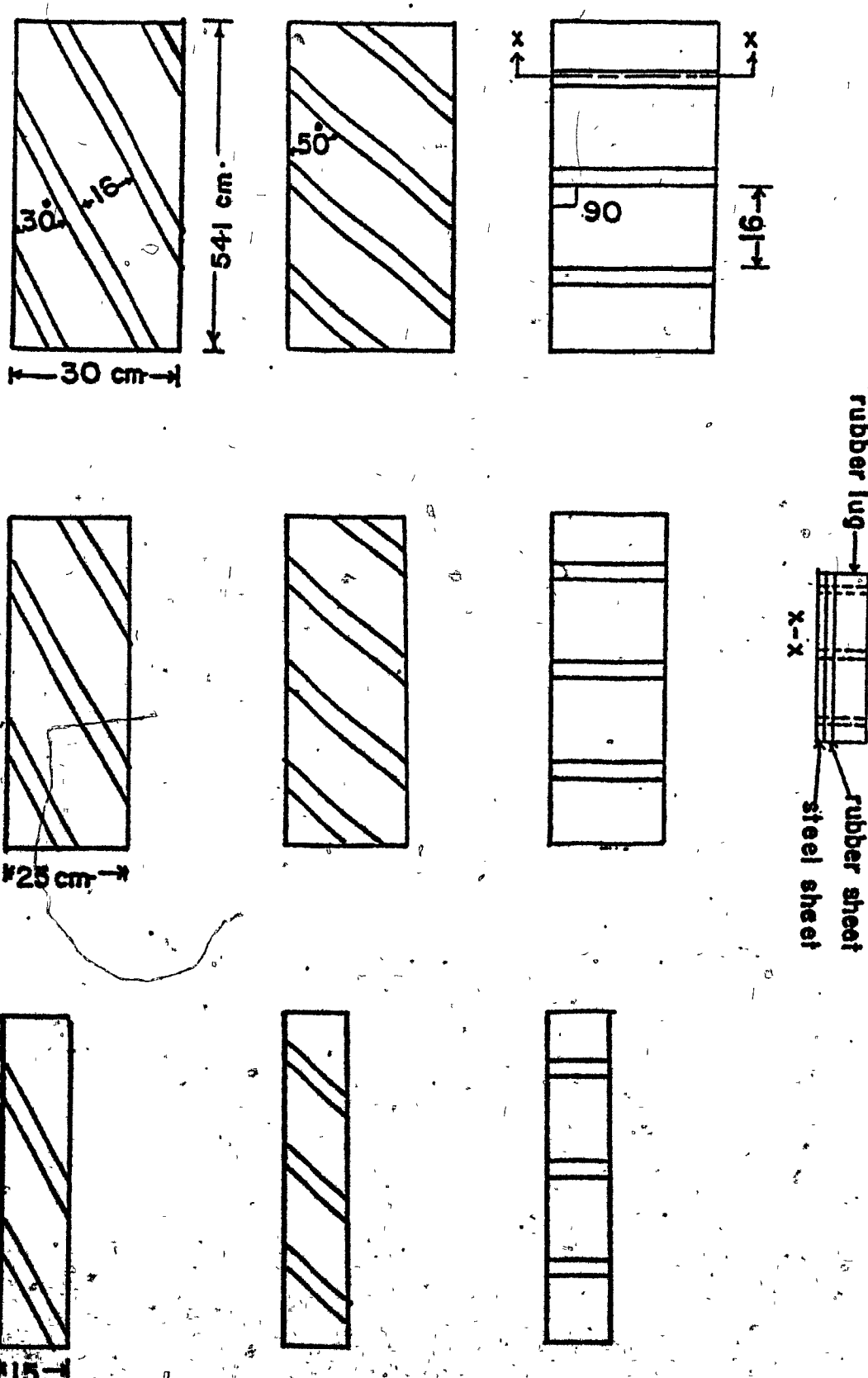

Figure 26. Models of the wheels tested in the field.

CHAPTER V

RESULTS AND DISCUSSION

The data shown in the figures presented in this chapter were very difficult to obtain in the field at very high or very low moisture content, except in the surface layer. The field moisture content in the sandy loam and clay soils was for most of the farming season between the wilting point and the soil liquid limit. Above the soil liquid limit, the soil parameters were not measured in the field because of the difficulty of operations in muddy fields. Therefore, the models developed in this study are applicable only when the soil moisture content lies within the above-noted range of soil moisture. In addition, the models were developed to predict the soil properties c, ϕ, c'_r, c'_s, δ_r, and δ_s within the top 10 cm of soil. These parameters could vary significantly within this soil layer as a result of the significant variation in soil moisture content for a particular day. Below the 10 cm soil depth, the variation in these parameters could be less, especially in a homogeneous soil profile (Bekker 1969). In addition, interaction between the lugged tires or tracked vehicle (to develop traction force) occurs in the first 15 cm of soil (Reece 1964). The models were developed for a soil with drainage systems

A. Soil properties

1. Soil cohesion (c) and internal frictional angle (ϕ) models

Mean values of four replications at each soil depth (d) and moisture content (MC) for the sandy loam and clay soils are given in Table 5. The relationships between the average values of the soil properties (c, ϕ, MC) at different soil depths are presented in Figures 27, 28, 29 and 30. The models (equation 23) gave good agreement between the calculated and the mean observed values shown in these figures. The constant values (C_1 and C_2) mentioned in equation 23 are presented in Table 6. It should be noted that the predicted values from this model presented as mean values of the parameters c and ϕ, and the actual values of these parameters in the field could vary around the mean value. Table 5 shows that the coefficient of variability ranged between 16.0% and 3.0% for the soil friction angle and between 31.0% and 4.0% for soil cohesion.

Lumb (1966, 1970) found a similar type of variation in the c and ϕ values in his study with a normal distribution around the mean value. However, the variation in the estimated cohesion values is higher than the estimated internal friction angle (ϕ).

The machine designer should take into consideration the magnitude of the above variations in order to make the machine capable of operating at a known range of values of c and ϕ.

TABLE 5. Mean value and standard deviation of the soil cohesion and friction angle at different depths, moisture content, and soil type

M.C.%	Depth cm	ϕ degree			Cohesion c kPa		
		Mean	S.D.*	C.V.%†	Mean	S.D.*	C.V.%†
			Sandy loam soil				
3.68	0	9.0	1.4	16	2.0	0.3	15
16.59	5	32.5	4.0	12	14.5	2.1	15
18.24	10	33.0	4.0	12	15.0	4.2	28
15.74	0	37.5	3.3	9	17.0	3.1	18
19.67	5	33.5	2.6	8	17.0	1.3	8
30.05	10	32.0	3.3	10	13.0	2.4	19
26.61	0	42.0	2.2	5	19.5	2.2	7
22.10	5	35.0	1.2	4	18.0	3.3	18
22.10	10	36.5	3.9	11	15.5	3.8	25
23.36	0	42.5	1.1	3	20.0	2.4	12
25.71	5	35.0	2.6	8	17.6	2.8	17
25.54	10	36.0	4.2	12	18.0	1.9	11
11.12	0	30.5	1.5	5	12.0	2.3	19
22.47	5	32.5	3.9	12	17.5	3.1	18
19.55	10	36.0	5.8	16	15.6	4.1	26
			Clay soil				
31.97	0	42.0	2.0	5	10.0	3.1	31
40.44	5	34.0	6.0	18	15.2	3.2	10
39.66	10	31.5	2.2	7	24.0	2.2	4
22.48	0	37.5	3.3	9	12.0	2.1	2
29.75	5	37.5	2.8	8	16.0	3.4	22
34.29	10	34.0	1.7	5	28.0	7.6	27
18.49	0	33.0	3.0	9	10.0	2.3	23
26.96	5	34.7	3.3	9	19.0	3.9	21
25.68	10	32.0	4.9	16	25.0	5.7	23
37.94	0	32.0	1.2	4	9.8	2.1	22
38.19	5	34.0	2.3	7	15.8	2.1	13
40.33	0	38.5	1.0	3	9.7	2.1	22

Note: each entry is an average of four replications.

* S.D. = standard deviation.

† C.V.% = coefficient of variation.

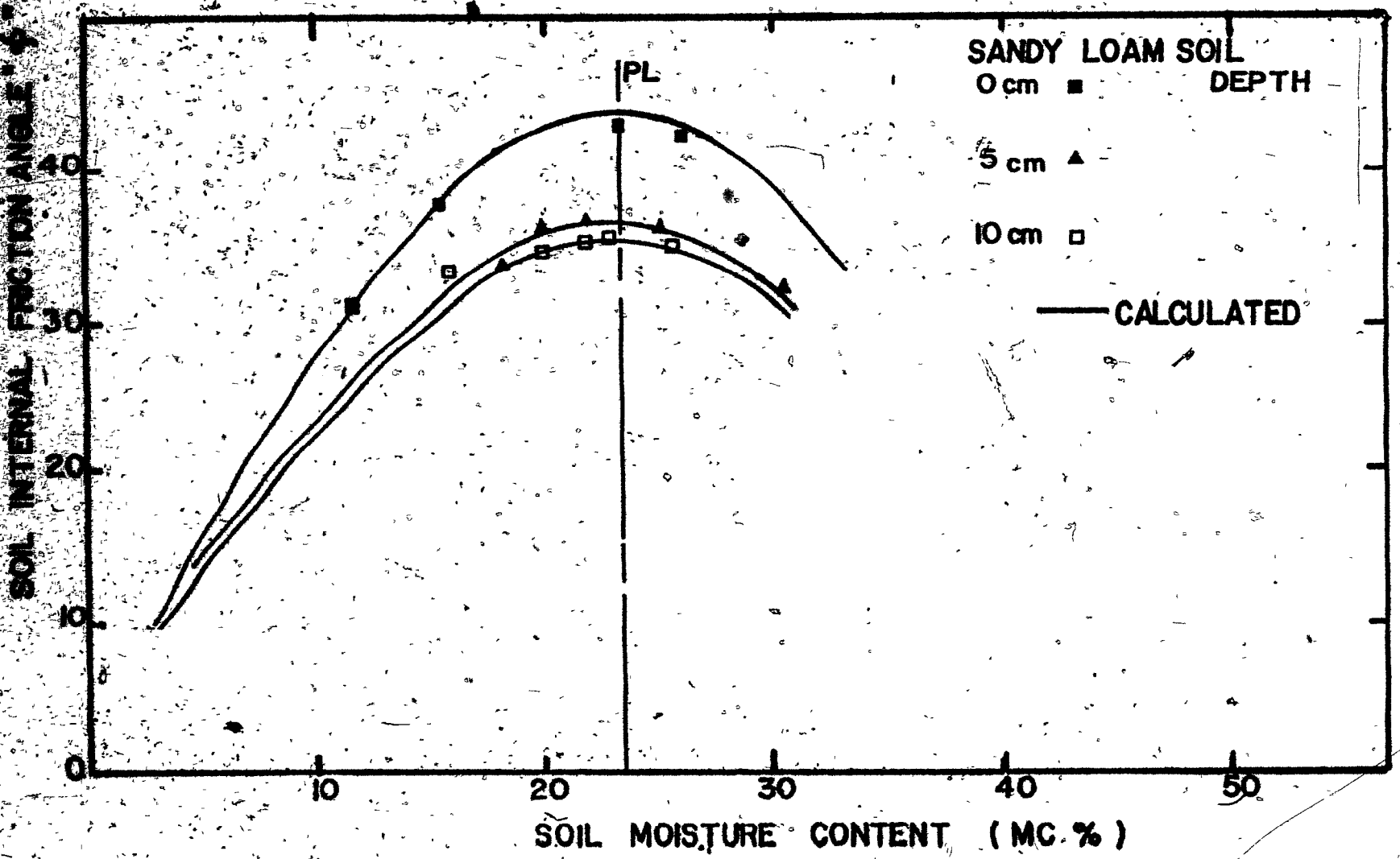

Figure 27. The relationships between soil moisture content and soil frictional angle at different depths for sandy loam soil.

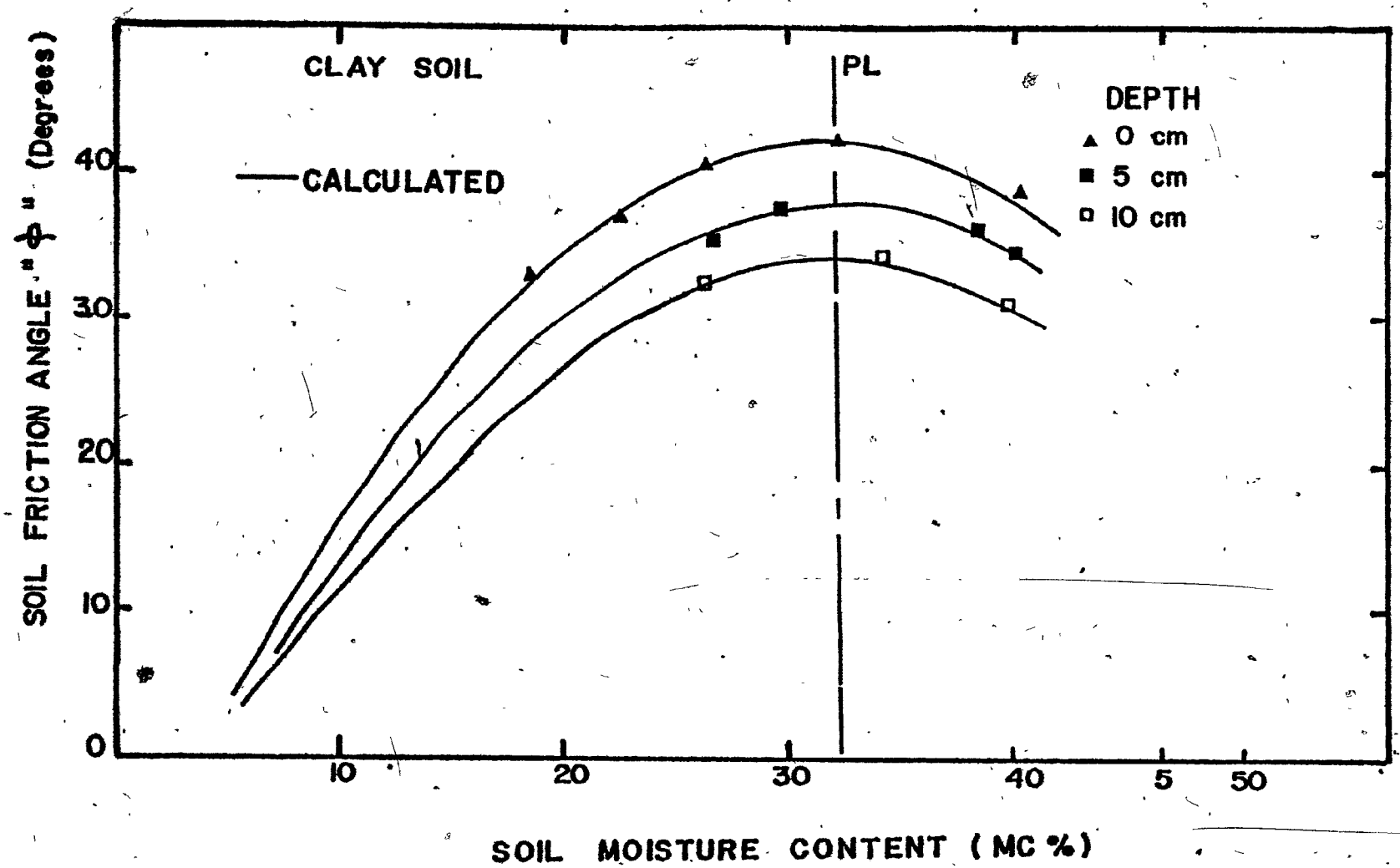

Figure 28. The relationships between soil moisture content and soil internal friction angle at different depths for clay soil.

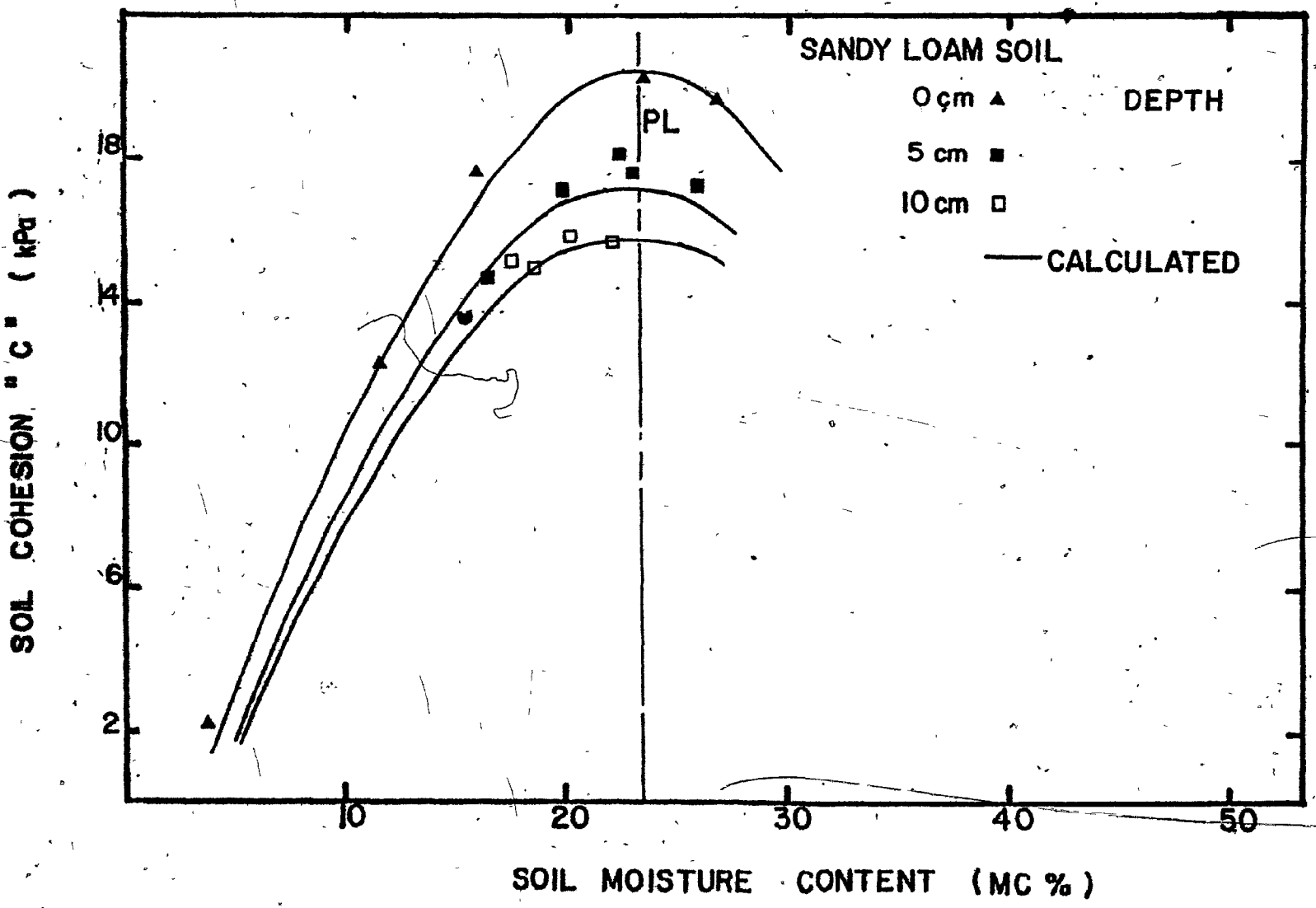

Figure 29. The relationships between soil moisture content and soil cohesion at different depths for sandy loam soil.

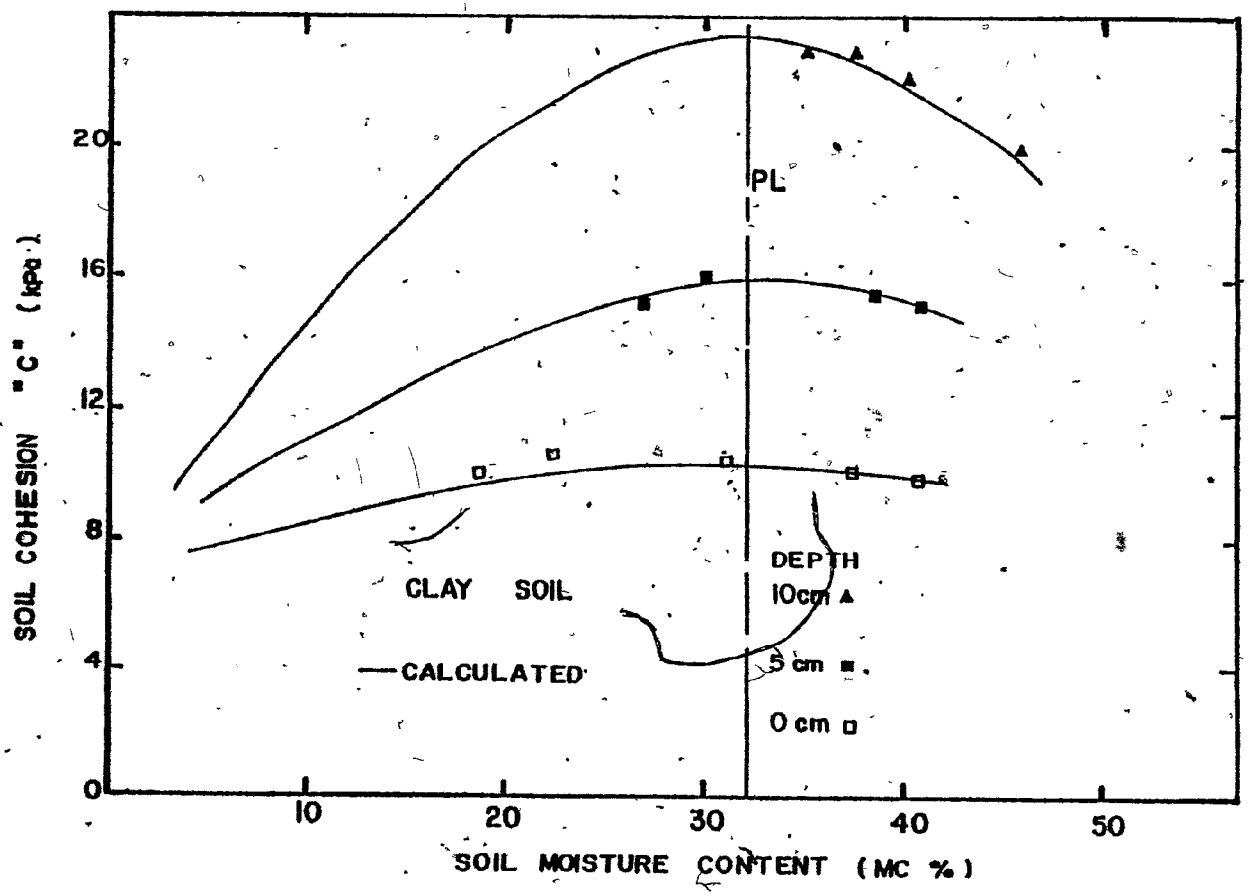

Figure 30. The relationships between soil moisture content and soil cohesion at different depths for clay soil.

TABLE 6. Coefficient values for the soil mechanical properties models at three depths for sandy loam and clay soil

Soil properties	Depth cm	Sandy loam soil		Clay soil	
		C_1*	C_2	C_1*	C_2
ϕ (degrees)	0	0.52	43.50	-8.23	37.24
	5		34.76		34.09
	10		35.91		31.92
δ_r (degrees)	0	17.65	12.20	12.81	16.38
	5		12.22		17.62
	10		15.42		17.95
δ_s (degrees)	0	14.62	5.35	6.82	10.51
	5		6.55		20.60
	10		10.12		23.89
c (kPa)	0	-5.58	33.69	6.87	2.35
	5		30.45		7.01
	10		23.37		13.60
c'_r (kPa)	0	3.35	6.56	3.75	4.25
	5		5.51		9.90
	10		5.51		23.77
c'_s (kPa)	0	-1.98	10.15	-0.21	6.79
	5		10.75		5.44
	10		12.29		4.45

*C_1 is constant in all the depths for one soil property.

In general, the magnitudes of the soil parameters (c and ϕ) increased with increasing soil moisture content up to the plastic limit and then decreased with increasing soil moisture beyond this limit. This finding is in agreement with those of Nichols (1932) and Payne and Fountaine (1952). The observed rates of the increase or decrease were greater in the sandy loam than the clay soil. In sandy loam soil the soil friction angle decreased with increasing soil depth but below 5 cm the variation becomes very small (Figure 27). On the other hand, ϕ continued to decrease with depth in the clay soil also (Figure 28). The soil cohesion value of sandy loam soil decreased with increasing soil depth (Figure 29); in the clay soil the soil cohesion increased with increasing soil depth (Figure 30). These results are similar to those obtained by Soltynski (1979) on Polish soils.

2. Soil-rubber and steel cohesion and friction angle models (c_r', c_s', δ_r, δ_s)

The mean values of four replications of the parameters c_r', c_s', δ_r, and δ_s for sandy loam and clay soils are presented in Tables 7, 8, 9 and 10. Equation (23) was the best curvilinear relationship that fits the data points. The constants (C_1 and C_2) used in this model are reported in Table 6. The good agreement between the predicted and the mean measured values for c_r', c_s', δ_r and δ_s for sandy loam and clay soils at different depths is shown in Figures 31 to 38. Tables 7 through 10 also show the coefficient of variation in the measured soil

TABLE 7. The mean and standard deviation values of the soil-steel friction angle and soil-rubber adhesion for clay soils

M.C.% Mean	Depth cm	Soil-steel friction angle (δ_s)			Soil-rubber adhesion (kPa)		
		Mean*	S.D.*	C.V.%	Mean*	S.D.*	C.V.%
38.19	0	33.0	7.4	23	9.5	1.8	19
37.95	5	29.5	3.5	12	11.2	2.0	18
18.75	0	27.7	1.2	5	8.1	2.5	31
26.25	5	30.0	4.5	15	9.8	1.9	19
27.25	10	30.0	2.7	9	14.4	2.6	18
31.97	0	35.0	4.9	14	9.6	1.5	16
40.44	5	28.0	2.7	10	11.2	2.7	19
39.66	10	37.2	10.0	27	14.0	2.2	16
22.48	0	33.0	5.5	17	8.4	1.8	21
29.75	5	31.0	4.5	14	11.8	1.6	14
34.29	10	29.5	5.6	19	14.7	2.0	14

*Note: each entry is an average of four replications.

TABLE 8. The values of the mean and standard deviation of soil-rubber friction angle and soil-steel adhesion for clay soils

M.C.% Mean	Depth cm	Soil-rubber friction angle (δ_r)			Soil-steel adhesion (kPa)		
		Mean*	S.D.	C.V.%	Mean*	S.D.	C.V.%
37.95	0	37.0	3.3	9	6.7	1.2	18
38.19	5	35.5	4.7	13	11.2	2.8	25
45.76	10	30.0	8.8	29	14.4	2.5	17
18.75	0	32.0	6.3	20	5.3	1.0	19
26.25	5	36.0	5.0	14	10.9	1.3	12
27.25	10	34.5	3.8	11	17.5	1.9	11
40.33	0	35.0	2.5	7	6.3	1.1	17
55.53	0	23.0	5.4	23	2.8	0.1	4
31.97	0	38.0	3.1	8	7.0	1.3	19
40.44	5	34.5	2.8	8	10.5	2.3	22
39.66	10	33.0	6.3	19	16.8	3.1	18
22.48	0	35.0	2.4	7	6.3	1.1	17
29.75	5	36.5	9.3	26	11.4	2.4	21
34.29	10	35.0	3.7	10	17.9	3.1	17

*Note: each entry is an average of four replications.

TABLE 9. The values of the mean and the standard deviation of the soil-rubber friction angle and soil-rubber adhesion for sandy loam soils

M.C.% Mean	Depth cm	Soil-rubber friction angle (δ_r)			Soil-rubber adhesion c_r' (kPa)		
		Mean*	S.D.	C.V.%	Mean*	S.D.	C.V.%
11.12	0	25.5	3.7	15	8.1	2.2	27
22.47	5	29.7	2.5	8	13.3	3.1	23
19.55	10	31.38	2.7	9	15.0	3.4	23
3.68	0	20.0	4.8	24	4.6	1.3	28
16.59	5	26.36	5.5	21	12.3	2.1	17
18.29	10	31.0	4.8	16	14.7	3.2	22
23.36	0	29.0	6.7	23	10.5	2.1	20
25.36	5	30.0	3.9	13	13.3	3.0	23
25.54	10	32.0	2.1	7	14.7	2.8	19
20.60	0	-	-	-	-	-	-
22.10	5	30.0	2.2	7	13.3	2.3	17
22.10	10	32.81	1.3	4	15.1	3.9	26
15.74	0	30.0	2.2	8	9.5	1.7	18
19.67	5	30.5	2.3	8	13.7	2.1	15
30.05	10	29.0	0.6	2	13.0	3.0	23

*Note: each entry is an average of four replications.

TABLE 10. The values of the mean and standard deviation of the soil-steel friction angle and soil-steel adhesion for sandy loam soils

M.C.% Mean	Depth cm	Soil-steel friction angle (δ_s)			Soil-steel adhesion (c_s' kPa)		
		Mean*	S.D.	C.V.%	Mean*	S.D.	C.V.%
25.75	5	19.5	1.5	8	8.4	1.1	13
25.54	10	22.5	2.8	13	9.8	1.9	19
26.61	0	17.0	2.5	17	7.4	1.2	16
22.10	5	19.0	1.8	9	8.4	2.3	27
22.10	10	22.0	1.7	8	10.0	2.3	23
15.74	0	16.3	1.5	1	6.5	0.9	14
19.67	5	20.2	1.0	5	8.4	1.3	15
30.05	10	20.0	2.1	11	8.6	1.8	21
11.12	0	17.0	3.6	21	5.6	1.5	27
22.47	5	19.5	2.3	12	8.8	1.8	20
19.55	10	22.5	3.8	17	9.8	1.7	17
3.68	0	13.0	2.8	22	1.1	0.2	18
6.59	5	19.0	1.5	8	7.0	1.3	19
18.29	10	22.0	2.0	9	9.6	2.7	28
23.36	0	17.0	1.0	6	8.1	2.3	28

*Note: each entry is an average of four replications.

parameters at different locations. These data are summarized in Table 11 and indicate higher coefficients of variation in the adhesion values than that in the friction angles. The high variation in these parameters (c'_r, c'_s, δ_r, δ_s) might be due to the fact that the shear graph used had a relatively small friction measurement surface area which does not make a good representation of the field situation. Nevertheless, it was the only standard instrument available which could be used to measure these parameters. It should be noted that the coefficient of variation presented in Table 11 includes the variations due to the soil moisture contents in the field, i.e., these ranges include all the sources of variation in the parameters c'_r, c'_s, δ_r, and δ_s.

TABLE 11. The coefficient of variation in the measured values of c'_r, c'_s, δ_r, and δ_s for two different soil types

Soil type	Soil parameters			
	c'_r	c'_s	δ_r	δ_s
	Per cent			
Sandy loam	15-27	13-28	2-24	1-22
Clay soil	14-31	4-25	8-29	5-23

The results shown in Figures 31 and 32 indicate that both in sandy loam and clay soils the soil-rubber friction angle (δ_r) increased slightly with increasing soil moisture content up to the plastic limit and then decreased with increasing soil moisture. In

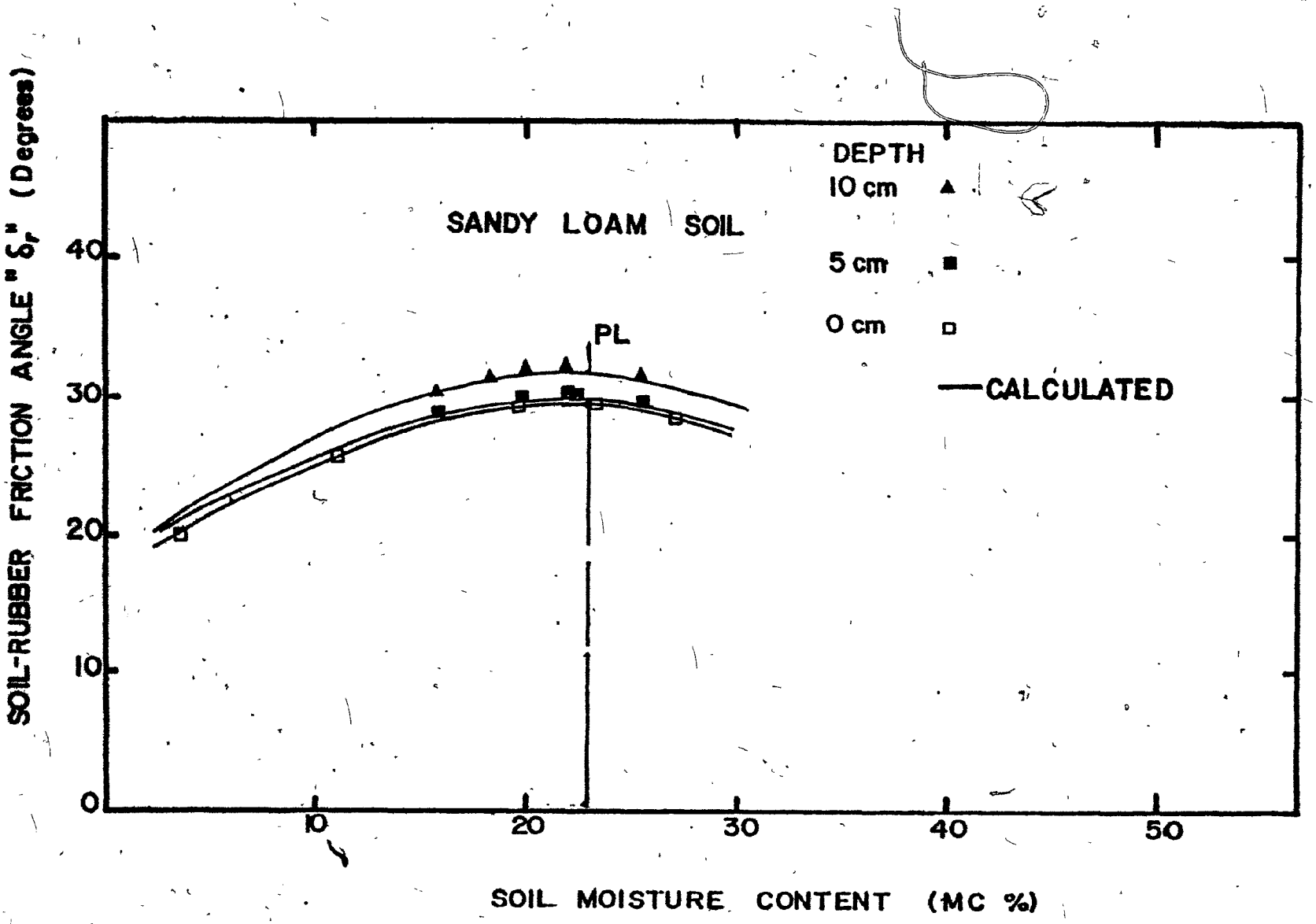

Figure 31. The relationships between soil moisture content and soil-rubber friction angle at different depths for sandy loam soil.

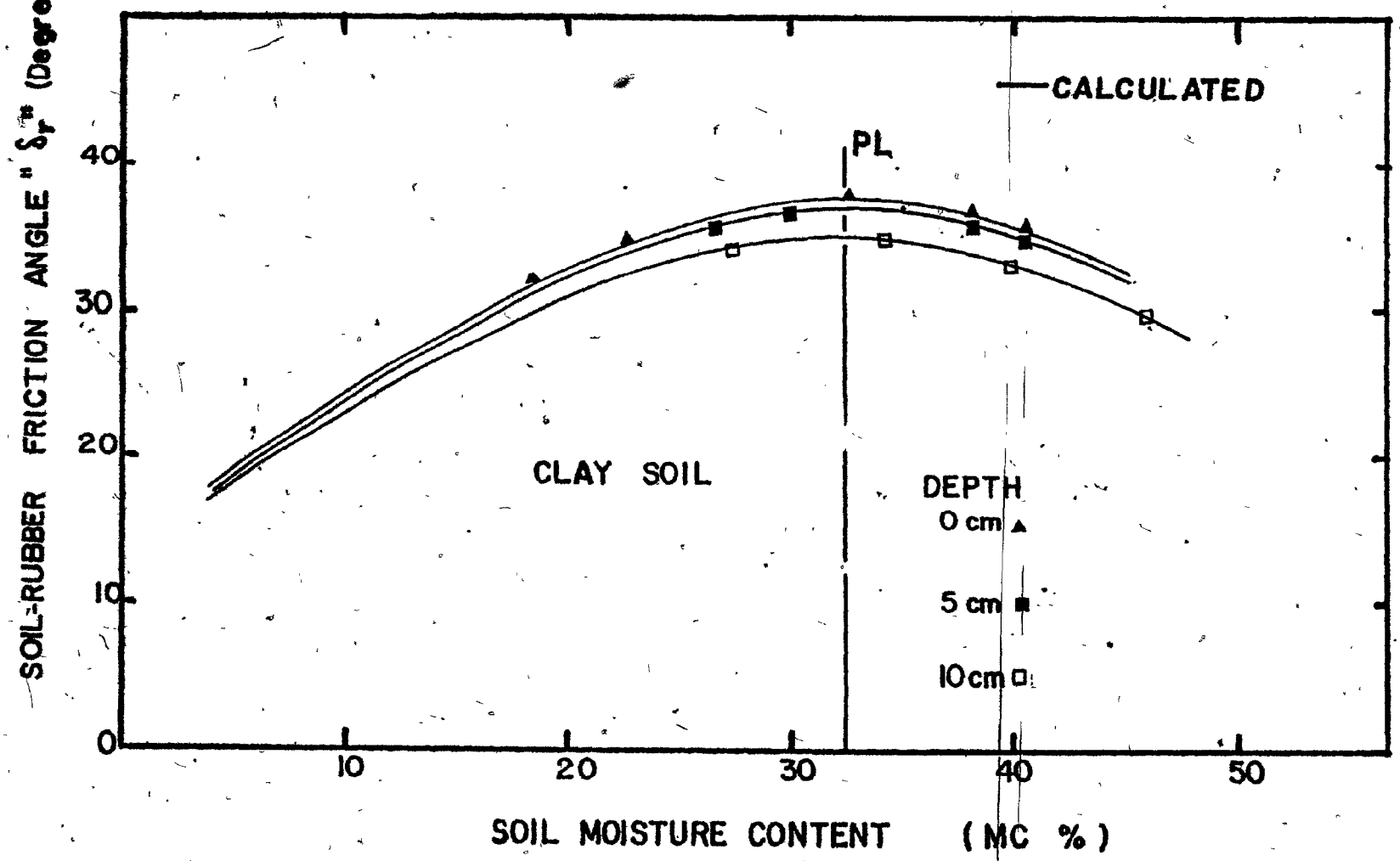

Figure 32. The relationships between the soil moisture content and soil-rubber friction at different depths for clay soil.

addition, the variation of this parameter with soil depth was small. However, there was a small decrease in the friction angle (δ_r) with depth in sandy loam soil; the opposite situation was found to exist in the clay soil.

The relationships between the rubber adhesion (c'_r) and soil moisture content are shown in Figures 33 and 34. The soil adhesion was maximum at around soil plastic limit for both the sandy loam and clay soils; the rate of increase or decrease was smaller in the clay soils. In addition, for both soil types the soil surface showed more adhesion force to the rubber than did the sub-surface soil. The variation in soil adhesion values with depth was higher than the variation in the friction angle δ_r.

Figures 35 and 36 indicate that maximum values of the soil-steel friction angle are obtained at the plastic limit; any change in the soil moisture from this limit resulted in a decrease in the δ_s value. The rate of increase or decrease of the δ_s values was smaller in sandy loam than in clay soils. The results also indicate that the friction angle (δ_s) decreases slightly with increasing soil depth for both sandy loam and clay soils.

The maximum values of the soil-steel adhesion (c'_s) were also at the plastic limit and these values decreased sharply if the soil moisture changed from the plastic limit (Figures 37 and 38). The rate of increase or decrease in the c'_s value was higher in sandy loam than in clay soils. Soil adhesion to steel decreased sharply with increasing soil depth, both in sandy loam and clay soils.

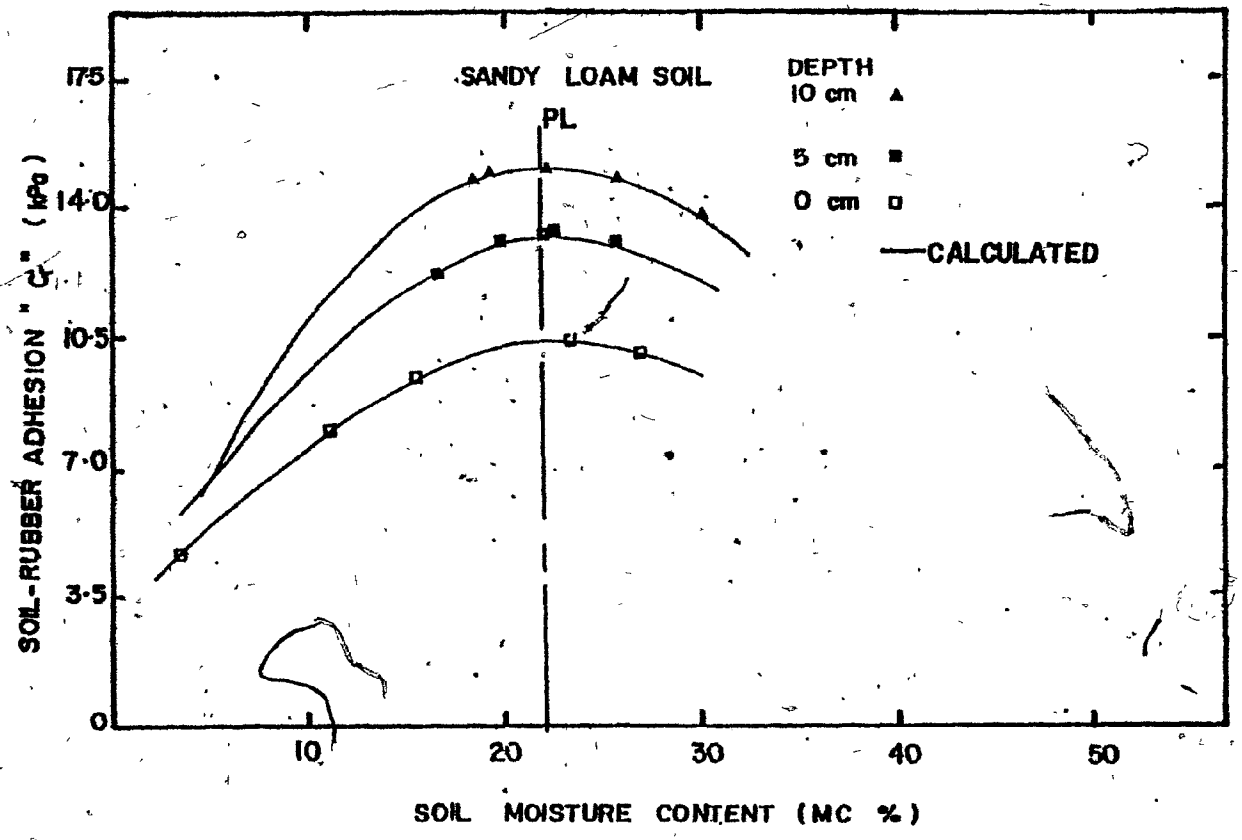

Figure 33. The relationships between the soil moisture content and soil-rubber adhesion at different depths for sandy loam soil.

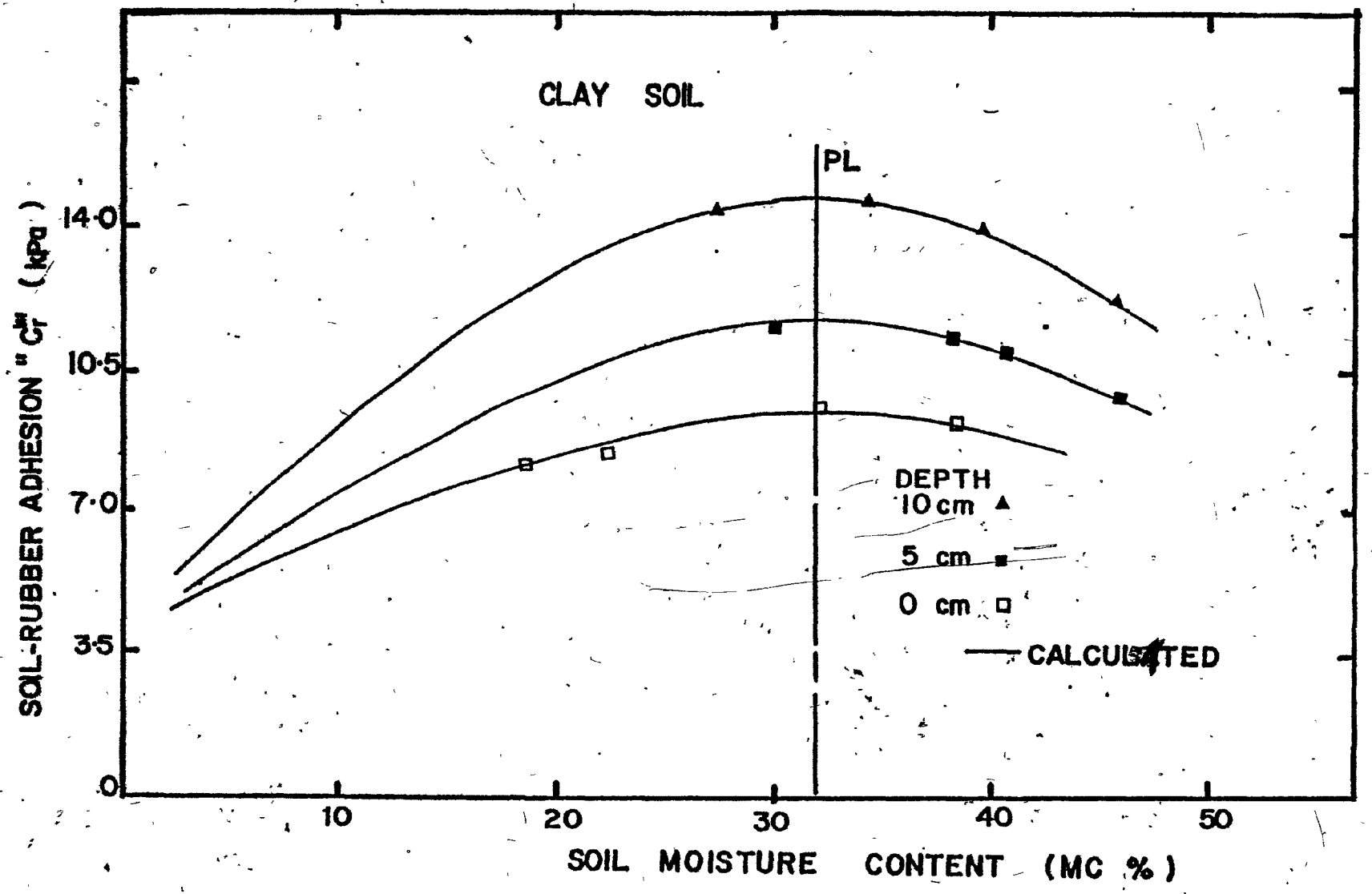

Figure 34. The relationships between soil moisture content and the soil-rubber adhesion at different depths for clay soil.

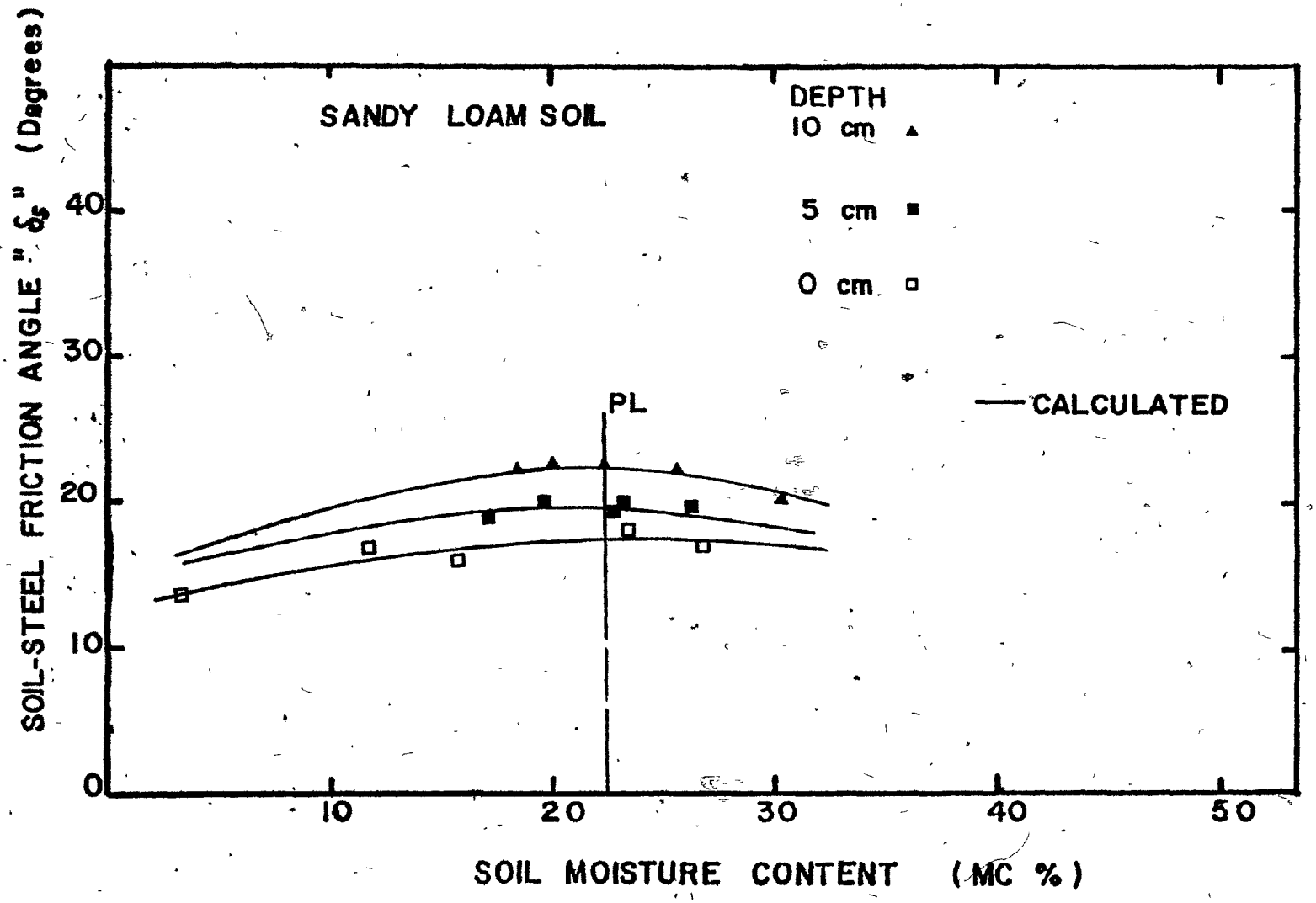

Figure 35. The relationships between the soil moisture content and soil-steel friction angle at different depths for sandy loam soil.

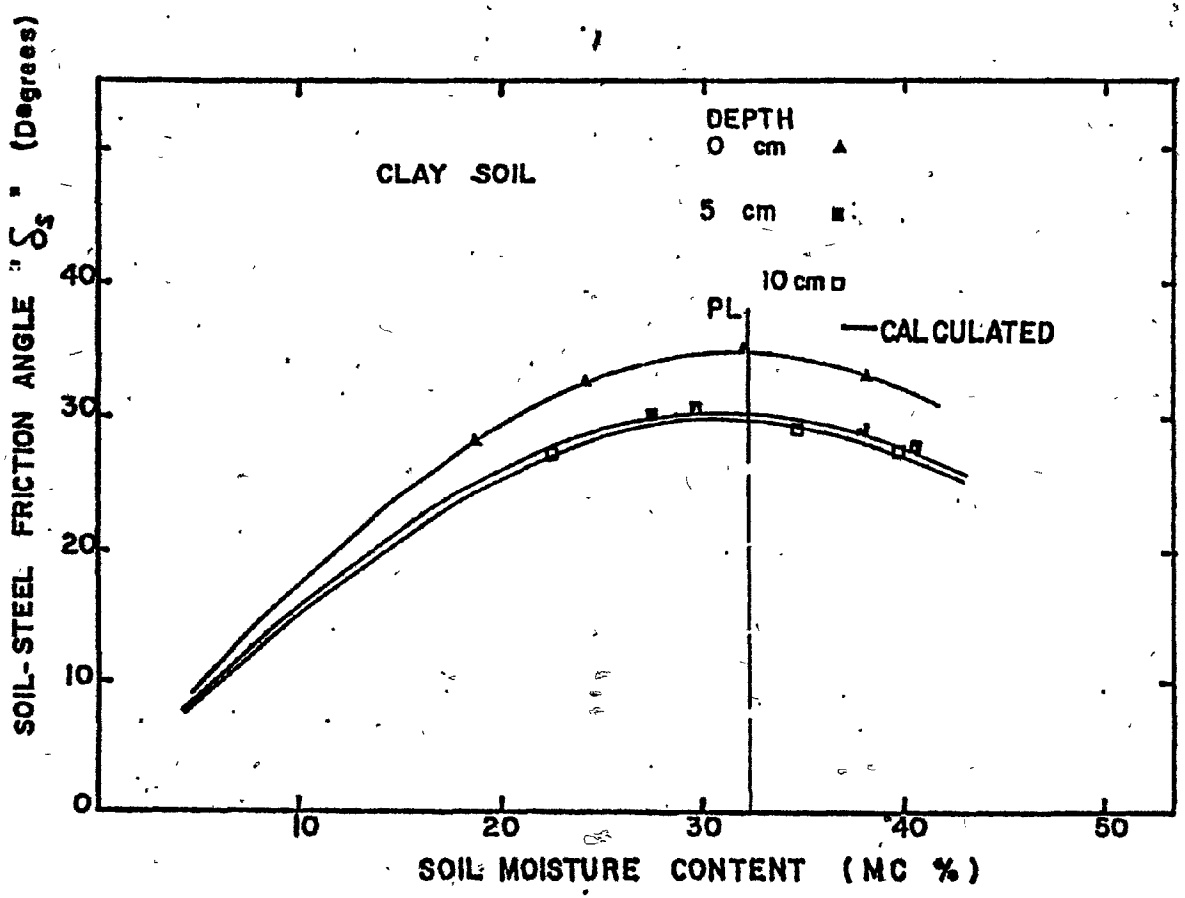

Figure 36. The relationships between soil moisture content and soil-steel friction angle at different depths for clay soil.

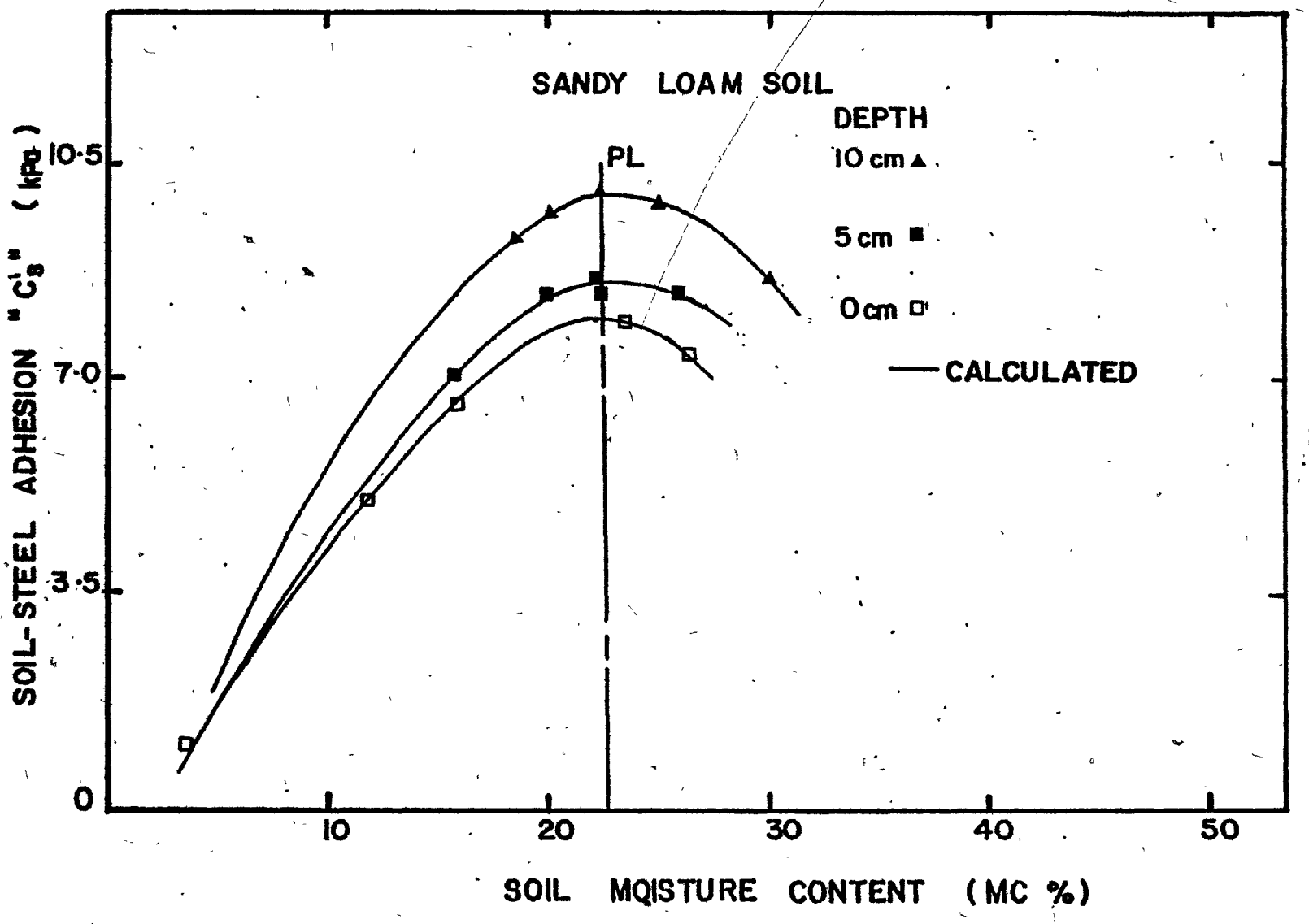

Figure 37. The relationships between soil moisture content and soil-steel adhesion at different depths for sandy loam soil.

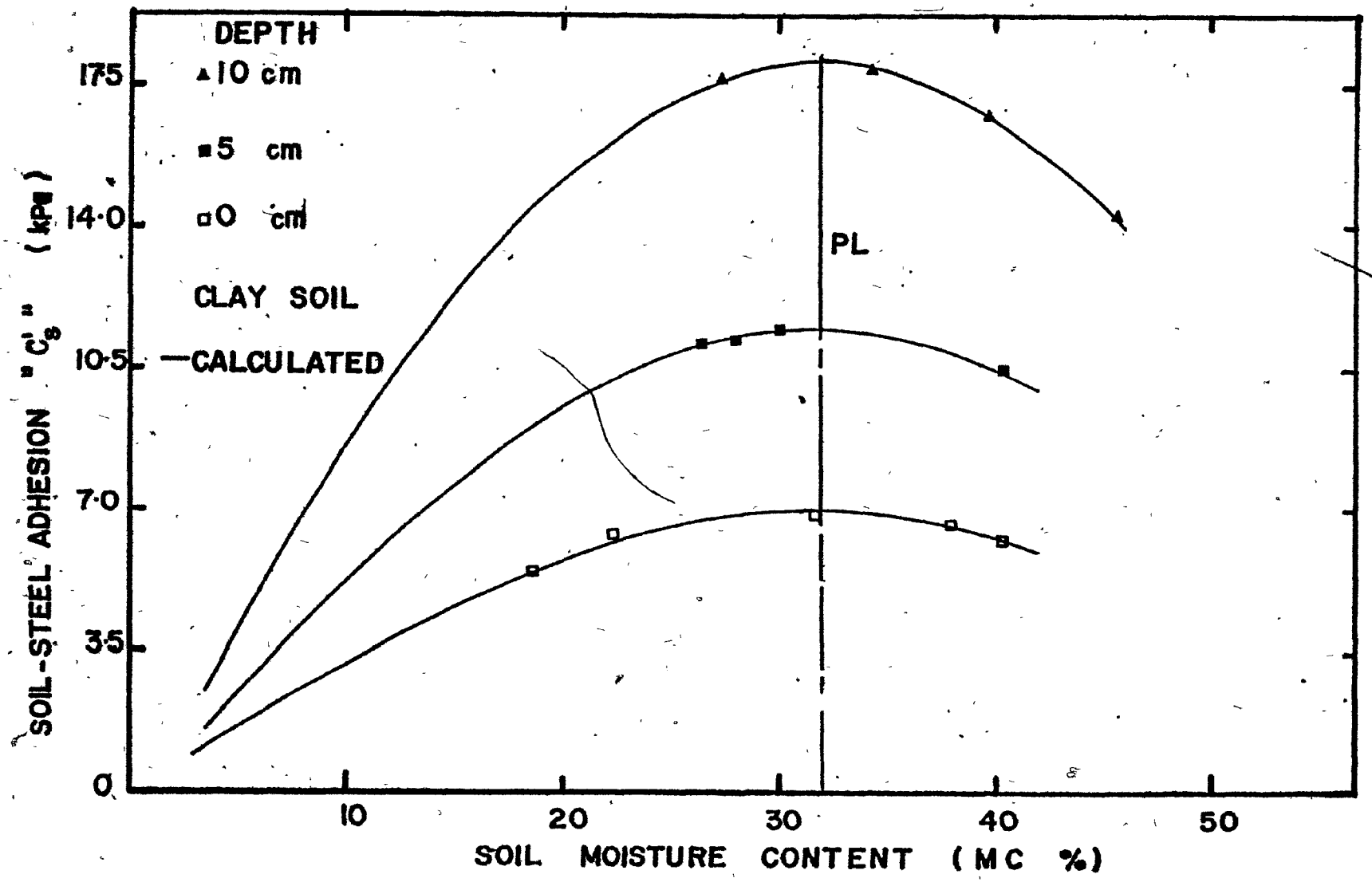

Figure 38. The relationships between soil moisture content and soil-steel adhesion at different depths for clay soil.

3. Modelling of the sinkage moduli kc, kϕ and n

Means of the data of the moduli kc, kϕ and n, are reported in Table 12. The means were plotted as a function of the soil moisture content for sandy loam and clay soils (Figures 39, 40 and 41). These results indicate that the models found in this study are in good agreement with the measured values. These models are:

For sandy loam:

$$kc = 26.8 + 4.15 \sin \left(\frac{\pi}{2} + \frac{3\pi}{2} \frac{MC}{LL} \right) \quad \ldots (36)$$

$$k\phi = 23.4 + 2.40 \sin \left(\frac{\pi}{2} + \frac{3\pi}{2} \frac{MC}{LL} \right) \quad \ldots (37)$$

$$n = 0.5 + \left[\sin \left(\frac{3\pi}{2} \frac{MC}{PL} \right) \right] (0.11) \quad \ldots (38)$$

For clay soil:

$$kc = 23.3 + 11.65 \sin \left(\frac{\pi}{2} + \frac{3\pi}{2} \frac{MC}{LL} \right) \quad \ldots (39)$$

$$k\phi = 15.4 + 4.1 \sin \left(\frac{\pi}{2} + \frac{3\pi}{2} \frac{MC}{LL} \right) \quad \ldots (40)$$

$$n = 0.79 + 0.1 \sin \left(\frac{3\pi}{2} \frac{MC}{PL} \right) \quad \ldots (41)$$

where

LL = soil liquid limit (%)

PL = soil plastic limit (%)

MC = gravimetric soil moisture content (%)

TABLE 12. The mean, standard deviation, and coefficient of variation of the kc, kϕ, and n parameters for sandy loam and clay soils

M.C.%	Mean values for			Standard deviation for			Coefficient of variation (%) for		
	n	kc	kϕ	n	kc	kϕ	n	kc	kϕ
				Sandy loam soil					
3.68	0.59	29.0	25.5	0.1	2.5	2.85	17.0	10.0	3.0
11.12	0.57	25.55	22.10	0.16	3.60	3.90	28.0	14.0	18.0
15.74	0.50	24.00	21.00	0.13	2.50	3.05	26.0	10.0	15.0
19.38	0.41	22.50	20.50	0.08	2.15	2.00	20.0	10.0	10.0
23.63	0.37	23.50	21.55	0.09	2.45	2.65	24.0	10.0	12.0
26.61	0.44	25.50	20.55	0.10	1.95	2.00	23.0	8.0	10.0
33.42	0.49	27.50	23.75	0.13	2.55	2.90	27.0	9.0	12.0
				Clay soil					
12.36	0.88	24.0	17.0	0.22	2.8	2.2	25.0	12.0	13.0
19.28	0.88	17.4	16.3	0.14	1.7	1.3	18.0	10.0	8.0
22.49	0.83	13.5	12.5	0.11	1.2	1.1	13.0	9.0	9.0
31.97	0.70	16.2	17.2	0.14	0.8	1.3	20.0	5.0	8.0
37.95	0.66	14.5	12.0	0.19	1.2	1.1	29.0	8.0	9.0
40.33	0.74	25.0	16.0	0.22	1.7	1.5	30.0	1.0	9.0

Note: each entry in the mean is for four replications.

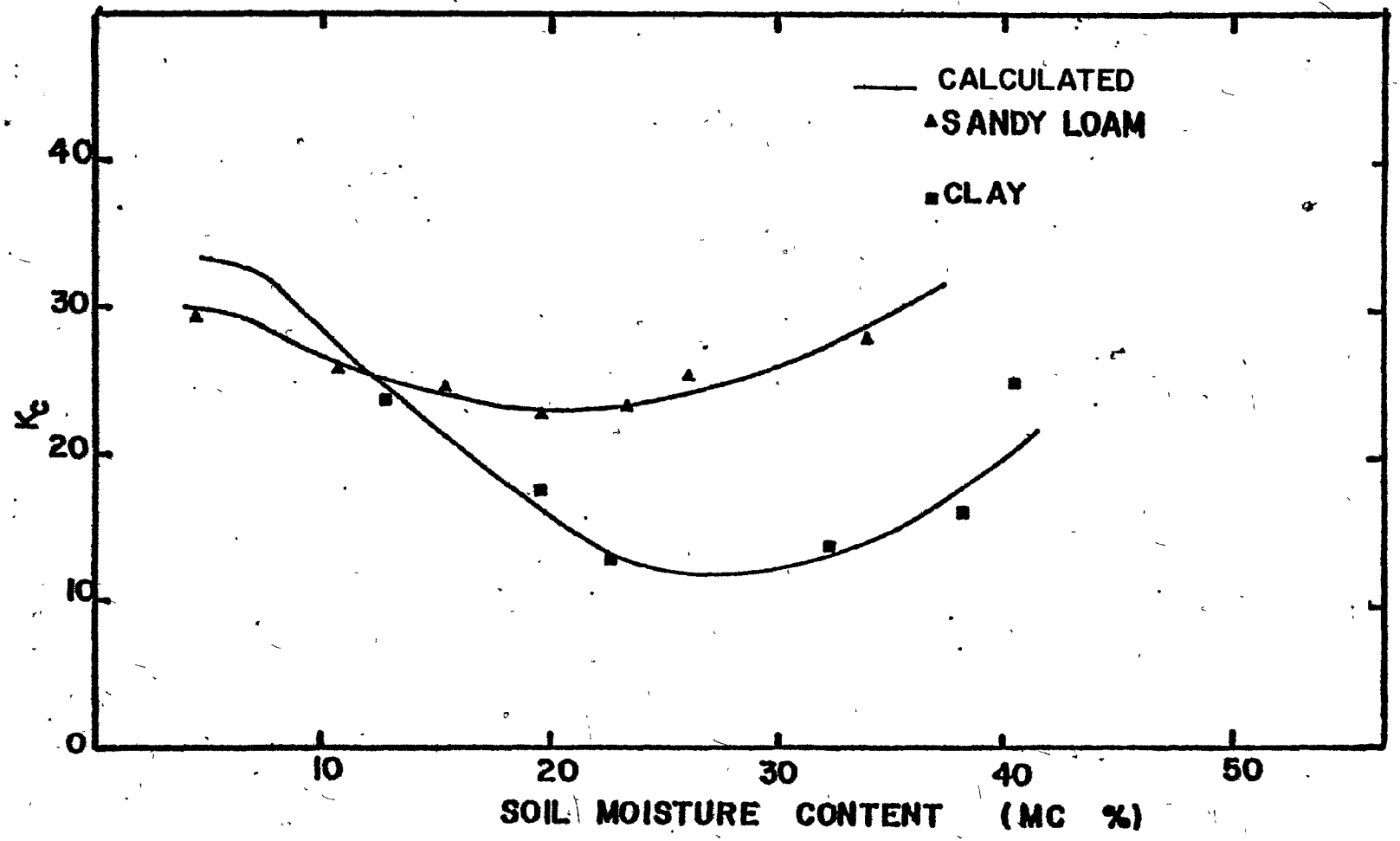

Figure 39. The relationships between soil moisture content and the sinkage modulus "K_c"

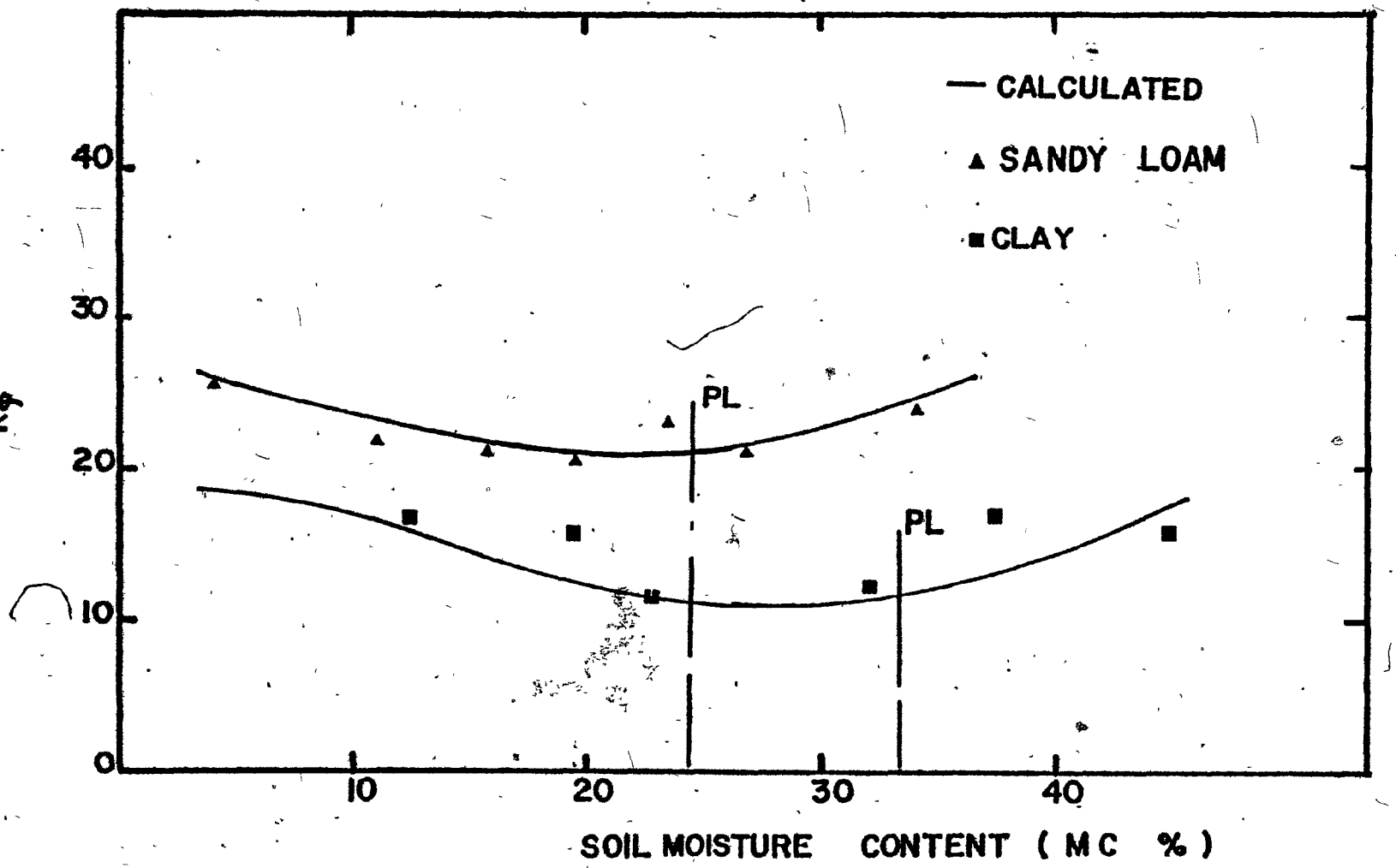

Figure 40. The relationships between soil moisture content and the sinkage modulus "K_ϕ" for sandy loam and clay soils.

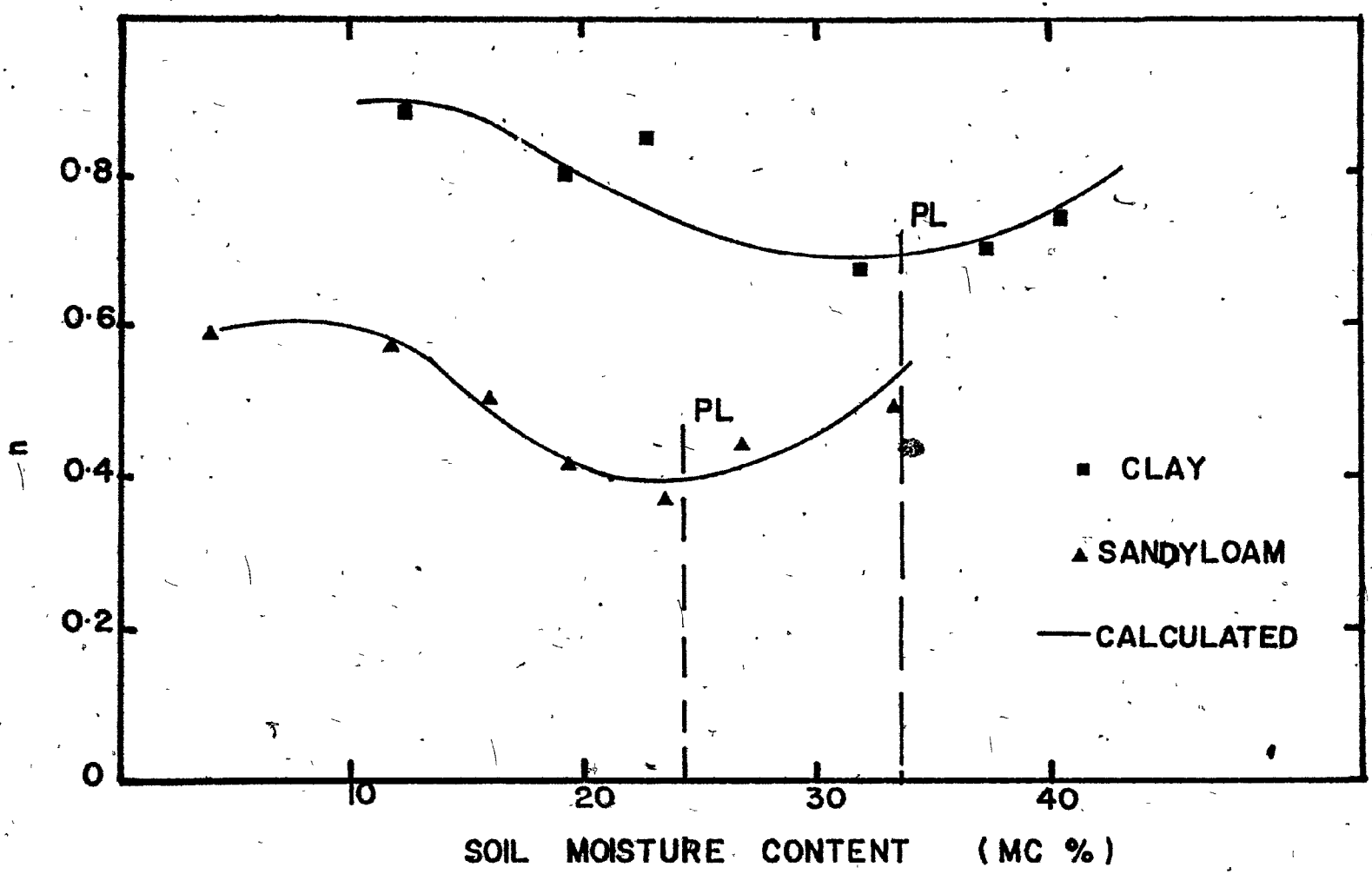

Figure 41. The relationships between soil moisture content and "n" factor for sandy loam and clay soils.

The results expressed in Figures 39, 40 and 41 show that the moduli kc, $k\phi$ and n decrease with increasing soil moisture content up to the plastic limit. Increasing the soil moisture content beyond the plastic limit resulted in only slightly increased kc and $k\phi$ values up to the maximum tested levels of soil moisture (liquid limit). However, it would appear that the soil compressibility becomes higher with increasing soil moisture content. Beyond the soil plastic limit the amount of water in the soil could support some of the normal load which results in an increase in the soil bearing capacity. This finding is in agreement with those of Bekker (1960, 1969). Similar results were obtained in the laboratory experiments performed by Wells and Treesuwan (1977). It should be noted that the sinkage of the farm vehicle in wet soil could be much higher than the calculated static values by using the kc, $k\phi$, and n parameters. This increase in the sinkage at high levels of moisture content due to the low strength of the soil results in higher slip and in turn leads to more digging in of the tires.

The results obtained in this study indicate that the kc and $k\phi$ moduli were higher in the sandy loam soil than in the clay soil. This behavior could be the result of the following two factors:

(a) The sand content in the sandy loam soil (70%) was higher than that of the clay soil (16.8%) and this gave the sandy loam soil less sinkage (Terzaghi and Peck 1948).

(b) The average bulk density of the sandy loam soil was higher than that of the clay soil.

Equation (8) can be written in another form as

$$Z = \left(\frac{N}{\left(\frac{kc}{b} + k\phi \right)} \right)^{1/n} \quad \ldots (42)$$

From equation (42), increasing the n factor results in a decrease in the soil sinkage (Z). Therefore, the smaller sinkage in the sandy loam soil compared with the clay soil is due to higher values of the n factor in clay than in sandy loam soil (Figure 41).

4. Modelling the soil moisture content

Equation (24) was used to model the daily soil moisture content. In this model, the daily rainfall and evaporation pan (class A) data were provided by the Macdonald College Farm Station; evapotranspiration values were calculated using the results presented in Figures 5 and 6. Volumetric water contents were converted to percentage by weight (dry weight basis).

Negi et al. (1979) carried out investigations in the same fields used in this study. The values of the field capacity and wilting point, percentage by volume, for soils in these fields as determined from their study were as follows:

	Sandy loam soil	Clay soil
Field capacity %	33.00	41.00
Wilting point %	19.00	20.00

Therefore, the plant available water in the root zone was 61.0 mm and 45 mm in clay and sandy loam soils, respectively, for a 30 cm root zone. These two values were used to plot the curves shown in Figure 5 and to calculate the soil moisture deficits and surpluses for the sandy loam and clay soils.

Figures 42 and 43 show graphs of the calculated and the measured soil moisture contents. These figures indicate that the measured values are in good agreement with the predicted values. It should be noted that each of the measured data points presented in these figures is an average of soil moisture content in the top 15 cm of soil at four different locations.

B. The variation in the soil mechanical properties during the farming season

The seasonal variations in average soil moisture content in both fields, sandy loam and clay soils, were determined by using the method presented by Chieng (1975) for a 22-year period (1945 to 1966) during the field preparation and growing season. For these 22 years the data for the evaporation pan were not available for the Macdonald College region. Therefore, the method presented in this thesis cannot be used to predict the soil moisture content of this period. The volumetric soil moisture contents obtained from Chieng's (1975) model for 30 cm root zone were transferred to a percentage (dry weight basis) and the wilting

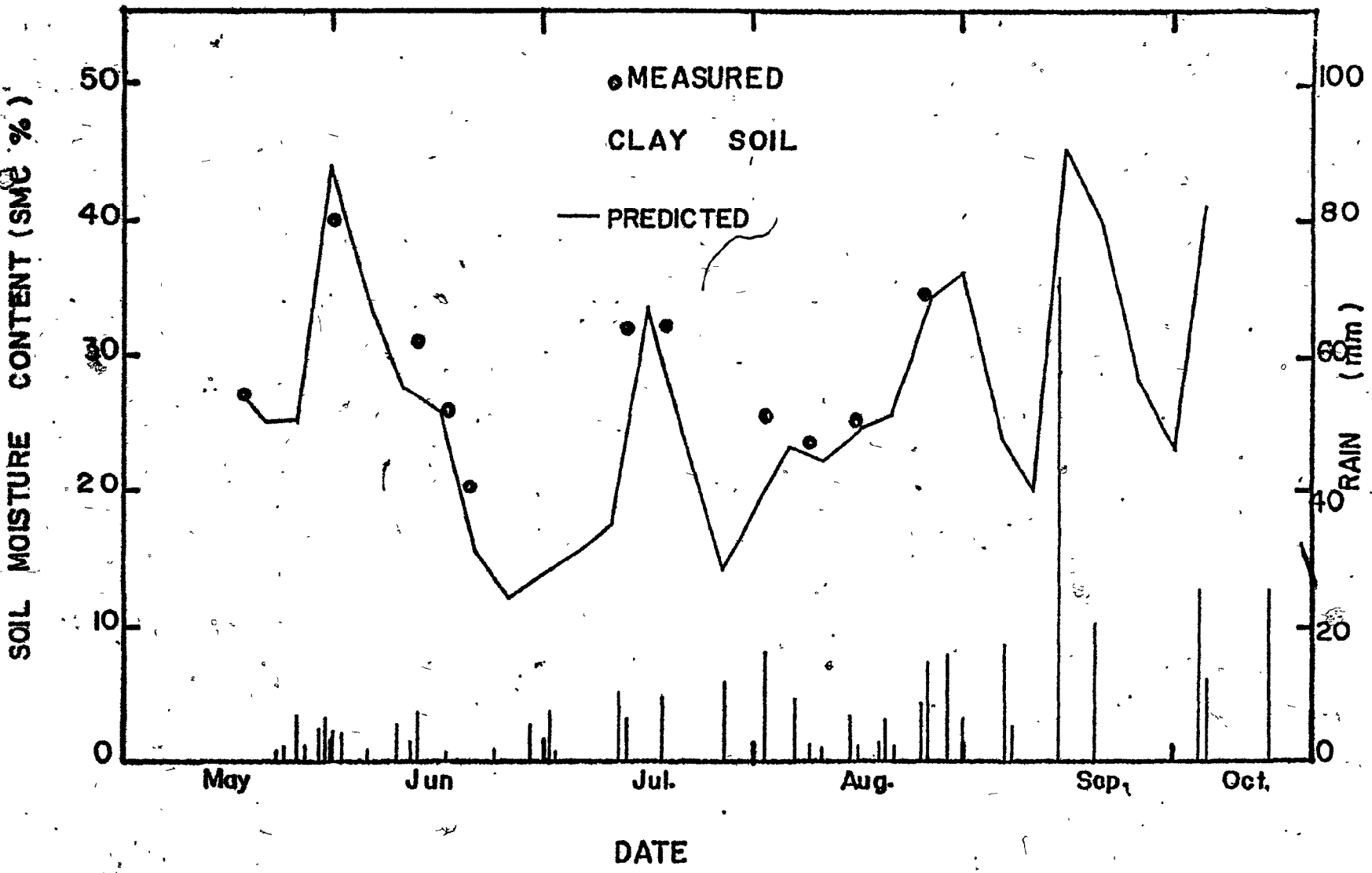

Figure 42. Predicted and measured soil moisture content during the farming season in clay soil (1979).

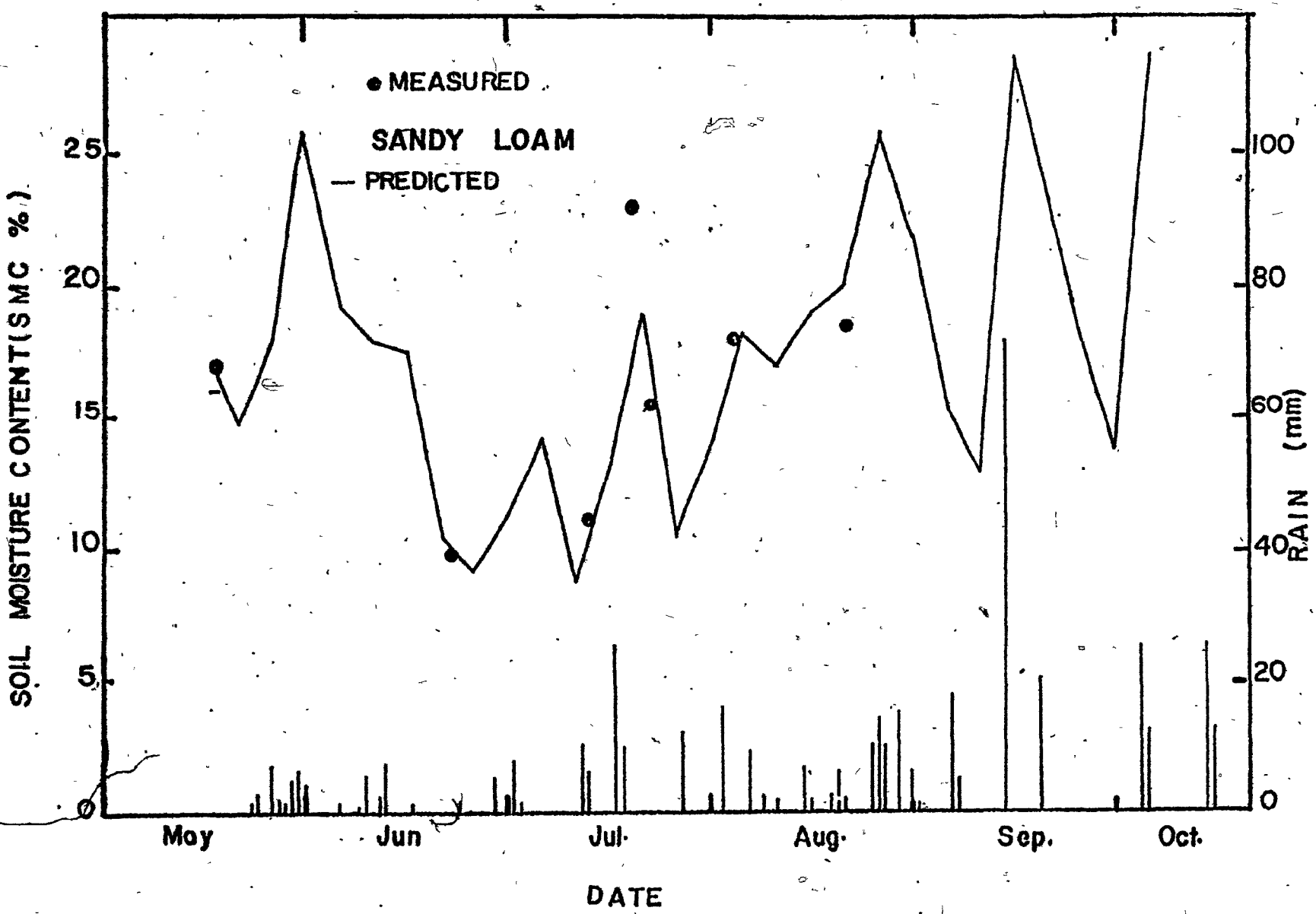

Figure 43. Predicted and measured soil moisture content during the farming season for sandy loam soil (1979).

point (dry weight basis) of each soil was added in order to predict the daily soil moisture content for the years 1941 to 1966. Tables B1 and B2 in Appendix B show the estimated soil moisture contents by weight for sandy loam and clay soils; these are averages of 25 years for 5-day periods taken during the farming season for sandy loam and clay soils (see Figure 44). These variations could be used with the models developed in this study to indicate the change in the soil mechanical properties that may occur.

Figures 45 to 50 illustrate the predicted change in each of the soil mechanical properties (c, ϕ, c'_r, c'_s, δ_r, δ_s) during the farming season for sandy loam and clay soils. In general, these figures show that the change in values of these properties for sandy loam soil are higher than in clay soil.

Figure 45 shows that the lowest values of the soil cohesion and soil friction angle could be found, in the field, in the last few days in May, the second half of June and the few days in the end of July and beginning of August in the sandy loam soil. In clay soil, however, the soil cohesion did not change very much during the growing season, and the smallest values could be expected during the second half of June. From this graph it would appear that the soil friction angle should be at a minimum in the second half of June, the beginning of August, and during the month of September. However, during these periods, which have the lowest values of c and ϕ, poor traction conditions would be expected but little soil cutting resistance, which

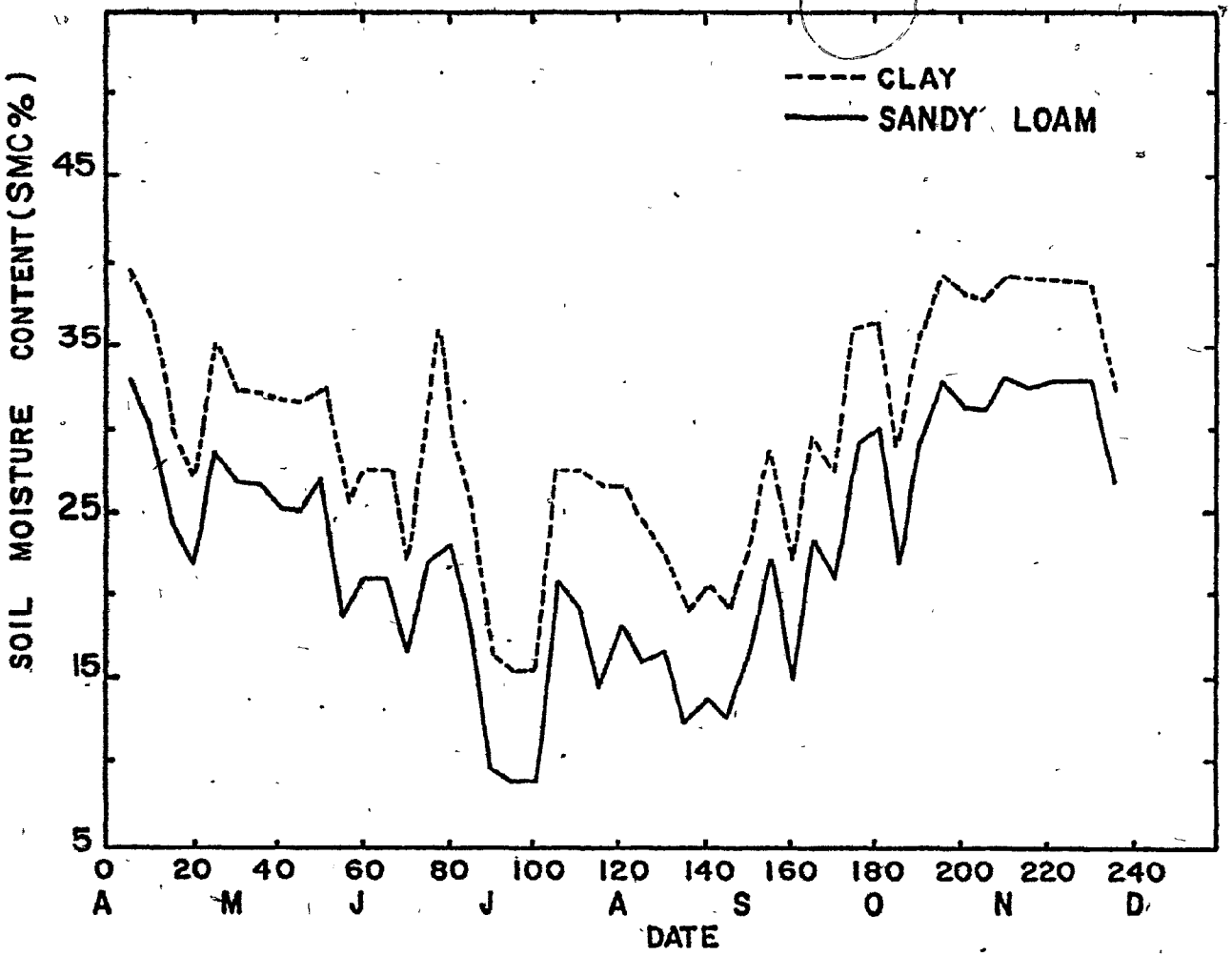

Figure 44. The mean values of soil moisture content (1941-1966) at Macdonald College farm for sandy loam and clay soils to 30-cm depth.

Figure 45. The variations in the soil cohesion and soil friction angle during the farming season for sandy loam soil (for average year 1941-1966).

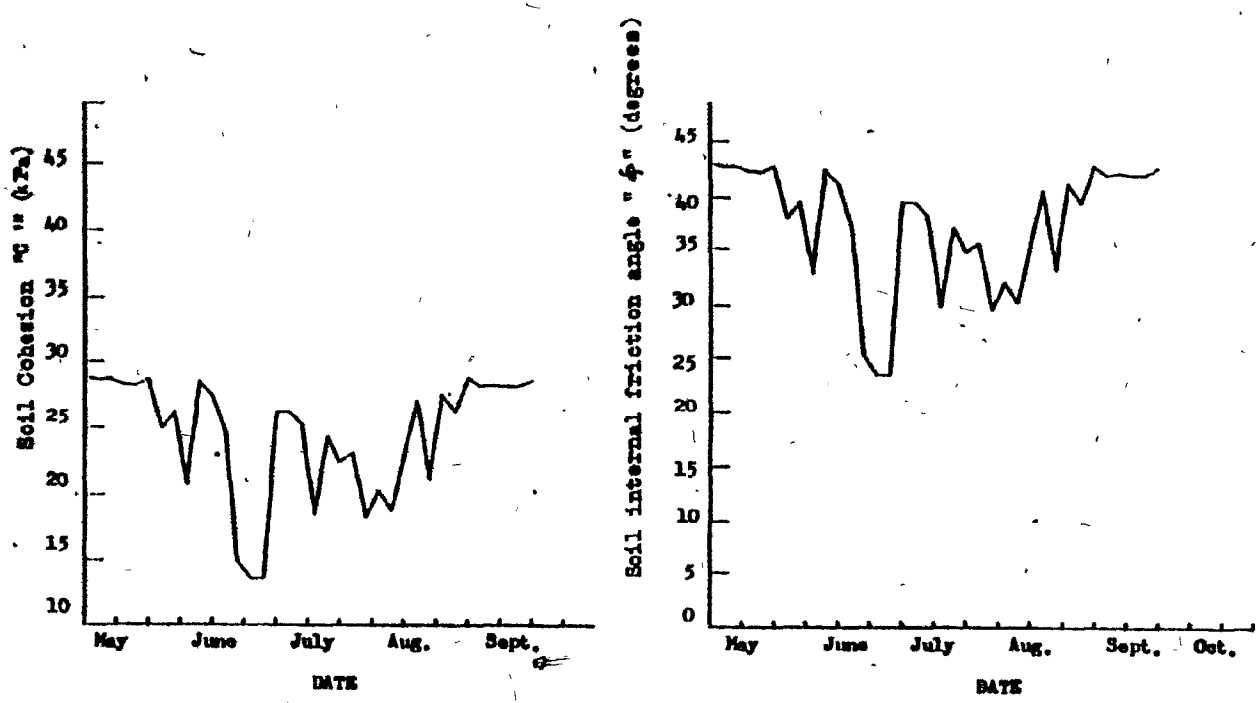

Figure 46. The variations in the soil rubber and steel friction angle during the farming season for sandy loam soil (for average year 1941-1966).

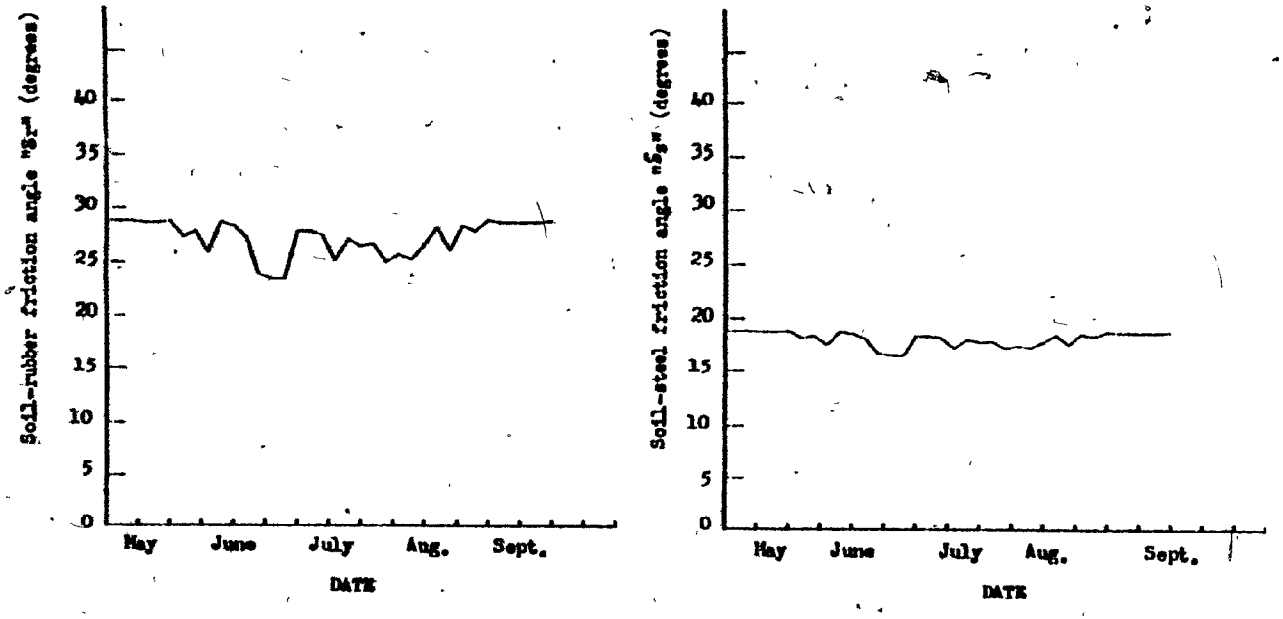

Figure 47. The variations in the soil steel and rubber adhesion during the farming season for sandy loam soil (for average year 1941-1966).

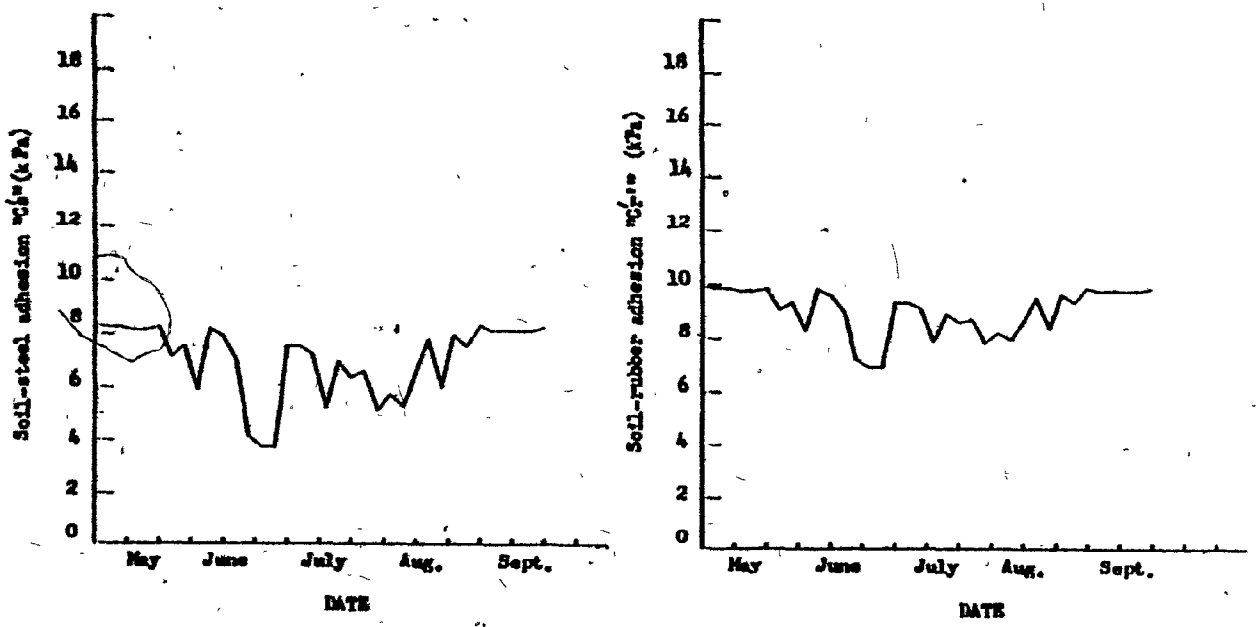

Figure 48. The variations in the soil cohesion and internal friction angle during the farming season for clay soil (for average year 1941-1966).

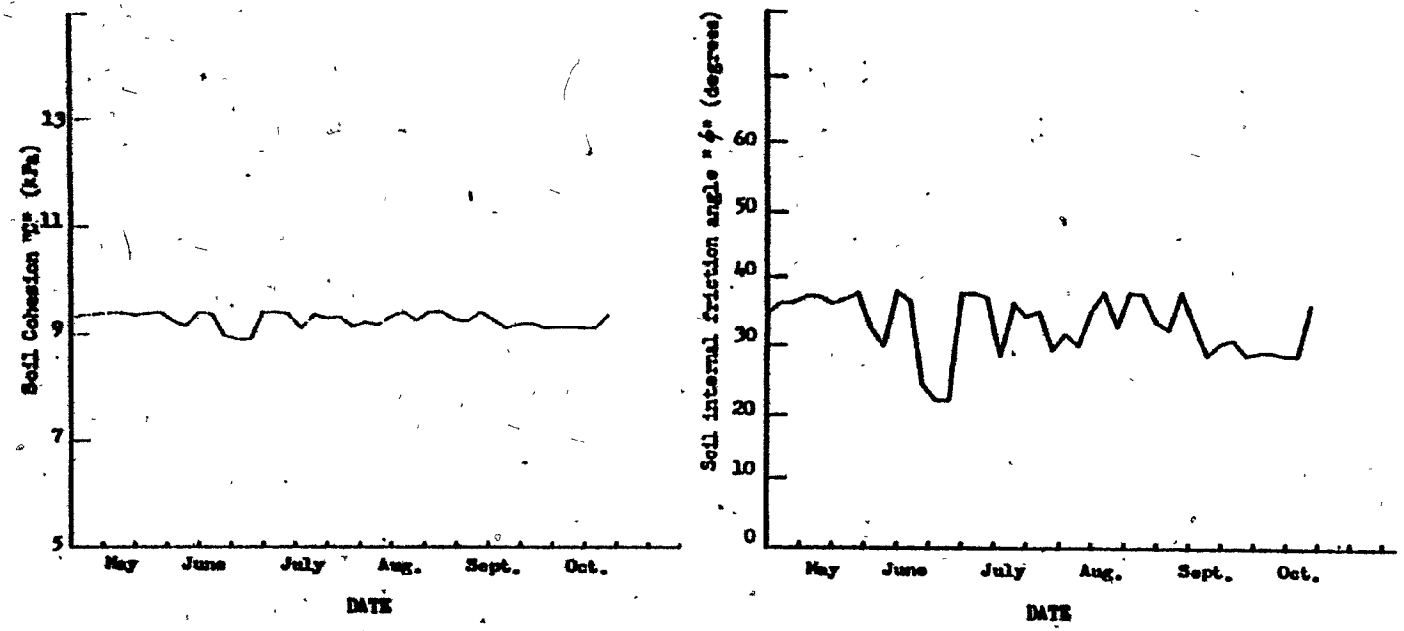

Figure 49. The variations in the soil steel and rubber adhesion during the farming season for clay soil (for average year 1941-1966).

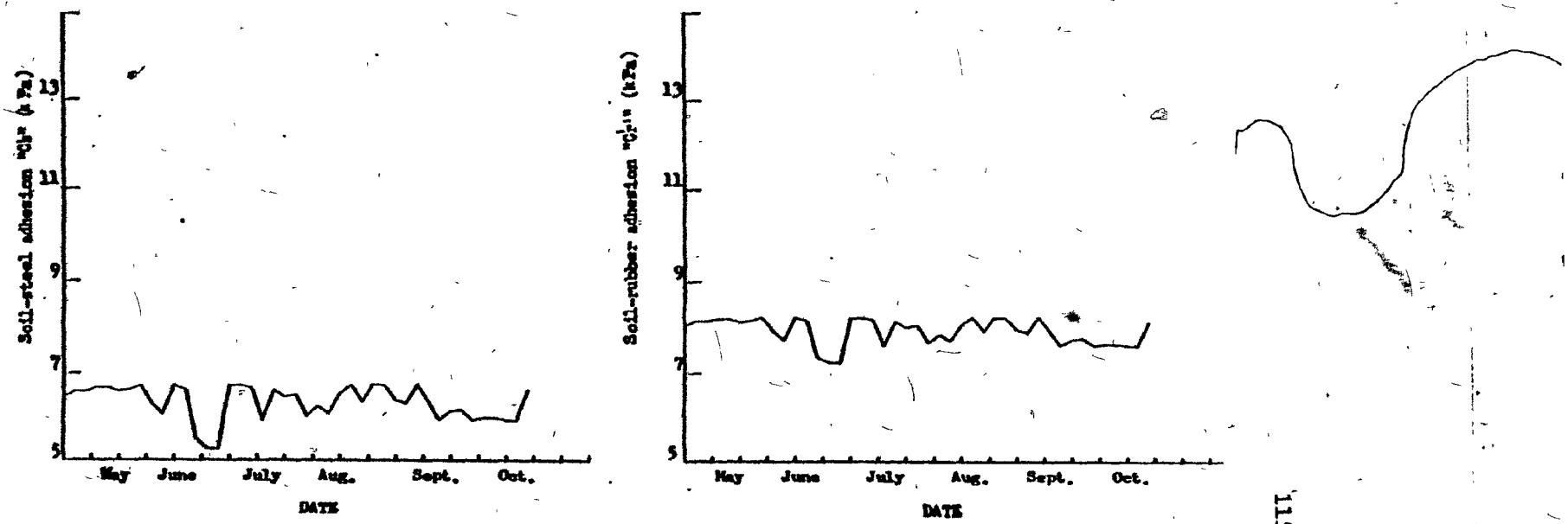

Figure 50. The variations in the soil steel and rubber friction angle during the farming season for clay soil (for average year 1941-1966).

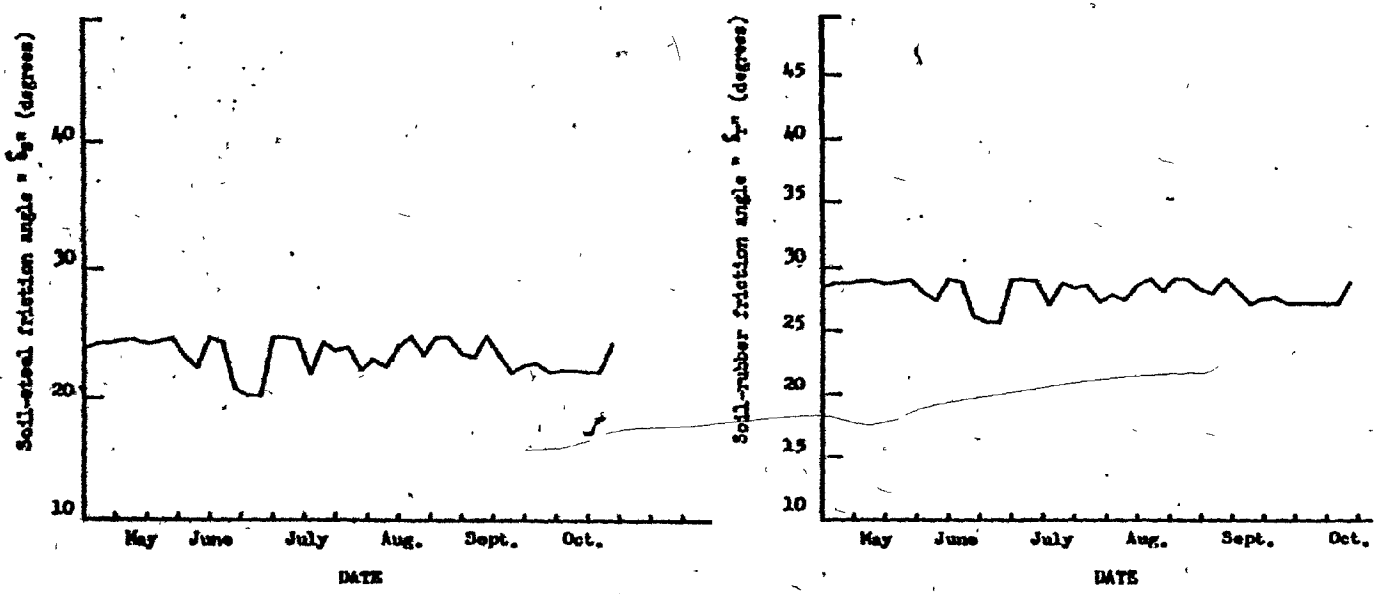

could result in soil compaction damage (Raghavan et al. 1975). Figure 46 indicates that the soil-rubber adhesion in sandy loam soil is lowest in the second half of June, but the variation in the soil-steel friction angles was not very high. In addition, during the same period of the month of June, the soil-friction angle with rubber or steel was predicted to be lowest for clay soil (Figure 50).

The soil adhesion values can give an idea of how strong the soil friction force would be against steel or rubber devices. The parameters c_r' and c_s' were lowest values during the last half of June and in the beginning of August in the sandy loam and clay soil (Figures 47 and 49). It should be noticed that the values of soil moisture content were calculated assuming that the amount of water above the field capacity will be removed quickly from the soil by subsurface drainage. If the soil has no drainage system it will take a much longer time to arrive at field capacity, which results in less time available for good working conditions during the farming season.

Figures 51 and 52 present the soil moisture content during the farming season (April to October) for the driest and wettest years within the period 1941 to 1967 for sandy loam and clay soils. The wettest year during this period was found to be 1954, which had 124 rainy days, while the driest year, 1944, had 82 rainy days. The data shown in these two figures were calculated from Chieng (1975). These data give information about two extreme years about the

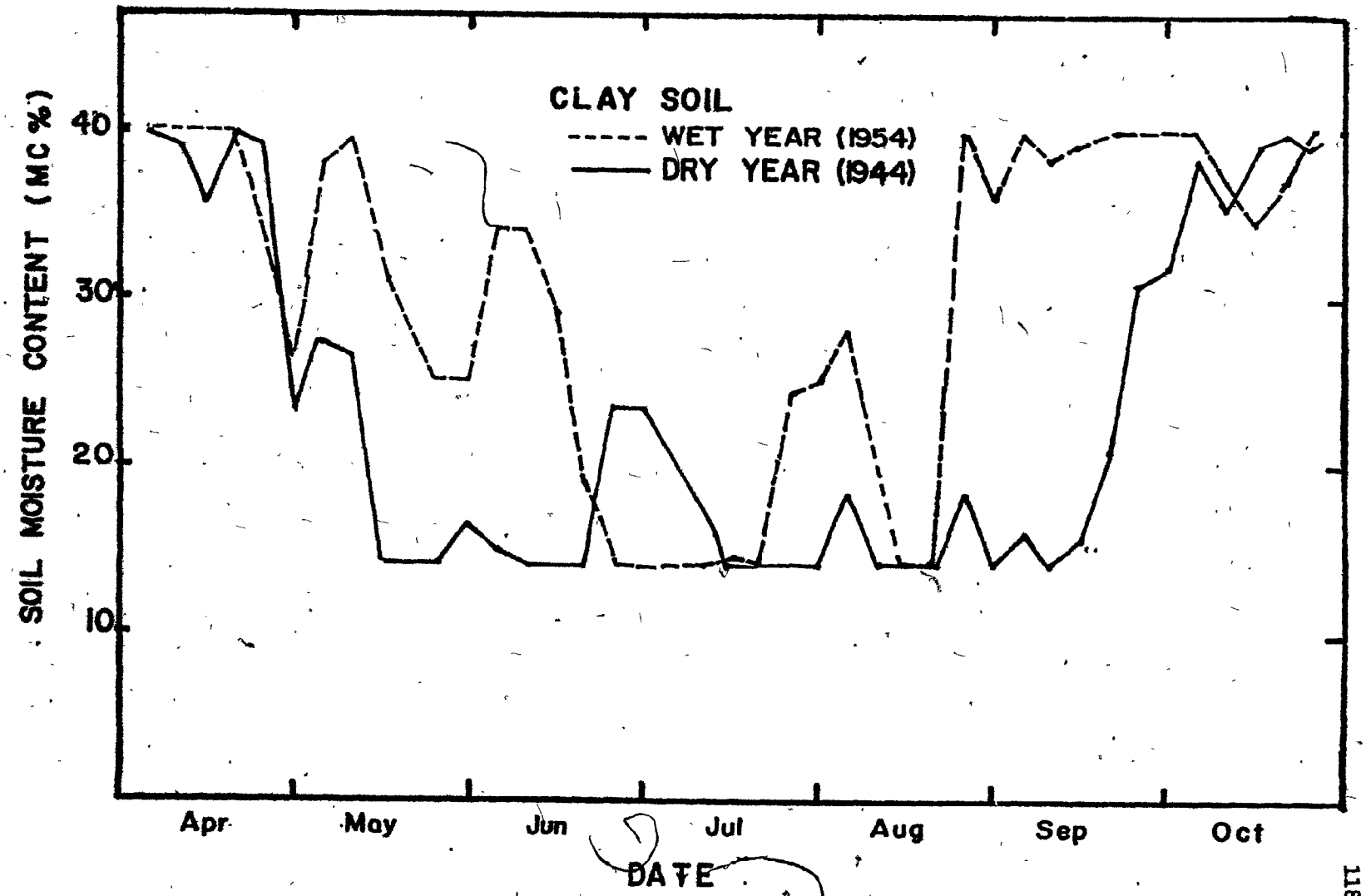

Figure 51. The relationships between soil moisture content and date for the driest and wettest year in southern Quebec during the interval 1941-1966.

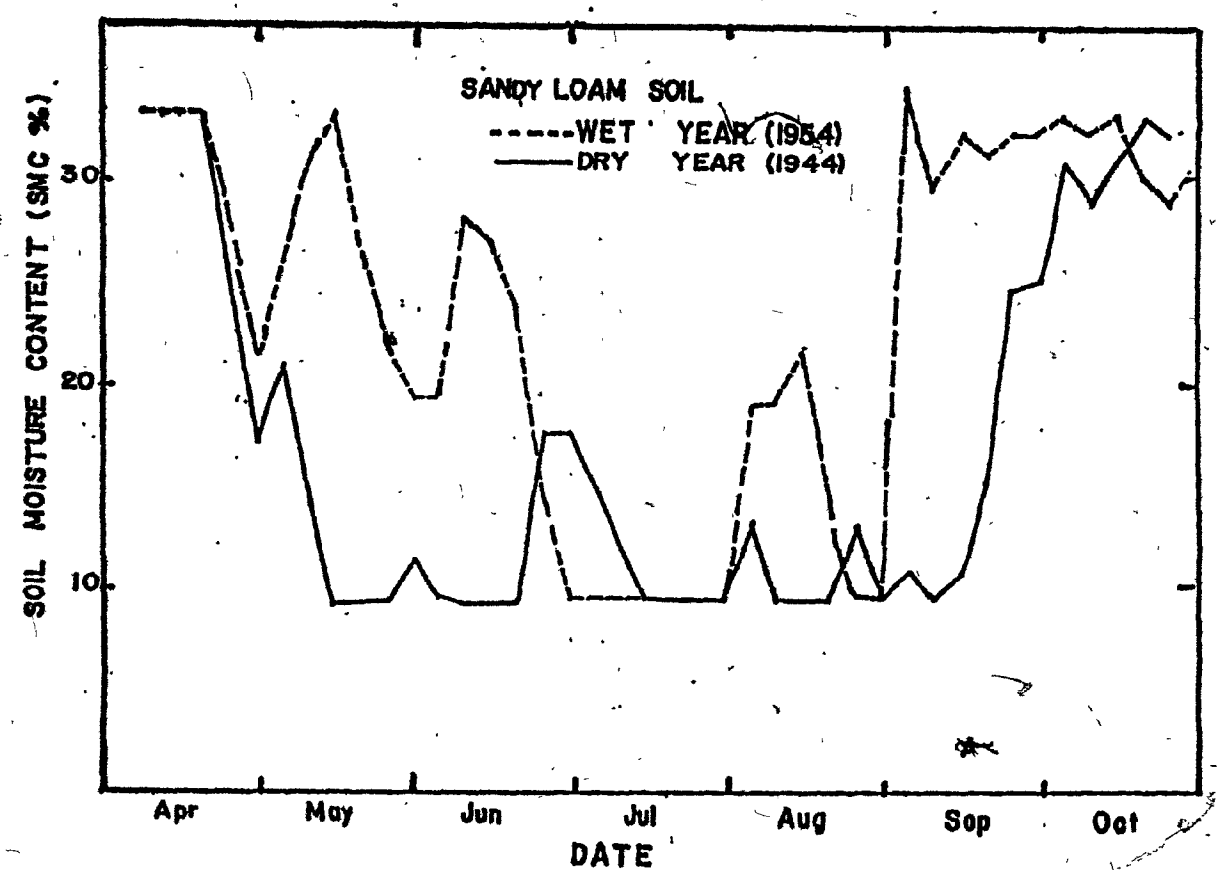

Figure 52. The relationships between soil moisture content and date for the most dry and and most wet year in southern Quebec.

number of wet or dry days during the farming season. The dry days indicate high values for soil mechanical properties (days of soil moisture content between the soil plastic limit and the wilting point), which means good working conditions. Soil with a moisture content higher than the plastic limit would be weak and "muddy" in texture, which leads to poor machinery working conditions. Therefore, the best working conditions are likely to be when the soil moisture content is less than the plastic limit. Since the sandy loam and clay soils having 23.6% and 32.1% soil moisture at the plastic limit, respectively, the period between 10 May and 20 September would be the best time for working the soil in a dry year and the period between 24 June and the end of August best for a wet year. Also, Figures 51 and 52 indicate that the minimum period for best working conditions in the field is between 24 June and the end of August in any given year. Normally at this time of the year there is no field work to be done for many field crops. However, that period could be used to do any field work for non-cultivated land, such as the installation of subsurface drainage tiles or land reclamation.

C. Traction characteristics of the lugged rubber tire

There are many areas in the field of agricultural engineering where use could be made of the models developed in this study. One of these areas in which only limited knowledge is available to the tire designer is the traction characteristics of different sizes and designs

of lugged tires. The models developed to predict the soil mechanical properties will be used in this section to study this problem.

The lug-wheel traction experiments in the field demonstrated the influence of angle of lug on soil thrust for different soil types and consistencies.

1. Effect of soil type and moisture content on the traction force

The theoretical estimation of soil thrust for all the tests was carried out according to the flow chart shown in Figure 15 using the computer program given in Table B15 in Appendix B. Tables B3 to B11 (Appendix B) and Figures 53 to 58 present the results obtained from all tested wheel models and the estimated values of total soil thrust due to the lug and to the friction between the wheel carcass and the soil for the two soil types and different water contents. These tables and figures show that the estimated and measured soil thrust are in good agreement. Therefore, the method explained in Chapter III could be used to predict the soil thrust due to the lug of a lugged tire.

Increasing soil moisture content increased the soil thrust up to the soil plastic limit for both sandy loam and clay soils, after which it declined (Figures 53 to 58). Soil thrust did not change significantly at very high moisture contents in sandy loam soil, whereas the clay soil had considerable strength under wet conditions and soil thrust decreased more gradually with increasing moisture contents.

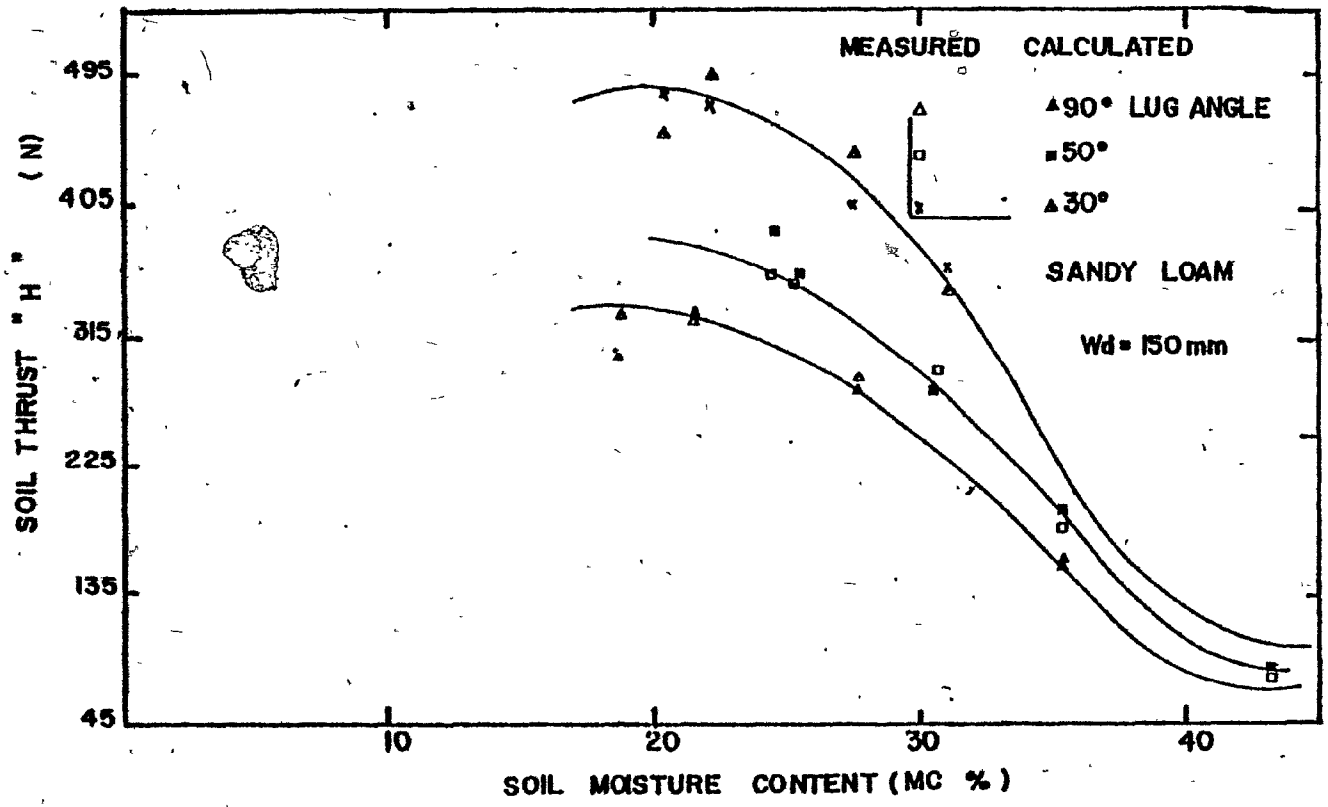

Figure 53. The estimated and measured effect of soil moisture content on soil thrust at different lug angles of 150-mm wide wheel for sandy loam soil.

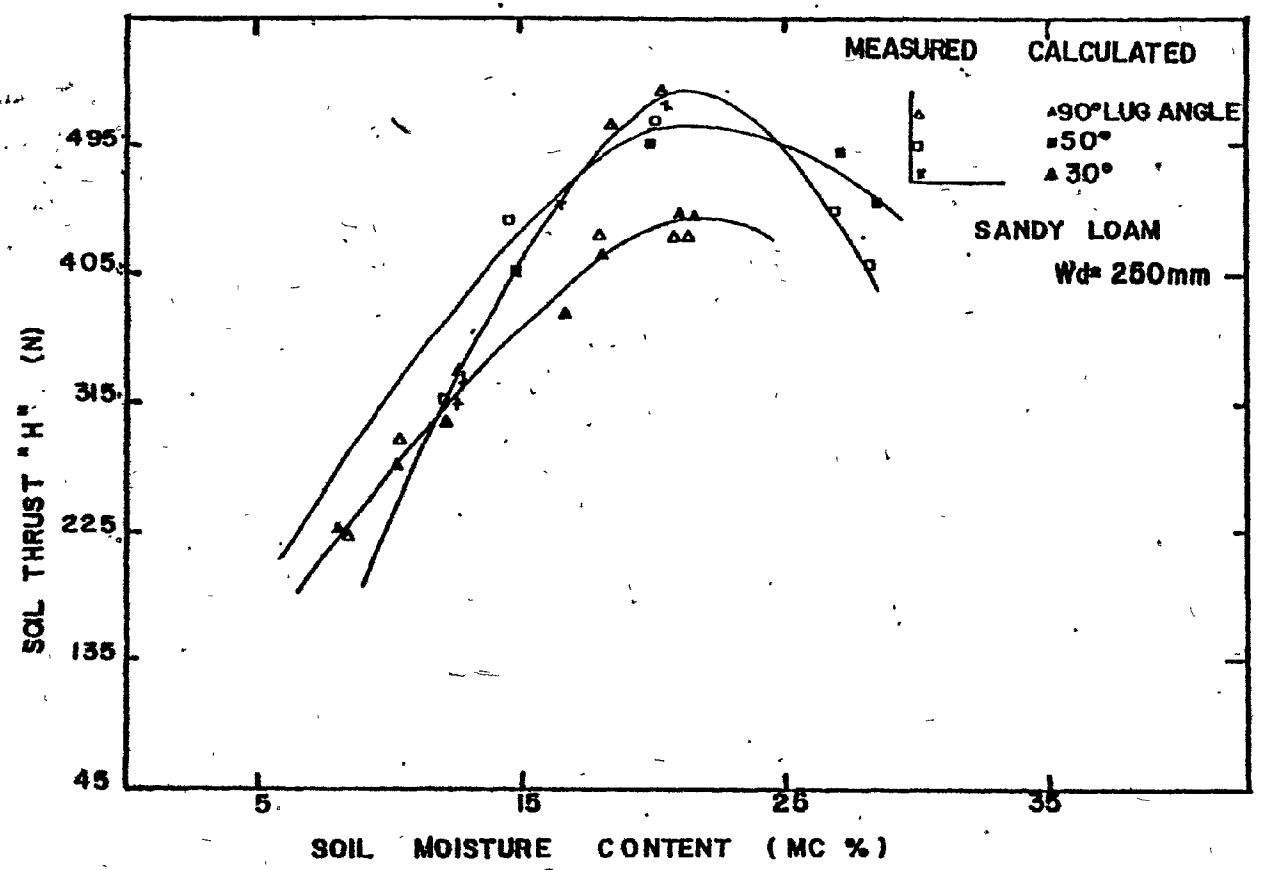

Figure 54. The estimated and measured effect of soil moisture content on the soil thrust at different lug angles of 250 mm wide wheel for sandy loam soil.

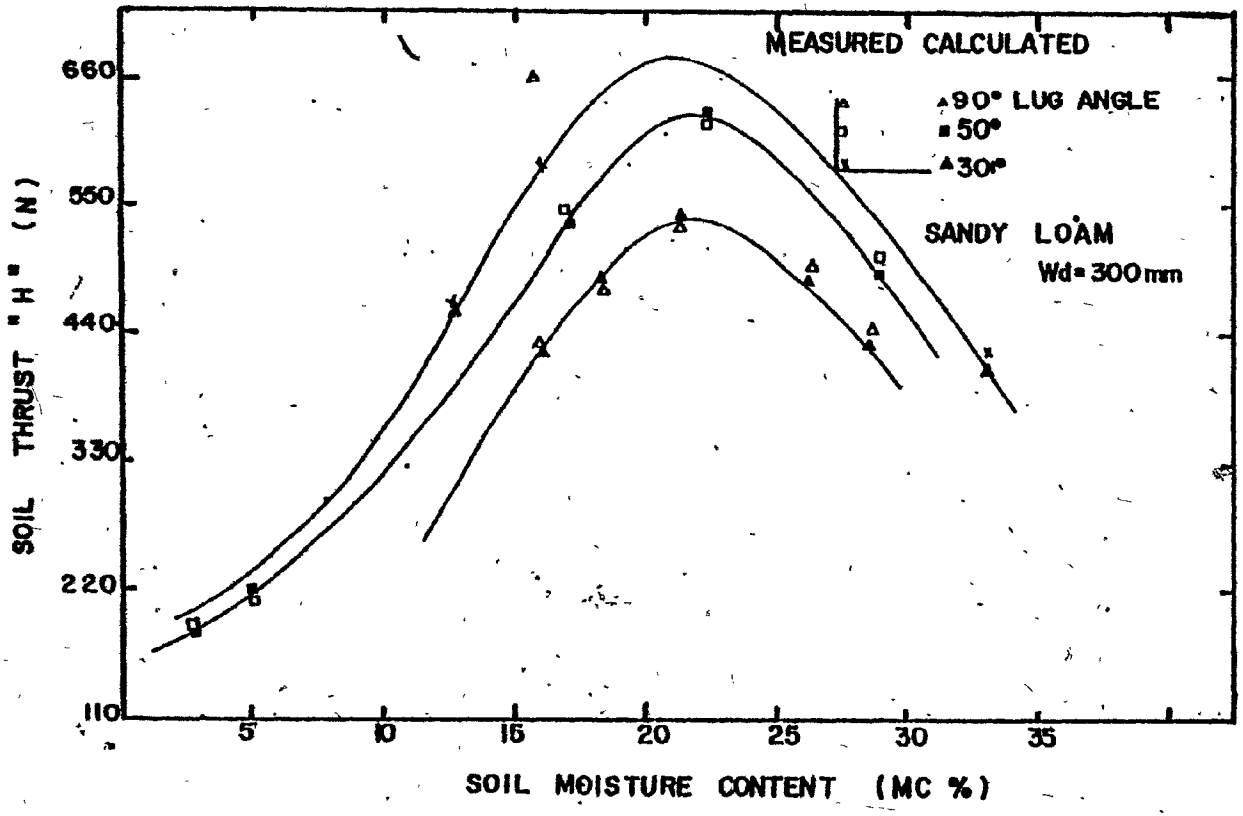

Figure 55. The estimated and measured effect of soil moisture content on the soil thrust at different lug angles of 300 mm wide wheel for sandy loam soil.

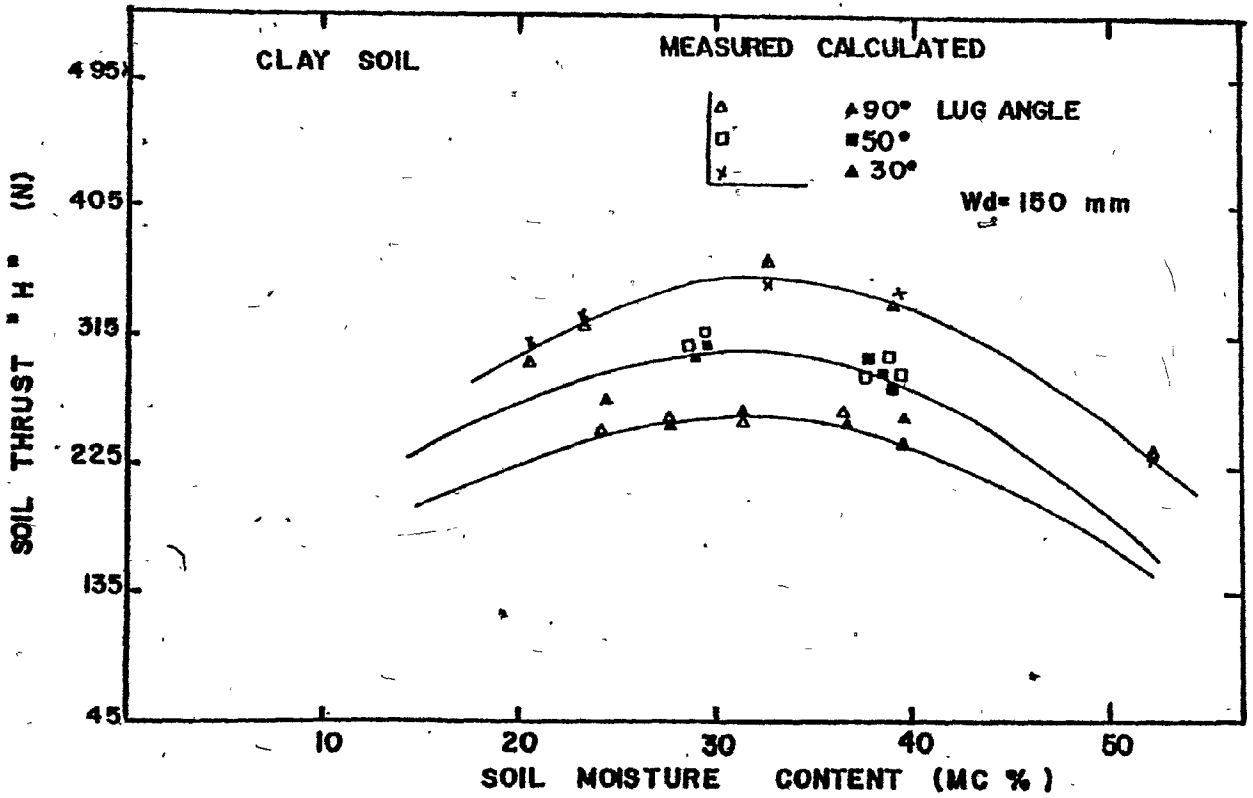

Figure 56. The estimated and measured effect of soil moisture content on the soil thrust at different lug angles of 150-mm wide wheel for clay soil.

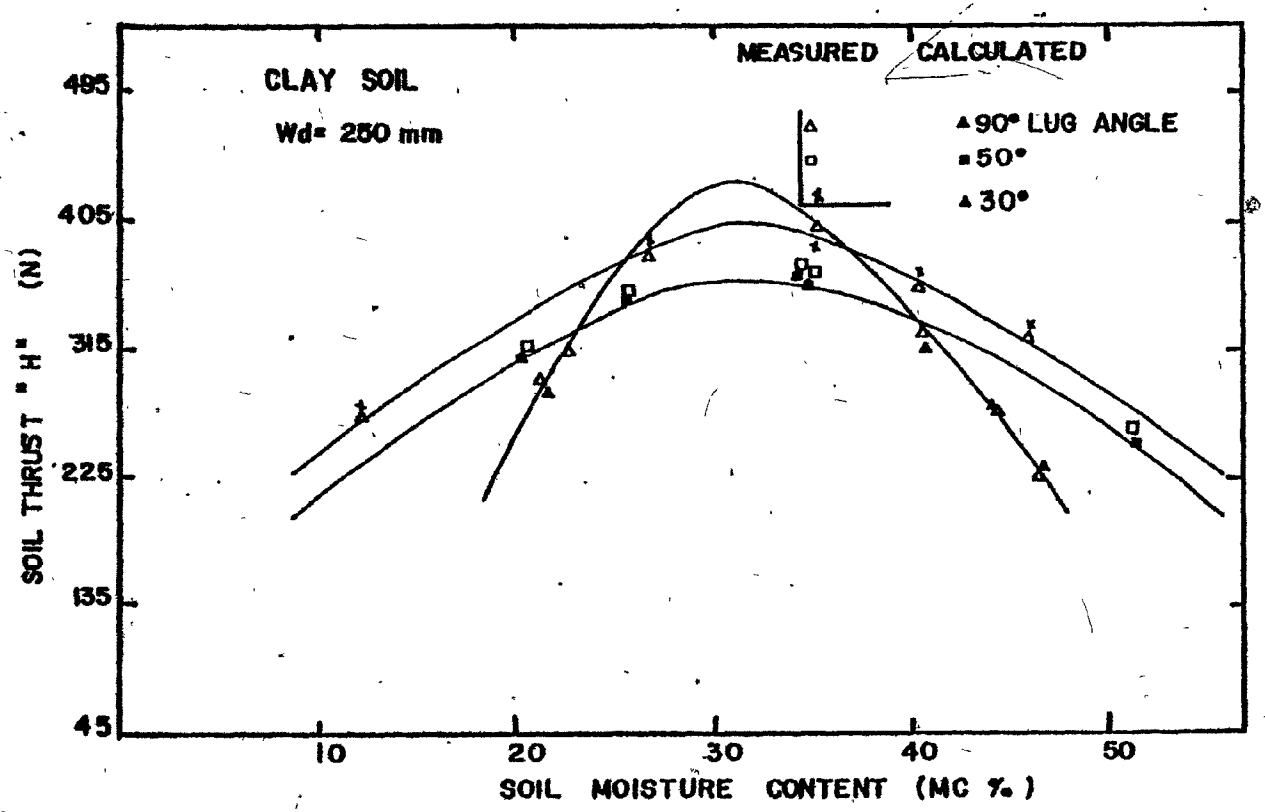

Figure 57. The estimated and measured effect of soil moisture content on the soil thrust at different lug angles of 250-mm wide wheel for clay soil.

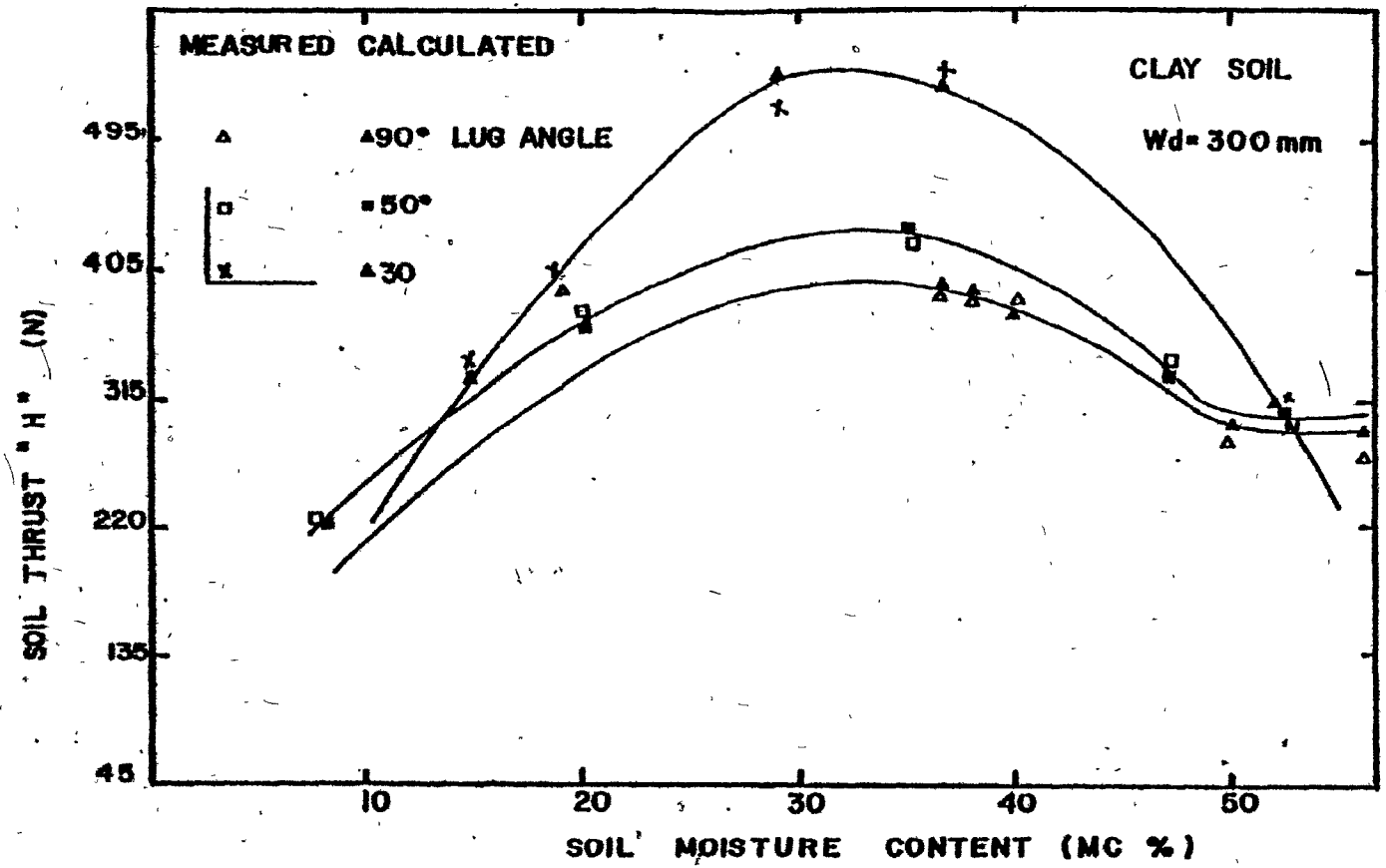

Figure 58. The estimated and measured effect of soil moisture content on the soil thrust at different lug angles of 300-mm wide wheel for clay soil.

2. Effect of lug angle on the soil thrust

Relationships between lug angle and soil thrust for different wheel widths in sandy loam and clay are given in Figures 59 and 61. Figures 60 and 62 present the relationships between the unit soil thrust (total soil thrust/wheel width) and lug angle.

It was noted that increasing the lug angle for the same wheel width decreased the lug length which in turn decreased the wheel soil thrust. On the other hand, decreasing the lug angle increased the lug length and thus increased the wheel soil thrust. Therefore, smaller lug angles led to the best soil wheel thrust. The minimum lug angle for a certain wheel-soil contact area can be obtained from

$$\theta = \tan^{-1} \frac{Wd}{b} \qquad \ldots (43)$$

where

b = length of the contact area between wheel and soil

Wd = wheel width

Changes in the lug angle above 80 degrees caused only a small change in soil thrust. Analysis of Figures 60 and 62 shows that the unit soil thrust increased with a decrease in lug angle in both sandy loam and clay soils. However, it can be stated that the trend of the relationships presented in Figures 53 to 62 did not change by changing wheel width or soil type and consistency.

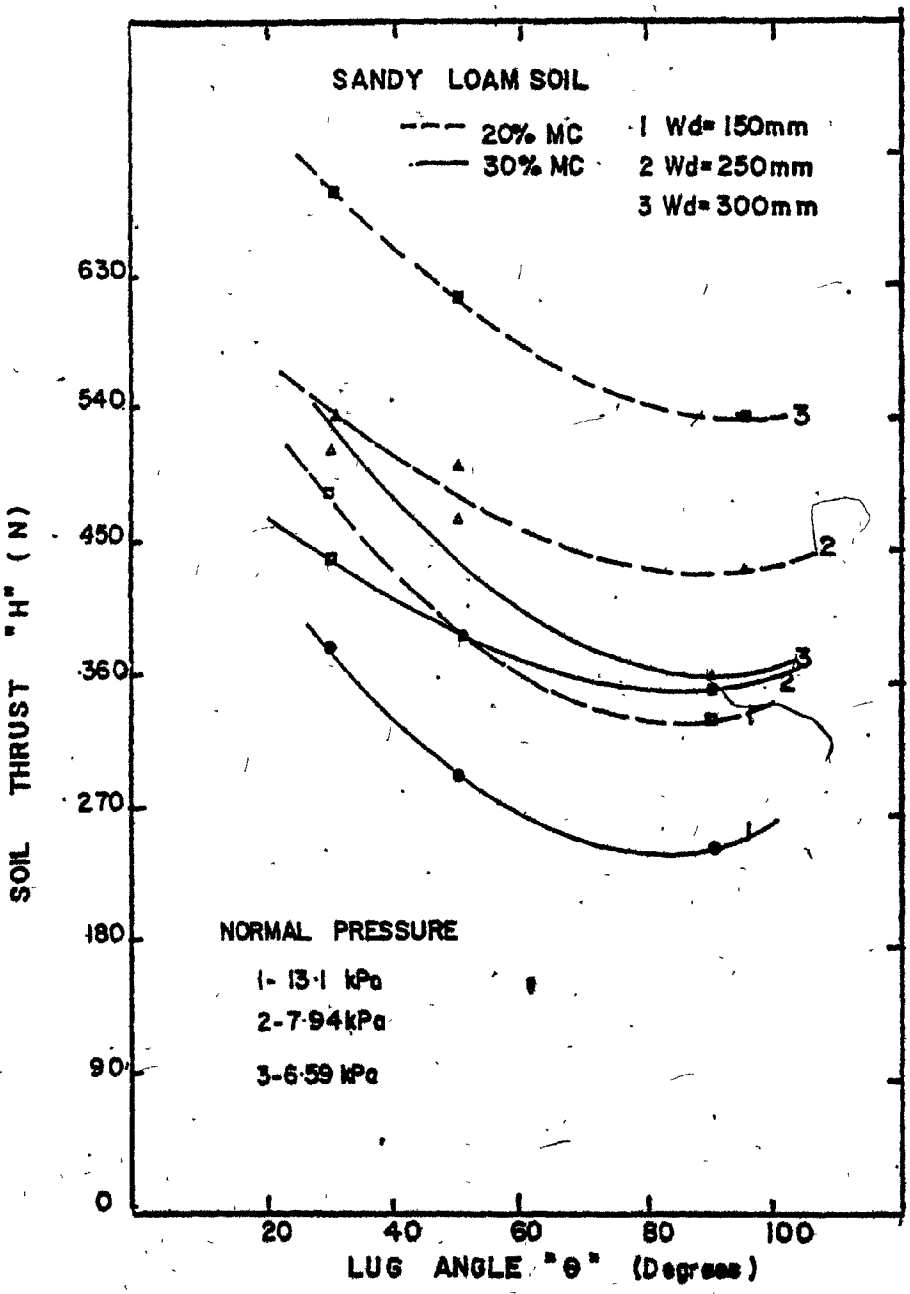

Figure 59. The relationships between lug angle and soil thrust at different wheel widths in sandy loam soil.

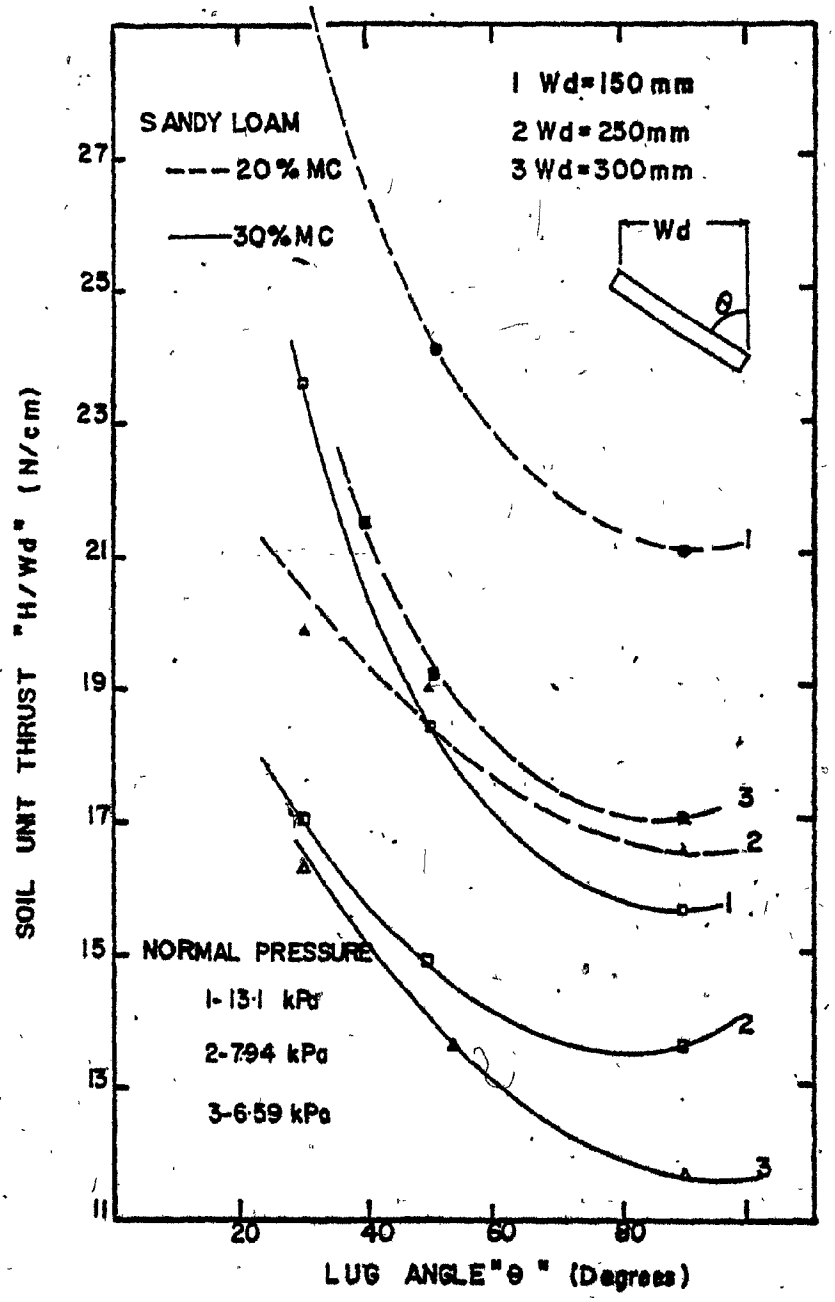

Figure 60. The relationships between lug angle and unit soil thrust at different wheel widths in sandy loam soil.

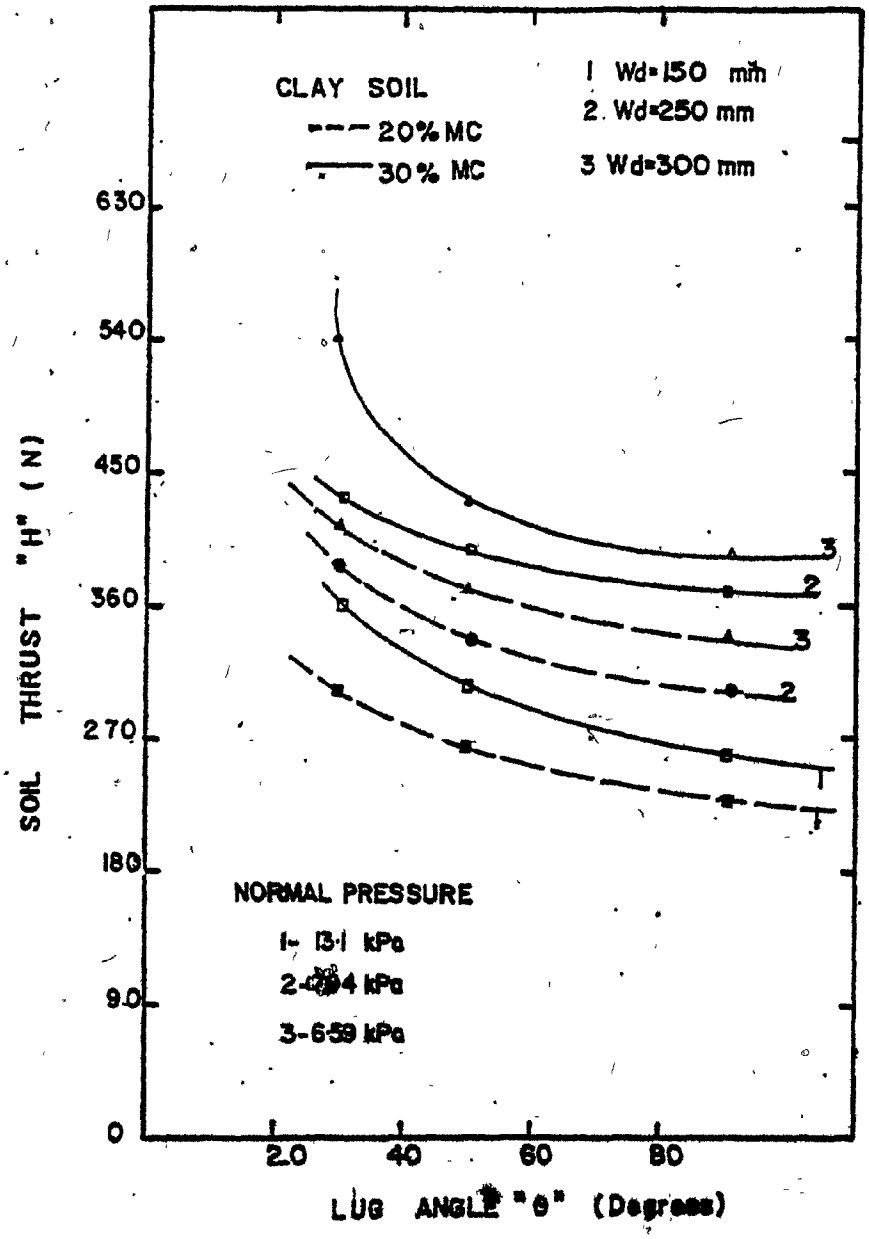

Figure 61. The relationships between lug angle and soil thrust at different wheel widths in clay soil.

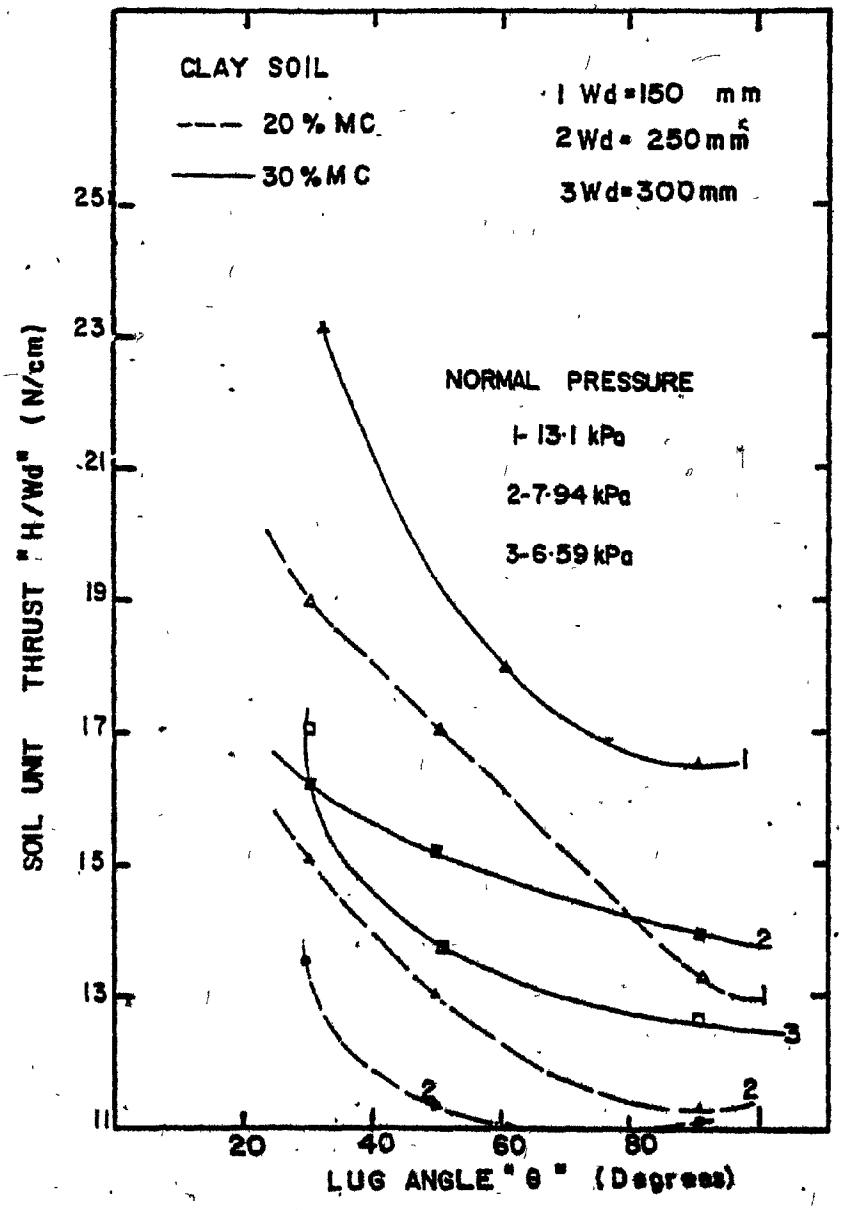

Figure 62. The relationships between lug angle and unit soil thrust at different wheel widths in clay soil.

3. Variation in the traction force during the farming season

From the average variation in the soil moisture content in sandy loam and clay soils (Figure 44) and the relationships presented in Figures 56 and 58, the soil thrust produced by a lugged tire with a width of 300 mm, during the farming season, can be obtained as shown in Figure 63. This figure indicates the variations in the soil thrust for a lugged tire with different lug angles for an average climatic year during the farming season. However, the lug angle 30° gave the best unit soil thrust during the farming season. Nevertheless, the tire user can select only one lug design in order to give the best traction force during the entire season. Also, the suitable time during the farming season can be defined from Figure 63 for certain requirements of traction force.

4. Suggested lug design

One row of lugs on the tire surface is suggested. This gives more soil thrust than the split lug design (Ali and McKyes 1978a). Figure 64 shows the shape of the suggested lug design for tractor tires to develop the best soil thrust due to the lugs. One row of lugs would cause a side force acting on the tire, thus producing additional bending moment on the wheel and the shaft. The effect of this side force on the steering stability of a tractor could be prevented by making the lug angle direction on the left tire opposite to the lug angle direction on the right tire (Figure 64).

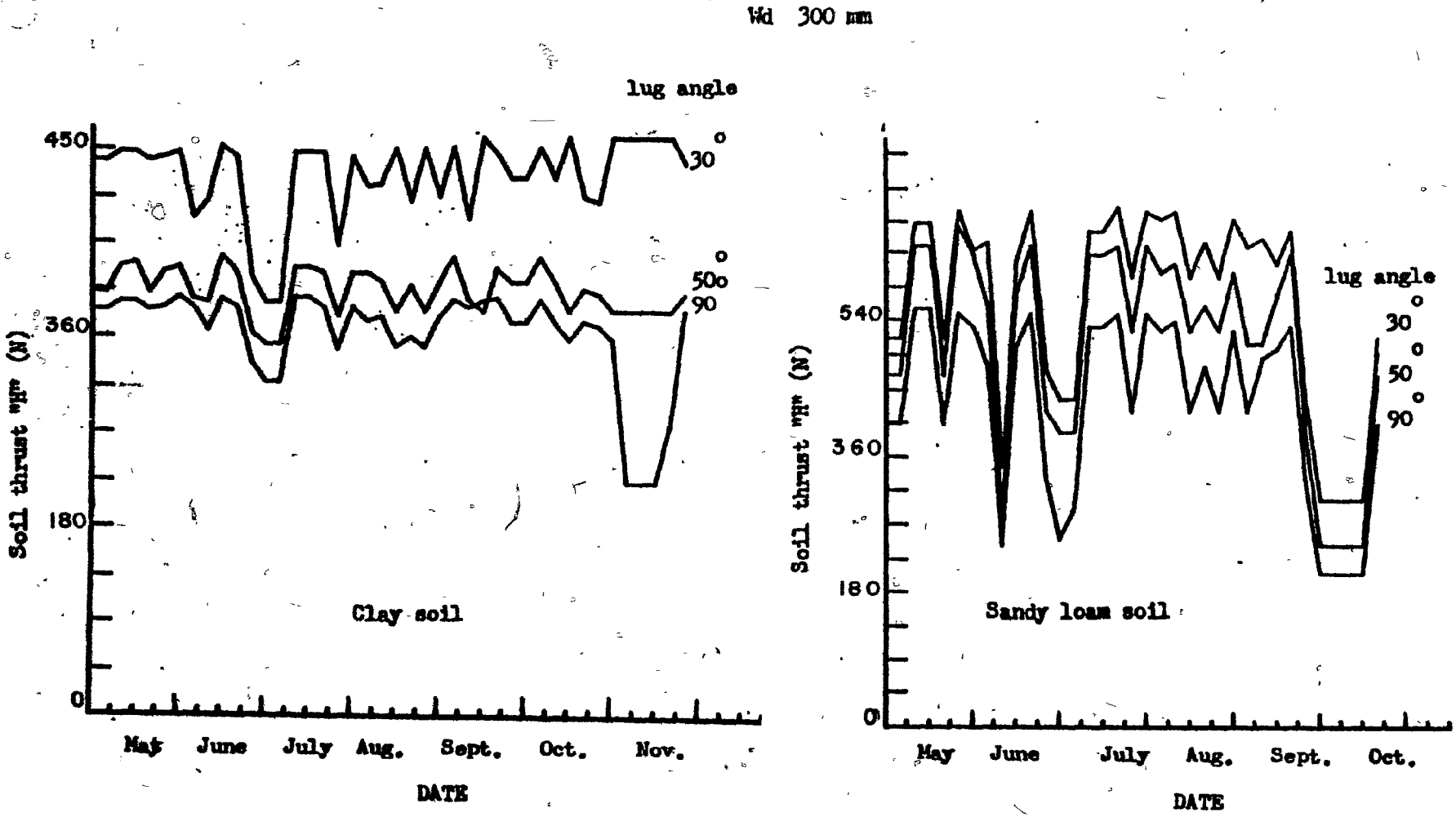

Figure 63. Relationship between the soil thrust and the date during the farming season with different lug angles and 300 mm wheel width in sandy loam and clay soils.

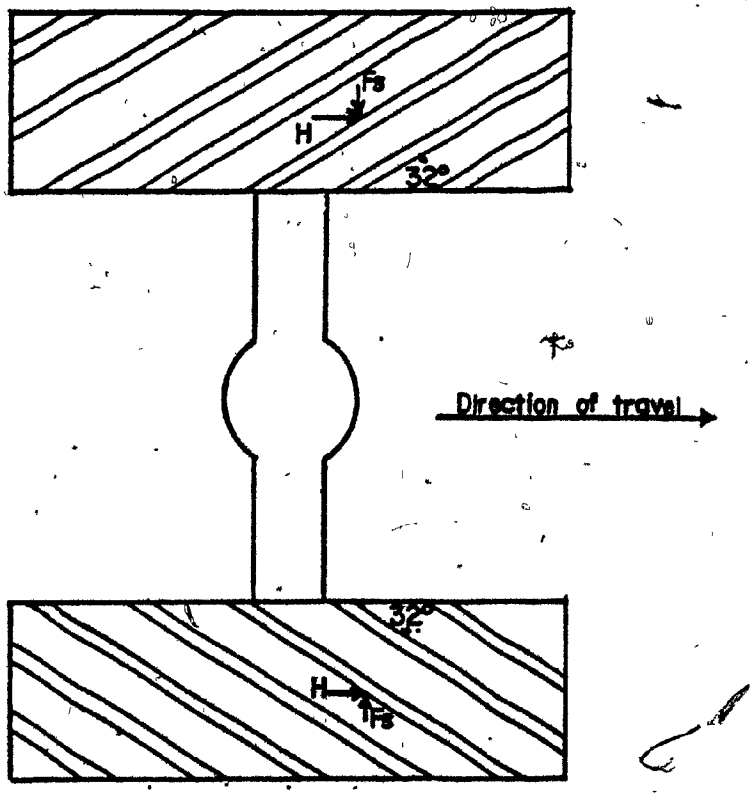

Figure 64. Example of the tread design which could be used in tractor right and left tires to avoid additional forces on the wheel axis.

In fact, this kind of tread design exists on the market (Tire Guides Inc. 1976), but not with the suggested lug angle, and there are evidently no problems reported from using it.

CHAPTER VI
SUMMARY AND CONCLUSIONS

The variations of soil mechanical properties (cohesion, c, internal friction angle, ϕ, soil rubber adhesion, c'_r, soil-rubber friction angle, δ_r, soil-steel adhesion c'_s, soil-steel friction angle, δ_s, the sinkage moduli, kc and $k\phi$, and sinkage factor n) have been studied under field conditions in a sandy loam and a clay soil. Models to predict these parameters were developed in this study. These models were functions of soil moisture content, soil plastic limit or liquid limit and two constants which depend on soil type and depth. These models could be used to predict the soil mechanical properties within a range of soil moisture content not exceeding the liquid limit. The models were applied to different soil depths (0, 5, and 10 cm). This range (from 0 to 10 cm) of soil depth has the largest variation in the parameters mentioned above at different times of the year. Also, interaction between soil and traction devices takes place within this layer of soil.

In order to predict the behavior of any farm machine or tractor by using these models, the soil moisture content during the farming season must be estimated. Therefore, a model to estimate the soil moisture content by a simple and adequate method was developed in this

study. Daily precipitation and evaporation from a class A pan are required by this model to predict the soil moisture content.

All the models developed in this study were verified by measured data from the field in sandy loam and clay soil. The predicted soil parameters or moisture content using these models were in good agreement with the measured data.

The traction characteristics of lugged tires were investigated by using the developed soil mechanical properties models. Prototype models of lugged tires were made by changing the shape of a wheel surface using 9 different lug designs. These designs had various lug angles (30, 50 and 90°) and wheel widths (150, 250, and 300 mm.). These lug designs were tested in two fields (sandy loam and clay soils) on the Macdonald College Farm, using a single wheel testing apparatus. The field experiments were carried out at different soil moisture contents ranging from very dry to very wet soil (above the liquid limit). Modifications to the theory of Hettiaratchi and Reece (1974) were used. The predicted value of soil thrust and the estimated soil mechanical properties from the models developed in this study were in good agreement. This study shows that the developed models of soil mechanical properties could be used successfully to predict the soil-machine interactions.

From the developed models and the field experiments, the following conclusions can be made:

1. The investigation confirmed that the soil mechanical properties (c, ϕ, c'_r, c'_s, δ_r, δ_s) increased with increasing soil moisture content up to the plastic limit and then decreased with increasing soil moisture for the sandy loam and clay soils.
2. The relationships between the soil moisture content and the parameters (c, ϕ, c'_r, c'_s, δ_r, δ_s) appeared to show the same trend at different soil depths (0, 5, 10 cm) for both soils.
3. The moduli kc and kϕ which are widely used to predict the sinkage load relationships decreased with increasing soil moisture content up to the soil liquid limit and then increased slightly with increased soil moisture content within the range of soil moisture contents studied. In addition, the factor n was reduced with increasing soil moisture up to the plastic limit and then increased slightly at higher soil moisture content.
4. Daily evaporation (class A pan), together with rainfall data, could be used in order to estimate the soil moisture content during the farming season according to the models developed in this study.
5. The good agreement between predicted and measured wheel soil-thrust of lugged tires shows that the developed models are acceptable for estimating soil mechanical properties.
6. Increasing soil moisture content resulted in increasing soil thrust up to the plastic limit under field conditions. For soil moisture content above the plastic limit, soil thrust becomes smaller. The behavior was found to be correct for the sandy loam and clay soils.

7. Changing the wheel width did not change the trend of the relationships between soil thrust and moisture content for the two soil types studied.
8. The magnitude of soil thrust increased by decreasing the lug angle. The force increased rapidly at angles less than 60°, while the rate of increase was smaller at higher lug angles. However, the smallest practical lug angle on the wheel surface which would give the best traction force can be obtained from the equation:

$$\theta = \tan^{-1} \frac{Wd}{b}$$

where

Wd = wheel width

b = wheel length in contact with soil

9. The trend of the relationships between lug angle and soil thrust was similar for the two soil types studied.
10. The variations in soil mechanical properties during the farming season were estimated for an average climatic year in southern Quebec.
11. The traction force of a lugged tire can be estimated successfully using the developed models in order to define the best time during the farming season to get the highest soil thrust for a farm vehicle.
12. The tire user should select a tire which has the minimum lug angle.

13. The farmer need use only one tire during the farming season for optimum traction force, since the trends of traction dependence on lug geometry did not alter appreciably with soil moisture content in the soils tested.

14. The models presented in this study could be used for other soil types as long as the constants C_1 and C_2 are evaluated for those soil types.

CHAPTER VII

CLAIMS TO ORIGINAL RESEARCH

As far as the author is aware, the following aspects of the study can be claimed as original work and contribution to knowledge:

1. The development of models for the soil properties c, ϕ, δ_r, c'_r, c'_s, and δ_s, as a function of soil moisture content and plastic limit (equation 20 and Table 6) for a sandy loam and clay soils.
2. The development of models for the sinkage moduli kc and kϕ and factor n for two soil types as a function of soil liquid or plastic limit and soil moisture content (equations 36 to 41).
4. Using the ratio of potential evapotranspiration to evapotranspiration along with the ratio of potential evapotranspiration to evaporation from an open pan to predict soil moisture content during the farming season as a step to estimate traction conditions.
5. The use of a newly designed field single wheel apparatus to test the effect of changing the surface of the wheel with different lug designs and their effects on traction.
6. The development of a procedure to calculate the soil thrust due to the lugs of a lugged tire.
7. Proposing a definition of the lug space value (equation 25).

As far as the author is aware, the following conclusions have not been reported in the literature and are a direct result of the present study.

(a) The small lug angles across the tire provide more traction force than higher angles.

(b) Changing the soil type and its consistency does not change the optimal lug design. The farmer can use only one lug angle for the entire farming season on a wide range of soil conditions and expect the greatest traction possible at all times.

(c) The variation of the soil mechanical parameters (c, ϕ, c_r', δ_r, c_s', δ_s) for an average climatic year in southern Quebec in sandy loam and clay soils was shown in Figures 45 to 50.

(d) The relationships between soil moisture content and soil thrust for lugged tires with different lug angles and wheel widths were demonstrated in sandy loam and clay soils.

CHAPTER VIII

RECOMMENDATIONS FOR FURTHER RESEARCH

In order to generalize the proposed soil mechanical properties models and their use, further investigation must be carried out. However, as a result of this investigation it can be suggested that the following topics would be valuable projects for future research.

1. Testing the suggested models for the soil mechanical properties in different soil types and different regions with very dry or muddy soil conditions.
2. A comprehensive study about the variation in the soil mechanical properties at specific times and locations for different soil types and regions.
3. Validate the proposed model of soil moisture content under different types of vegetation and regions.
4. Optimization of the lug position and dimensions on the wheel surface for the best power efficiency of the farm tractor under different operating conditions.
5. Study the effect of lug dimension and distribution, on the tire surface, on wheel rolling resistance under different slip rates.
6. Study the shape of soil failure in three dimensions ahead of a narrow and deep lug for different soil types and conditions.

7. Study the relationship between the lug angle (θ) and direction of soil movement on the lug face (ε) for different soil conditions, types, and normal loads on the soil surface.

REFERENCES

Agricultural Engineering Year Book. 1976. ASAE, St. Joseph, Michigan.

Ali, O. S., and E. McKyes. 1978a. Effect of lug position on soil thrust for lug models. CSAE 20(2): 119-126.

_____. 1978b. Traction characteristics of lugs for tires. Trans. of ASAE 21(2): 239-243 and 248.

American Society for Testing Materials. 1968. Testing rubber. D.1761.

Artemov, F. F., and I. N. Serebryakov. 1967. The influence of auxiliary lugs on the tractive performance of the 6-ton self-propelled chassis. Traktory i sel Khozmashiny No.7, p. 17-18.

Ayers, H. D. 1968. Role of soil moisture in the hydrological cycle. Proc. Hydrol. Sym. No.6. Soil moisture, p. 3-24.

Baier, W., and G. W. Robertson. 1966. A new versatile soil moisture budget. Can. J. of Plant Sci. 46: 299-315.

Bailey, A. C., and J. A. Weber. 1965. Comparison of methods of measuring soil shear strength using artificial soils. Trans. ASAE 8(2): 153-160.

Bailey, A. C., E. C. Burt, and J. H. Taylor. 1976. Thrust-dynamic weight relationships of rigid wheels. II. The effect of soil and wheel surface. Trans. of ASAE 19: 37-40.

Bekker, M. G. 1952. Theory of land locomotion. The Univ. of Michigan Press.

_____. 1960. Off-the-road locomotion. The Univ. of Michigan Press.

_____. 1969. Introduction to terrain vehicle systems. The Univ. of Michigan Press, Ann Arbor.

Bhattacharya, A. K. 1977. Hydrologic and economic models for surface drainage. Ph.D. thesis. Macdonald College, McGill Univ., Montreal, Canada.

Bond, J. J., and W. O. Wills. 1969. Soil water evaporation: surface residue rate and placement effects. Soil Sci. Amer. Proc. 33: 445-448.

_____. 1970. Soil water evaporation: first stage drying as influenced by surface residue and evaporation potential. Soil Sci. Amer. Proc. 34: 924-928.

Cackett, H. E., and R. R. Metelerkamp. 1963. The relationship between evapotranspiration and the development of field bean crop. Rhod. J. Agr. Res. 1: 18-21.

Chieng, Sie-Tan. 1975. The effects of subsurface drain depths and drainage rates on water table levels. M.Sc. thesis. Macdonald College of McGill University, Montreal, Canada.

Chieng, S. T., R. S. Broughton, and N. Foroud. 1978. Drainage rates and water table depths. Journal Irr. and Drainage Div. ASCE, Vol. 104, No. IR4, Proc. Paper 14260, Dec. 1978, p. 413-433.

Dwyer, M. I., P. R. Comely and D. W. Evernden. 1974. The field performance of some tractor tyres related to soil technical properties. J. Agr. Eng. Res. 19: 35-50.

Foroud, N., and R. S. Broughton. 1974. The effects of different drainage coefficients on the duration of high water table in southwestern Quebec. CSAE Annual Meeting, Ste-Foy, Quebec, Canada.

Fountaine, E. R. 1954. Investigations into the mechanism of soil adhesion. J. Soil Sci. 2(5): 251-263.

Fountaine, E. R., and N. J. Brown. 1959. Shearing resistance of top soils under small normal loads. J. of Agr. Eng. Res. 4(1): 53-59.

Freitag, D. R., R. L. Schafer and R. D. Wismer. 1970. Similitude studies of soil machine systems. J. of Terramechanics 2(7): 25-59.

Gee-Clough, D., M. McAllister and D. W. Evernden. 1977. The effect of lug height on the tractive performance of tractor drive wheel tyres. NIAE Departmental Note No. Dn/T/679/1415.

Ghani, A. M. 1966. Determination of shear stress of a fine cloddy soil with a "guarded" shear head. 2nd International Conference Terrain Vehicle Systems, Quebec 1966.

Gill, W. R. and G. E. VandenBerg. 1967. Soil dynamics in tillage and traction. Agriculture Handbook No.316.

Gross, W. A. and A. D. Elliott. 1946. Traction as influenced by soils and their condition. Transaction of the Society of Automotive Engineering (Dec. 1946), p. 27-28.

Hettiaratchi, D. R. P. and A. R. Reece. 1967. Symmetrical three dimensional soil failure. J. of Terramechanics 3(4): 45-67.

_____. 1974. The calculation of passive soil resistance. Geotechnique 24: 289-310.

Holmen, R. M. and G. W. Robertson. 1963. Application of the relation between actual and potential evapotranspiration in dry land agriculture. Trans. of the ASAE 6(1): 65-67.

_____. 1964. The calculation of the soil moisture budget. International Assoc. Sci. Hydrol. Land Erosion, Precipitation, Hydrometry, Soil Moisture 65: 454-461.

Ikeda, T. and S. P. E. Persson. 1968. A track shoe for soft soil. Trans. of ASAE 6(11): 746, 749, 753.

Lake, E. B. 1968. Soil moisture deficits and surpluses in south-western Quebec. M.Sc. Thesis, Macdonald College, McGill Univ., Montreal, Canada.

Lambe, T. W. and R. V. Whitman. 1969. Soil mechanics. John Wiley & Sons, Inc., New York.

Lee, I. K. (ed.). 1974. Soil mechanics - New horizons. American Elsevier Publishing Company, Inc., New York.

Lemon, E. R. 1956. The potentialities for decreasing soil moisture evaporation loss. Soil Sci. Amer. Proc. 20: 120-125.

Lewis, E. B. and R. H. Burgy. 1964. Hydrologic balance from an experimental watershed. J. Hydrol. 2: 197-212.

Lumb, P. 1966. The variability of natural soils. Canadian Geotechnical J. 3: 74-97.

_____. 1970. Safety factors and probability distribution of strength. Canadian Geotechnical J. 7: 225-242.

McKyes, E. and O. S. Ali. 1977. The cutting of soil by narrow blades. J. of Terramechanics 14(2): 43-58.

McKyes, E. and E. Stemshorn. 1977. Effect of machinery traffic in Quebec apple orchards and possible means for minimizing them. Paper No. 77-212 presented at the 1977 Annual Meeting of CSAE.

Mitchell, J. K. 1976. Fundamentals of soil behavior. John Wiley & Sons Inc., New York.

Monteith, J. D. 1965. Evaporation and environment. Symposia of the Society for Experimental Biology, Cambridge Univ. Press, Cambridge, England, 19: 205-234.

Neal, N. M. 1966. Friction and adhesion between soil and rubber. J. Agric. Eng. Res. 11(2): 108-112.

Negi, S., E. Douglas, F. Taylor, E. McKyes and V. Raghavan. 1979. Effect of machinery traffic and tillage operations on soil physical properties and plant yields. Report for Quebec Ministry of Agriculture. Department of Agricultural Engineering, Macdonald Campus, Quebec, Canada.

Nichols, M. L. 1932. The dynamic properties of the soil. III. Shear values of uncemented soils. Trans. of ASAE 26: 47-50.

O'Callaghan, J. R., K. M. Farrebly and P. J. McCullen. 1964. Limitations of the torsion shear test. J. of Agr. Eng. Res. 1(14): 114-117.

Osman, M. S. 1964. The mechanics of soil cutting blade. J. of Agr. Eng. Res. 9(4): 313-328.

Pandey, K. P. and T. P. Ojha. 1973. Effect of lug angle on tractive performance of rigid wheel in puddled soil. Harvester 15: 29-33.

Payne, P. C. J. and E. R. Fountaine. 1952. A field method of measuring shear strength of soils. J. of Soil Science 1(3): 137-144.

Payne, P. C. J. 1956. A field method of measuring soil/metal friction. J. of Soil Science 2(7): 235-241.

Penman, H. L. 1941. Laboratory experiments on evaporation from fallow soil. J. Agr. Sci. 31: 454-465.

_____. 1948. Natural evaporation from open water, bare soil and grass. Proc. Roy. Soc. Agr. 193(1032): 120-145.

_____. 1949a. The dependence of transpiration on weather and soil conditions. Journal of Soil Science 1: 74-89.

_____. 1949b. Meteorology and agriculture. General survey of meteorology and agriculture and an account of the physics of irrigation control., Quant. J. R. Met. Soc. 75: 325.

Raghavan, G. S. V., E. McKyes, B. Beaulieu, F. Merineau and I. Amir. 1975. Study of traction and compaction problems on eastern Canadian agricultural soils. Report to Agric. Canada Engineering Research Services. Agr. Eng. Dept., Macdonald College.

Raghavan, G. S. V. and E. McKyes. 1979. Performance of traction wheels in clay soil. Trans. of the ASAE 22(2): 229-232.

Randolph, J. W. 1926. Tractor lug studies on sandy soil. Trans. of ASAE 21: 67-80.

_____. 1927. Tractor lug studies on sandy soil. Trans. of ASAE 21: PM5-8.

Reece, A. R. 1964. Effect of grousers on off-the-vehicle performance. Journal of Agr. Research 9(4):360-371.

Reed, J. F. and J. W. Shields. 1950. The effect of lug height and of rim width on the performance of farm tractors tires. SAE National Tractor Meeting, Milwaukee.

Saxton, K. E., H. P. Johnson and R. H. Shaw. 1974. Watershed evapotranspiration estimated by combination method. Trans. ASAE 17(4): 668-672.

Schofield, A. and P. Wroth. 1968. Critical state soil mechanics. McGraw-Hill Book Company, New York.

Shimshi, D., D. Yaran, E. Bresler, M. Weisbrod and G. Strateemer. 1975. Simulation model for evapotranspiration of wheat: empirical approach. ASCE Irrigation and Drainage Division 101 (IR1): 1-19.

Smith, J. L. 1964. Strength moisture-density relations of fine-grain soil in vehicle mobility research. U.S. Army Engineer Waterways Experiment Station, Technical Report No.3-636. Vicksburg, Ms.

Soltynski, A. 1979. The mobility problem in agriculture. J. of Terramechanics 16(3): 139-149.

Stong, J. V. and W. F. Buchele. 1962. Effect of soil parameters on strength of tillable soils. Paper No.63-132, ASAE.

Taylor, J. H. 1973. Lug angle effect on traction performance of pneumatic tractor tires. Trans. of ASAE 1(16): 16-18.

_____. 1974. Lug space effect on traction of pneumatic tractor tires. Trans. of ASAE 1(17): 195-197.

_____. 1976. Comparative traction performance of R-1, R-3, and R-4 tractor tires. Trans. of ASAE 1(19): 14-16.

Terzaghi, K. and R. P. Peck. 1948. Theoretical soil mechanics. John Wiley and Sons, New York.

Tire Guides Inc. 1976. Tread design guide, 2119. Route 110, Farmingdale, N.Y. 11735. Vol. 11.

VandenBerg, G. E. and I. F. Reed. 1962. Traction performance of radial-ply and conventional tractor tires. Trans. of ASAE 2(5): 125-129.

Van Hylckama, T. E. A. 1956. The water balance of the earth. Drexel Inst. Tech. Lab. of Climatology, Pub. Climatology 9(2): 59-117.

Vasey, G. H. and I. T. Naylor. 1958. Field tests on 14-30 tractor tires. J. Agr. Eng. Res. 3(1): 1-8.

Wells, L. G. and O. Treesuwan. 1977. The response of various soil strength indices to changing water content. Paper No.77-1055, presented at the June 1977 Annual Meeting of ASAE, North Carolina.

Wong, J. Y. and M. G. Bekker. 1977. Terrain vehicle systems analysis special program. Dept. of Mechanical and Aeronautical Engineering, Carleton University.

Wong, J. Y. 1979. Data processing methodology in the characterization of the mechanical properties of terrain. Symposium Transportation problems in resource industries. Calgary, Alberta, October 2nd and 3rd, 1979.

Wroth, C. P. and D. M. Wood. 1978. The correlation of index properties with some basic engineering properties of soils. Canadian Geotechnical Journal 2(15): 137-145.

Yong, R. N. and R. Sylvestre-Williams. 1969. Analysis and prediction of grouser thrust on sand. Soil mechanics series, No.26, McGill University, Montreal.

Yong, R. N. and C. K. Chen. 1970. Analytical and experimental studies of soil cutting. Paper No. 70-676, ASAE Winter Meeting, December 8-11, 1970.

_____. 1976. Cone penetration of granular and cohesive soils. ASCE Engineering Mechanics Division, 102: 345-364.

Yong, R. N., A. F. Youssef and H. El-Manlouk. 1977. Soil deformation and slip relative to grouser shape and spacing. Presented at ASAE Winter Meeting in Chicago, December 1977.

Young, T. C. and J. T. Ligon. 1972. Water table and soil moisture probabilities with tile drainage. Trans. ASAE 15(3): 448-451.

Youssef, M. S., E. L. Ramli, A. H. and M. ElDemary. 1965. Relationships between shear strength, consolidation, liquid limit, and plastic limit for remoulded clays. Proceedings of the 6th International Conference on Soil Mechanics and Foundation Engineering, Montreal, P.Q. 1: 126-129.

APPENDIX A

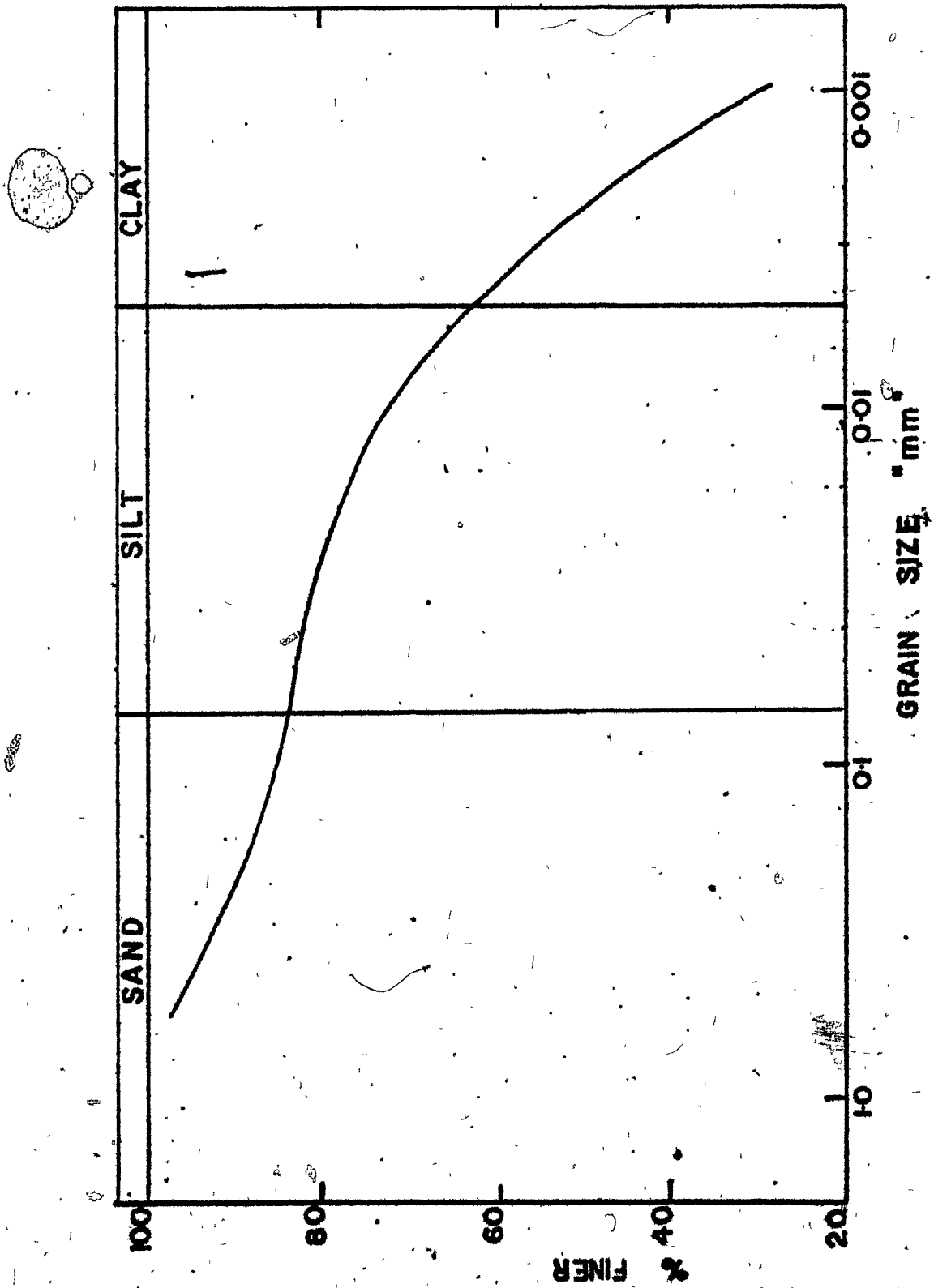

Figure A-1. Grain size distribution of the clay soil.

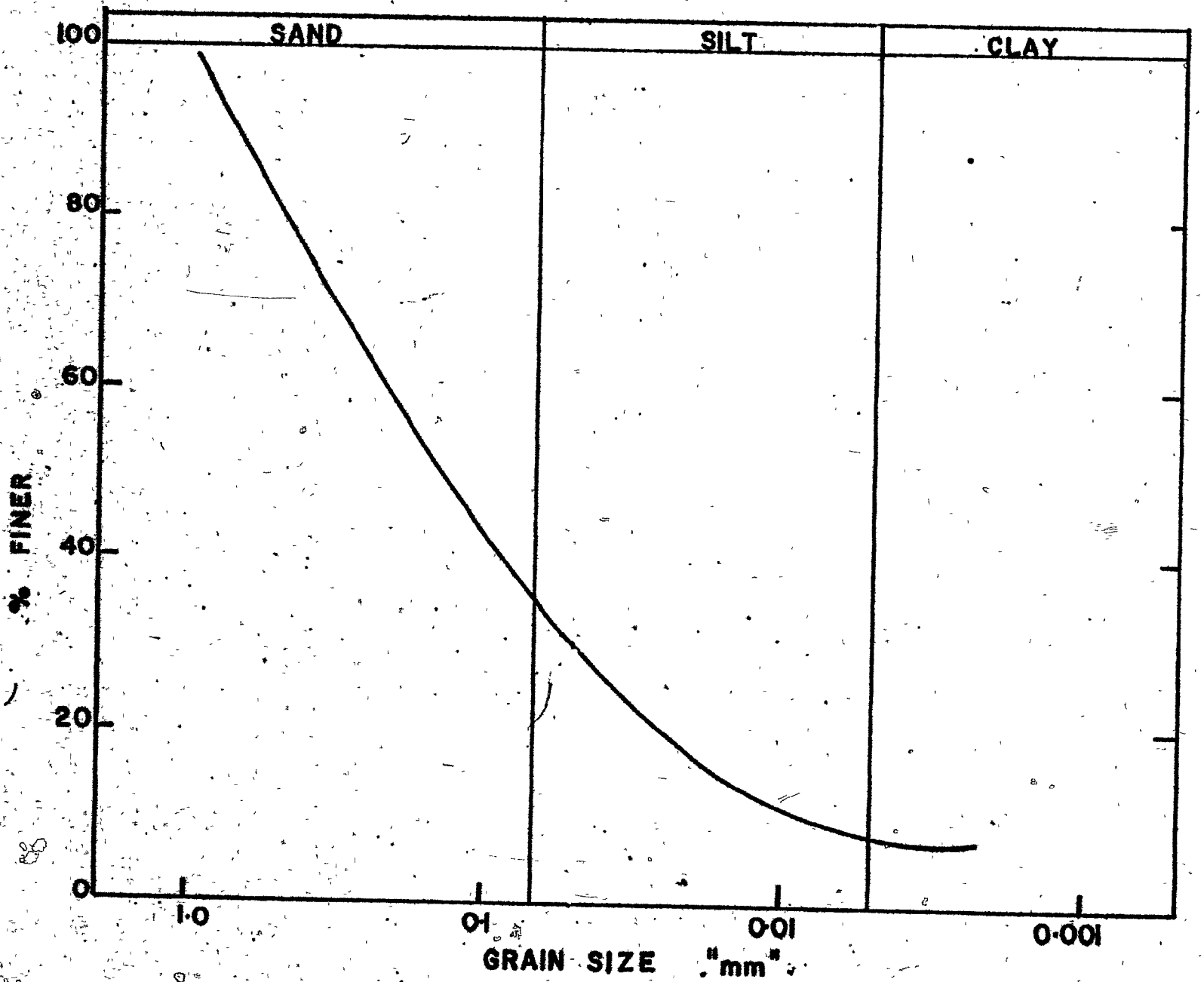

Figure A-2. Grain size distribution of the sandy loam soil.

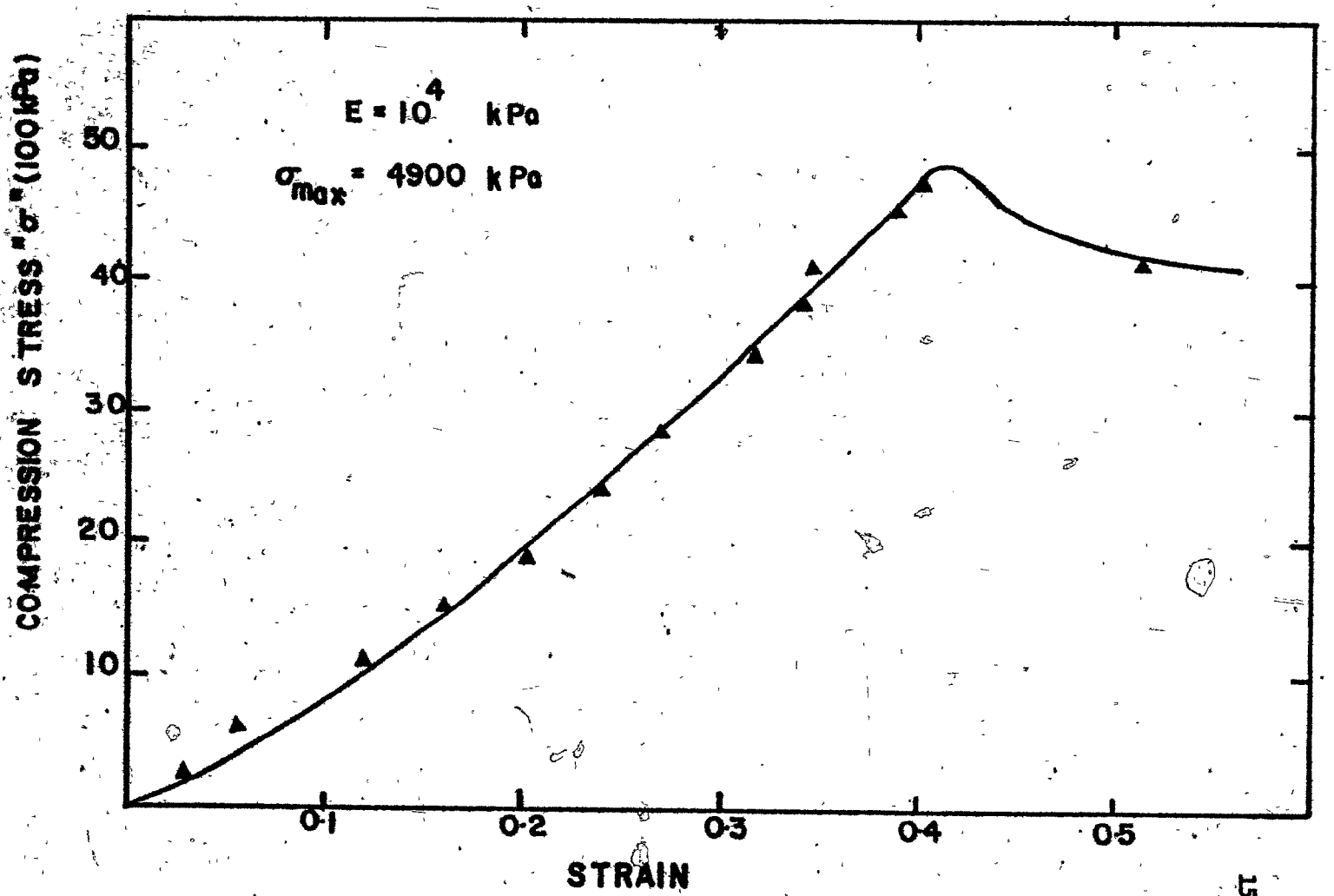

Figure A-3. Stress-strain performance of the rubber in tension.

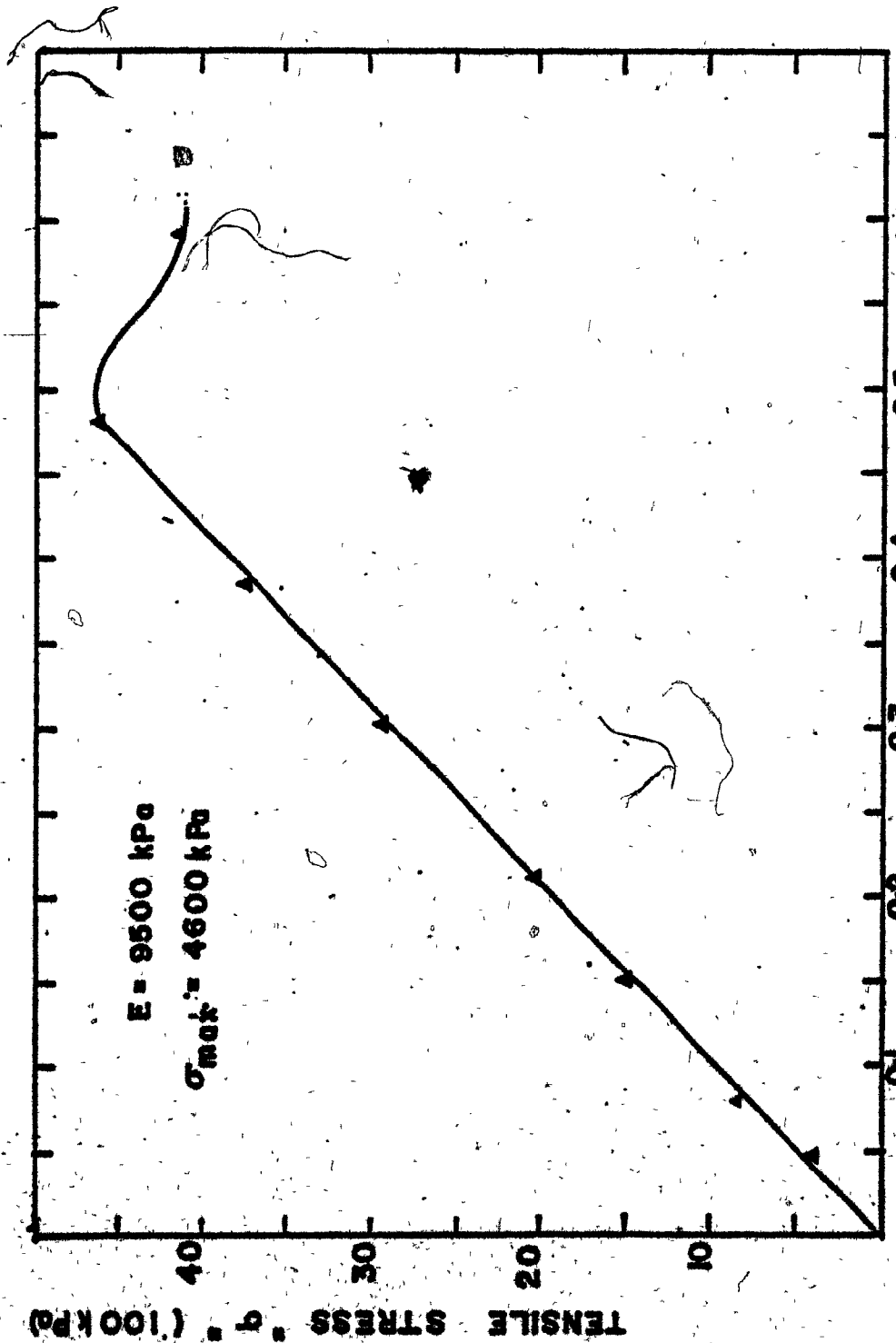

Figure A-4 : Stress-strain performance of the rubber in tension.

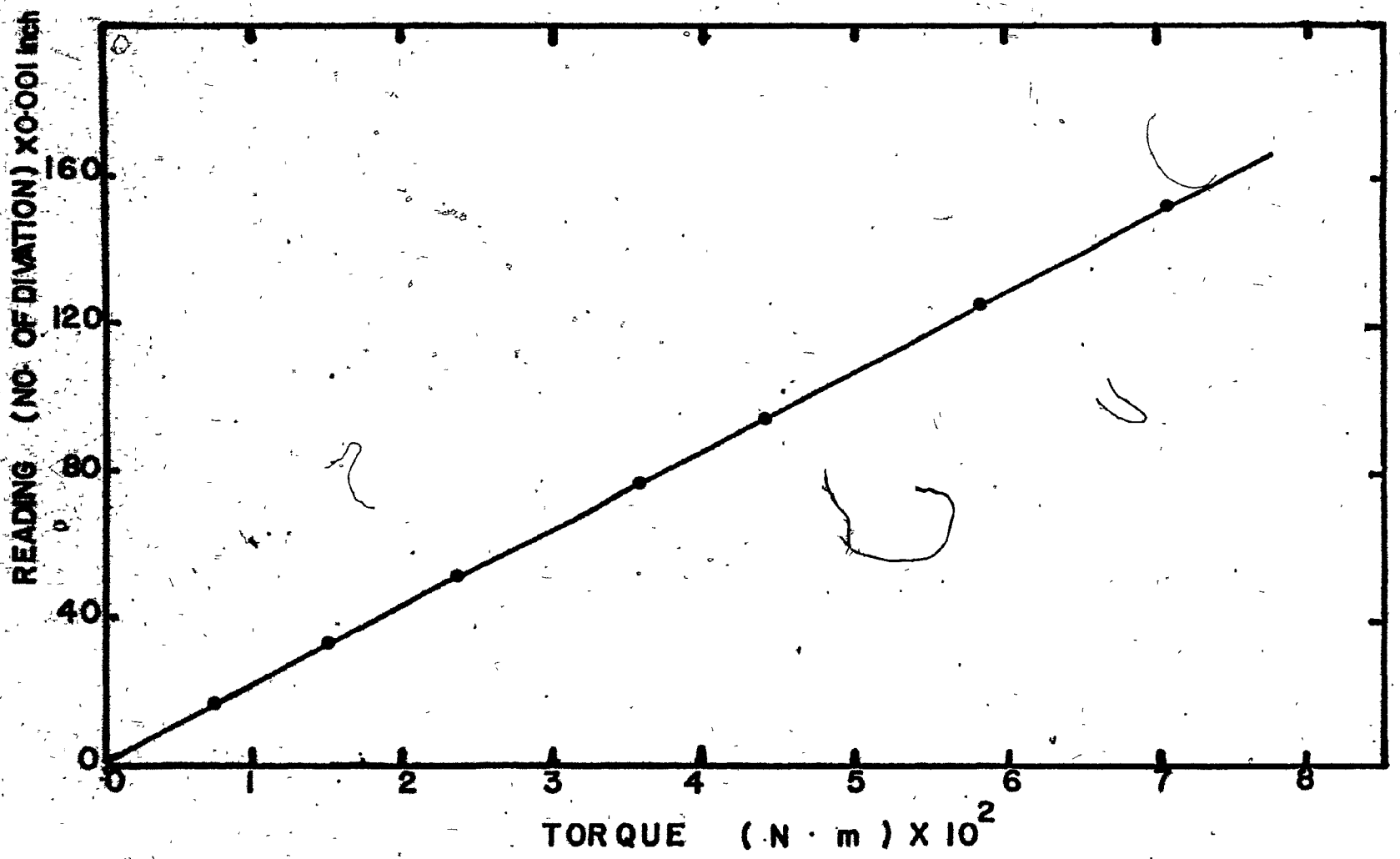

Figure A-5. Calibration of the shear ring apparatus.

MC = 39.26 %

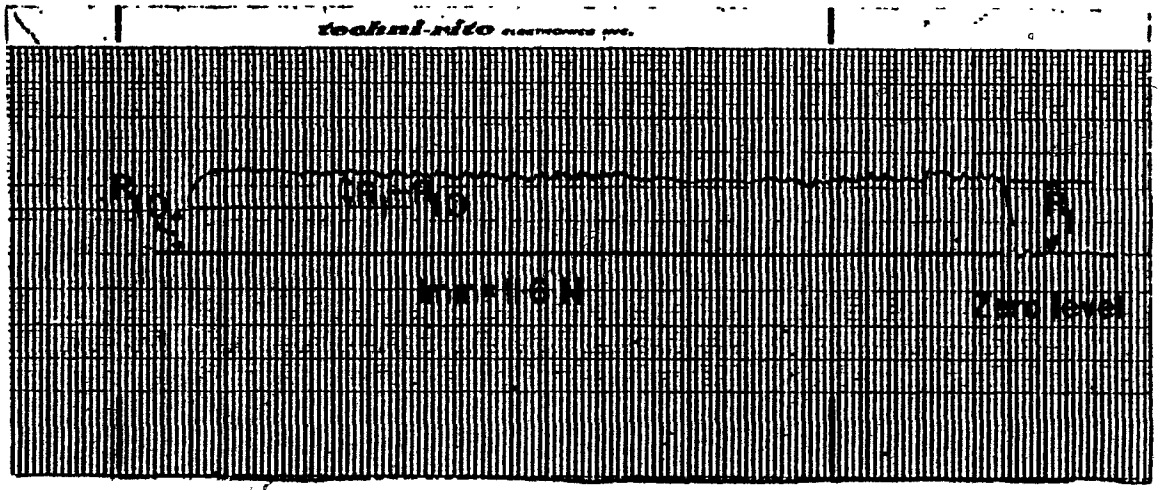

Figure A-6. Typical recording chart for the field test of sandy loam soil.

TABLE A1. The mean values, standard deviation (S.D.) and coefficient of variation (C.V.%) for soil moisture contents at different depths and times during the growing season

Depth cm	Sandy loam soil			Clay soil		
	Mean*	S.D.	C.V.%	Mean*	S.D.	C.V.%
0	11.12	1.13	10.19	31.97	3.84	12.11
5	22.47	1.98	8.82	40.44	2.29	5.68
10	19.55	2.05	10.50	39.65	4.47	12.27
0	23.36	0.64	2.70	22.48	1.62	7.25
5	25.71	0.34	1.32	29.75	3.15	10.59
10	25.55	2.50	9.81	34.29	1.29	3.07
0	22.10	0.15	0.70	37.94	1.52	4.01
5	22.08	0.20	0.91	38.19	0.91	2.39
10	26.61	0.48	1.83	45.75	0.55	1.22
0	3.68	0.32	8.83	18.89	0.56	2.96
5	16.59	1.27	7.67	26.34	0.93	3.53
10	18.29	1.05	5.77	27.27	0.43	1.58

*Mean of four measurements.

APPENDIX B

TABLE B1. Soil moisture content (percentage by weight) as average of 22-year period (1945 to 1966) from April to November for Macdonald College Farm for sandy loam soil for 30 mm root zone

Date	April	May	June	July	August	September	October	November
5	32.95	26.87	14.84	9.00	16.33	22.51	21.81	32.74
10	31.00	25.39	32.15	21.00	16.99	15.18	29.81	32.81
15	24.45	25.24	23.29	21.00	12.69	23.56	33.00	33.00
20	22.00	27.03	18.59	19.55	14.35	21.00	31.82	33.00
25	29.65	19.17	19.98	12.90	13.12	29.55	31.50	26.94
30	26.94	21.00	9.00	18.34	16.57	30.41	33.00	

TABLE B2. Soil moisture content (percentage by weight) as average of 22-year period (1945 to 1966) from April to November for Macdonald College Farm for clay soil for 30 cm root zone

Date	April	May	June	July	August	September	October	November
5	39.46	33.38	21.35	15.51	22.84	29.02	28.82	39.25
10	36.51	31.90	38.66	27.51	23.50	21.69	36.32	39.32
15	30.96	31.75	29.80	27.51	20.20	31.07	39.51	39.51
20	28.51	33.54	25.10	26.06	20.86	27.51	38.33	39.51
25	35.16	25.68	16.49	18.60	19.63	36.06	38.01	33.45
30	33.45	27.51	15.51	24.85	23.57	36.92	39.51	

TABLE B3. Predicted soil mechanical properties and soil wheel thrust and the measured soil wheel thrust for a lugged tire at 150 mm wheel width with normal pressure 13.1 kPa and two soil types

Soil moisture M.C.%	Soil density γ kg/m^3	Soil friction ϕ degree	Soil-rubber friction δ_r degree	Soil cohesion C kPa	Soil-rubber adhesion c'_r kPa	Soil thrust due to the lug	Soil thrust due to the friction	Total estimated soil thrust H (N)	Measured soil thrust H (N)
				Sandy loam soil					
16.66	1400	41.64	29.08	27.81	6.62	191	110	301	332
19.09	1300	42.03	29.19	28.12	6.59	263	109	373	320
21.39	1200	43.52	29.61	29.30	6.36	227	106	333	325
27.61	1600	42.51	29.32	28.50	5.02	192	96	288	289
35.31	1400	31.61	26.29	19.81	2.23	84	75	159	157
				Clay soil					
27.63	1200	27.29	28.79	9.36	8.03	116	131	247	247
31.19	1200	28.13	29.17	9.41	8.13	133	131	264	258
36.35	1200	27.39	28.84	9.36	8.04	124	131	255	258
39.33	1500	25.92	28.18	9.27	7.87	133	136	263	270
24.49	1400	25.66	28.09	9.25	7.84	143	130	173	264

Contact area = 472.5 cm^2
Wheel speed = 0.305 km/hr

Lug length = 150 mm
Lug angle = 90°

TABLE B4. Predicted soil mechanical properties and soil wheel thrust and the measured soil wheel thrust for a lugged tire at 150 mm wheel width with normal pressure 13.1 kPa and two soil types

Soil moisture M.C.%	Soil density γ kg/m^3	Soil friction ϕ degree	Soil-rubber friction δ_r degree	Soil cohesion C kPa	Soil-rubber adhesion c'_r kPa	Soil thrust due to the lug	Soil thrust due to the friction	Total estimated soil thrust H (N)	Measured soil thrust H (N)
				Sandy loam soil					
24.49	1300	43.94	29.72	29.64	5.82	189	101	290	360
25.41	1400	43.71	29.66	29.46	5.61	258	100	358	337
30.43	1100	39.67	28.54	26.24	4.12	191	90	289	292
35.33	1400	31.57	26.28	19.77	2.22	122	75	197	180
42.82	1100	13.28	21.20	5.18	1.05	49	38	87	76
				Clay soil					
28.56	1400	27.62	28.94	9.38	8.07	169	130	299	309
29.22	1400	27.80	29.03	9.39	8.09	179	130	309	326
37.57	1500	26.88	28.61	9.33	7.98	167	129	296	281
38.29	1400	26.52	28.45	9.31	7.94	161	129	290	301
39.08	1500	26.07	28.24	9.28	7.88	146	129	275	305

Contact area = 472.5 cm^2
Wheel speed = 0.305 km/hr
Lug length = 200 mm
Lug angle = 50°

TABLE B5. Predicted soil mechanical properties and soil wheel thrust and the measured soil wheel thrust for a lugged tire at 150 mm wheel width with normal pressure 13.1 kPa and two soil types

Soil moisture M.C.%	Soil density γ kg/m^3	Soil friction ϕ degree	Soil-rubber friction δ_r degree	Soil cohesion C kPa	Soil-rubber adhesion c'_r kPa	Soil thrust due to the lug	Soil thrust due to the friction	Total estimated soil thrust H (N)	Measured soil thrust H (N)
				Sandy loam soil					
20.29	1300	42.93	29.44	28.83	6.49	367	87	454	476
22.24	1500	43.76	29.67	29.50	6.27	411	85	496	472
27.66	1700	42.48	29.31	28.47	5.01	366	78	444	404
21.19	1500	38.67	28.26	25.44	3.85	276	74	350	360
				Clay soil					
20.33	1600	22.28	26.54	9.03	7.43	183	110	293	310
23.03	1400	24.63	27.59	9.18	7.71	209	111	320	326
32.63	1400	28.15	29.18	9.41	8.13	257	111	368	345
38.82	1300	26.23	28.31	9.29	7.90	226	111	337	342
52.12	1500	12.09	21.95	8.36	6.23	136	100	236	231

Contact area = 472.5 cm^2
Wheel speed = 0.305 km/hr
Lug length = 300 mm
Lug angle = 30°

TABLE B6. Predicted soil mechanical properties and soil wheel thrust and the measured soil wheel thrust for a lugged tire at 250 mm wheel width with normal pressure 7.94 kPa and two soil types

Soil moisture M.C.%	Soil density γ kg/m^3	Soil friction ϕ degree	Soil-rubber friction δ_r degree	Soil cohesion C kPa	Soil rubber adhesion c'_r kPa	Soil thrust due to the lug	Soil thrust due to the friction	Total estimated soil thrust H (N)	Measured soil thrust H (N)
				Sandy loam soil					
8.23	1500	23.12	23.93	13.03	5.62	100	137	237	325
10.27	1500	27.93	25.27	16.87	6.06	127	145	272	288
18.08	1400	41.01	28.91	27.30	6.65	266	147	413	427
21.04	1400	43.35	29.56	29.17	6.41	308	140	448	426
20.98	1500	43.32	29.55	29.15	6.42	308	140	448	426
				Clay soil					
20.24	1400	22.19	26.50	9.02	7.42	134	171	305	270
25.61	1400	26.34	28.36	9.29	7.92	169	177	346	325
34.24	1400	27.97	29.10	9.40	8.11	188	178	366	314
35.34	1300	27.72	28.98	9.38	8.08	178	178	356	392
51.02	1200	13.68	22.67	8.46	6.41	94	154	248	225

Contact area = 787.5 cm^2
Wheel speed = 0.305 km/hr
Lug length = 250 mm
Lug angle = 90°

TABLE B7. Predicted soil mechanical properties and soil wheel thrust and the measured soil wheel thrust for a lugged tire at 250 mm wheel width with normal pressure 7.94 kPa and two soil types

Soil moisture M.C.%	Soil density γ kg/m^3	Soil friction ϕ degree	Soil-rubber friction δ_r degree	Soil cohesion C kPa	Soil-rubber adhesion c'_r kPa	Soil thrust due to the lug	Soil thrust due to the friction	Total estimated soil thrust H (N)	Measured soil thrust H (N)
				Sandy loam soil					
14.58	1400	36.35	27.61	23.59	6.60	264	143	407	438
18.77	1400	41.74	29.11	27.89	6.61	352	136	488	512
19.77	1500	42.57	29.34	28.55	6.54	360	134	494	512
27.01	1500	42.93	29.44	28.84	5.19	327	117	444	500
28.46	1500	41.81	29.13	27.94	4.77	357	113	470	413
				Clay soil					
12.14	1400	12.13	21.97	8.36	6.23	121	146	267	260
26.26	1300	26.88	28.61	9.33	7.98	209	169	367	369
35.03	1300	27.79	29.02	9.39	8.09	232	169	401	373
40.37	1300	25.24	27.87	9.22	7.79	191	167	358	373
45.87	1300	20.23	25.62	8.89	7.19	154	161	315	314

Contact area = 787.5 cm^2
Wheel speed = 0.305 km/hr
Lug length = 32.6 mm
Lug angle = 50°

TABLE 38. Predicted soil mechanical properties and soil wheel thrust and the measured soil wheel thrust for a lugged tire at 250 mm wheel width with normal pressure 7.94 kPa and two soil types

Soil moisture M.C.%	Soil density γ kg/m^3	Soil friction ϕ degree	Soil-rubber friction δ_r degree	Soil cohesion C kPa	Soil-rubber adhesion c'_r kPa	Soil thrust due to the lug	Soil thrust due to the friction	Total estimated soil thrust H (N)	Measured soil thrust H (N)
				Sandy loam soil					
11.83	1700	31.28	26.20	19.54	6.31	293	113	406	315
12.81	1700	33.21	26.74	21.08	6.44	231	77	408	328
16.66	1500	39.40	28.46	26.02	6.67	389	0	389	427
20.22	1500	42.88	29.43	28.80	6.50	556	0	556	516
				Clay soil					
21.75	1500	23.58	27.12	9.11	7.59	269	203	472	270
22.74	1700	24.41	27.49	9.17	7.69	266	18	284	270
40.23	1700	25.34	27.92	9.23	7.80	280	15	295	283
43.06	1400	23.07	26.89	9.08	7.53	237	22	259	268
46.52	1600	19.50	25.29	8.84	7.10	203	28	231	225

Contact area = 787.5 cm^2
Wheel speed = 0.305 km/hr
Lug length = 500 mm
Lug angle = 30°

TABLE 39. Predicted soil mechanical properties and soil wheel thrust and the measured soil wheel thrust for a lugged tire at 300 mm wheel width with normal pressure 6.59 kPa and two soil types

Soil moisture M.C.%	Soil density γ kg/m^3	Soil friction ϕ degree	Soil-rubber friction δ_r degree	Soil cohesion C kPa	Soil-rubber adhesion c_r' kPa	Soil thrust due to the lug	Soil thrust due to the friction	Total estimated soil thrust H (N)	Measured soil thrust H (N)
				Sandy loam soil					
16.15	1600	38.72	28.27	25.48	6.67	263	169	432	243
18.25	1500	41.24	28.97	27.49	6.67	331	165	496	483
21.17	1500	43.42	29.58	29.23	6.39	396	157	553	539
26.21	1200	43.38	29.57	29.02	5.41	360	141	502	505
28.45	1600	41.82	29.13	27.95	4.77	312	134	446	450
				Clay soil					
36.48	1000	27.34	28.81	9.36	8.04	200	201	401	393
37.89	1300	26.72	28.54	9.32	7.96	191	200	391	382
39.84	1200	25.60	28.03	9.25	7.83	176	196	366	382
49.44	1900	15.86	23.65	8.60	6.67	116	180	296	264
56.19	1100	5.72	19.09	7.94	5.47	142	152	294	229

Contact area = 945.0 cm^2
Wheel speed = 0.305 km/hr
Lug length = 300 mm
Lug angle = 90°

TABLE 810. Predicted soil mechanical properties and soil wheel thrust and the measured soil wheel thrust for a lugged tire at 300 mm wheel width with normal pressure 6.59 kPa and two soil types

Soil moisture M.C.%	Soil density γ kg/m^3	Soil friction ϕ degree	Soil-rubber friction δr degree	Soil cohesion C kPa	Soil-rubber adhesion c'_r kPa	Soil thrust due to the lug	Soil thrust due to the friction	Total estimated soil thrust H (N)	Measured soil thrust H (N)
				Sandy loam soil					
2.72	1400	8.33	19.82	1.23	3.97	60	121	181	185
5.01	1600	14.72	21.60	6.33	4.73	91	136	227	213
17.56	1600	40.50	28.76	26.89	6.66	384	156	540	550
22.28	1400	43.83	29.69	29.55	6.23	49	143	192	629
29.03	1700	41.26	28.98	27.51	4.59	373	124	497	517
				Clay soil					
6.72	1400	3.51	18.09	7.79	5.21	242	7	249	400
20.00	1400	21.96	26.39	9.01	7.40	182	185	367	377
35.12	1100	27.77	29.01	9.39	8.09	242	190	432	348
47.04	1200	18.89	25.01	8.80	7.03	175	180	355	413

Contact area = 945.0 cm^2
Wheel speed = 0.305 km/hr
Lug length = 392 mm
Lug angle = 50°

TABLE B11. Predicted soil mechanical properties and soil wheel thrust and the measured soil wheel thrust for a lugged tire at 300 mm wheel width with normal pressure 6.59 kPa and two soil types

Soil moisture M.C.%	Soil density γ kg/m^3	Soil friction ϕ degree	Soil-rubber friction δ_r degree	Soil cohesion C kPa	Soil-rubber adhesion c'_r kPa	Soil thrust due to the lug	Soil thrust due to the friction	Total estimated soil thrust H (N)	Measured soil thrust H (N)
				Sandy loam soil					
12.74	1300	33.08	26.71	20.98	6.43	295	169	464	472
15.73	1300	38.13	28.11	25.00	6.66	486	169	655	595
33.14	1400	35.66	27.42	23.03	3.11	305	111	416	427
				Clay soil					
14.85	1900	15.94	23.69	8.61	6.68	151	181	332	348
18.97	1300	20.90	25.91	8.94	7.27	200	191	391	404
28.66	1300	27.64	28.95	9.38	8.07	340	201	541	518
36.73	1400	27.24	28.77	9.35	8.02	333	201	534	539
52.40	1300	11.67	21.77	8.33	6.18	134	169	303	314

Contact area = 945.0 cm^2
Wheel speed = 0.305 km/hr
Lug length = 600 mm
Lug angle = 30°

TABLE B12. Computer program to calculate the soil thrust, due to the lugs, of a lugged tire

```
$WATFIV           ID,PAGES=50,TIME=50
C     PROGRAM TO CALCULATE THE TRACTION FORCE OF A LUGGED TIRE UND
C    1 DIFFERENT CONDATION
C     SANDY LOAM SOIL
      DIMENSION E1(150),E2(150),E3(150),E4(150),E5(150),E7(150),E8(150),
     1E9(150),E10(150),E11(150),E12(150),E13(150),E14(150),E16(150),
     2E17(500),P(150) ,E15(150),E6(150)
      Z=2.0
      DO 1 I=1,56
      READ (5,100) E4(I),E1(I)
100   FORMAT (F5.2,F8.6)
1     CONTINUE
      E5(1)=23.64
      E5(2)=32.1
      E6(2)=42.0
      E6(1)=32.45
      DO 2 M=1,56
      E7(M)=(40.**ALOG(2.7806)*SIN(1.57*E4(M)/E5(1)))+0.5238
      E8(M)=0.3046**ALOG(2.4363)*SIN(1.57*E4(M)/E5(1))-0.05
      E9(M)=(0.8035**ALOG(1.255))*SIN(1.57*E4(M)/E5(1))+0.456)/14.26
      E10(M)= 29.145**ALOG(2.094)*SIN(1.57*E4(M)/E5(1))+17.655
      WRITE(6,900) E7(M),E8(M),E9(M),E10(M)
900   FORMAT (4F15.4)
2     CONTINUE
C     CLAY SOIL
      DO 3 I=57,115
      READ (5,110) E4(I),E1(I)
110   FORMAT (F5.2,F8.6)
3     CONTINUE
      DO 4 M=57,115
      E7(M)=(28.0**ALOG(2.9409))*SIN(1.57*E4(M)/E5(2))-8.229
      E8(M)=0.145**ALOG(6.9084)*SIN(1.57*E4(M)/E5(2))+0.0702
      E9(M)=((3.0516**ALOG(0.6478))*SIN(1.57*E4(M)/E5(2))+0.5437)/14.26
      E10(M)=23.05**ALOG(2.4377)*SIN(1.57*E4(M)/E5(2))+12.8136
      WRITE(6,1000)E7(M),E8(M),E9(M),E10(M)
1000  FORMAT(4F15.4)
4     CONTINUE
C     RAED THE K FACTOR FOR THE SANDY LOAM SOIL
      DO 5 I=1,56
      READ (5,120) E11(I),E12(I),E13(I),E14(I),E16(I),E17(I)
120   FORMAT (6F4.2)
5     CONTINUE
C     READ THE K FACTORS FOR THE CLAY SOIL
      DO 6 I=57,115
      READ(5,130) E11(I),E12(I),E13(I),E14(I),E16(I),E17(I)
130   FORMAT(6 F4.2)
6     CONTINUE
      DO 8 K=1,115
      READ(5,140) E3(K),E2(K),E15(K)
140   FORMAT(3F5.1)
8     CONTINUE
      DO 7 K=1,115
      Y=E10(K)/E7(K)
      D=0.4*(1-Y)*(E7(K)*3.14/180)*(1/TAN(E7(K)*3.14/180))
      F1=1-0.5*SINH(2*(1.57+E7(K)*3.14/180-1.833))*EXP(TAN(E7(K)*
     13.14/180))
      F2=1/TANH(1.57+0.175)
      F3= TANH(1.57-E7(K)*3.14/360)
      IF(D*F1.GT.174) GO TO 7
      W1=EXP(D*F1)
```

```
      W2=EXP(0*F2)
       W3=EXP(0*F3)
      P1=E11(K)*((E12(K)/E11(K))**W1*Y)
      P2=E13(K)* (E14(K)/E13(K))**W2*Y
      P3=E16(K)* (E17(K)/E16(K))**W3*Y
      X=1.0*K
      X1=E15(K)/100.0
       P(K)=(E1(K)*Z**2*P1+E8(K)*Z*P2+X1*Z*P3)*E3(K)
     1*COS(E10(K)*3.14/180)
      P4=Z*E3(K)*E9(K)+P(K)*SIN(E2(K)*3.14/180)*TAN(E10(K)*3.14/180)
      IF(P4.EQ.0.0) GOTO 5000
      GO TO 6000
 5000 P(K)=0.0
      B=0.0
      C=0.0
      R=0.0
      P4=0.0
      T=0.0
      A=31.5*E3(K+4)
      GO TO 3000
 6000 T=SQRT(P(K)**2+P4**2)
      B=(45-E7(K)/2)*3.14/180
      V=SIN(E10(K)*3.14/180)/SIN(E7(K)*3.14/180)
      IF(V.GT.1.0) GO TO 2000
      C=(3.14/4)-(3.14/180)*(E7(K)/2+E10(K)/2)-ARSIN(SIN(E10(K)*3.14/
     1180)/(SIN(E7(K)*3.14/180)))/2
      GO TO 7000
 2000 C=-(3.14/180)*(E7(K)/2+E10(K)/2)
 7000 R=Z*((TAN(E7(K)*3.14/180)+1/TAN(B))/(1.+TAN(C)*TAN(E7(K)*3.14/180)
     1))
      G=31.5
      H=E2(K)*3.14/180
      IF (E3(K)*COS(H).GT.31.5) GO TO 4000
      A=(G-E3(K)*COS(H))*E3(K)*SIN(H)+(E3(K)**2*COS(H)*SIN(H))-(R*
     1E3(K)-R**2*TAN(1.57-H)/2)
      GO TO 3000
 4000 A=TAN(H)*G**2/2-R*G/COS(H)-R**2/2*(TAN(1.57-H)+TAN(H))
      E3(K)=G/COS(H)
      GO TO 3000
 3000 TF=A*E9(K)+X1*TAN(E10(K)*3.14/180)*A
      T1=T+TF
      WRITE (6,150) E4(K),E1(K),E7(K),E10(K),E8(K),E9 (K),P(K),P4,T,X
     1,E1,TF
  150 FORMAT(12F10.4)
      CONTINUE
      STOP
      END
```